UNIVERSITY OF HAWAII
LIBRARY
JUN 7 '50

# The PHILOSOPHICAL MAGAZINE

FIRST PUBLISHED IN 1798

L. 41 SEVENTH SERIES No. 316 MAY, 1950

## A Journal of Theoretical Experimental and Applied Physics

EDITOR
PROFESSOR N. F. MOTT, M.A., D.Sc., F.R.S.

EDITORIAL BOARD
SIR LAWRENCE BRAGG, O.B.E., M.C., M.A., D.Sc., F.R.S.
ALLAN FERGUSON, M.A., D.Sc.
SIR GEORGE THOMSON, M.A., D.Sc., F.R.S.
PROFESSOR A. M. TYNDALL, C.B.E., D.Sc., F.R.S.

PRICE 10s.
Annual Subscription £5 2s. 6d. payable in advance.

TED AND PUBLISHED BY TAYLOR & FRANCIS LTD., RED LION COURT, FLEET ST., LONDON. E.C.4

# Annals of Science

A QUARTERLY REVIEW OF
THE HISTORY OF SCIENCE
SINCE THE RENAISSANCE

EDITORS

D. McKIE, D.Sc., Ph.D.,
University College, London.

HARCOURT BROWN, M.A., Ph.D.,
Brown University, Providence, R.I., U.S.A.

H. W. ROBINSON,
Former Librarian,
Royal Society of London.

ANNUAL SUBSCRIPTION
**£2 0s. 0d.**
OR
10s. 6d.
PER PART
POST FREE

**TAYLOR & FRANCIS, LTD., Red Lion Court, Fleet Street, LONDON, E.C.4**

---

ALERE FLAMMAM

# THE MATHEMATICAL WORKS OF JOHN WALLIS, D.D., F.R.S.

*by*

**J. F. SCOTT, Ph.D., B.A.**

"His work will be indispensable to those interested in the early history of The Royal Society. I commend to all students of the Seventeenth Century, whether scientific or humane, this learned and lucid book."—Extract from foreword by Prof. E. N. da C. Andrade, D.Sc., Ph.D., F.R.S.

**Recommended for publication by University of London**

**12/6** net

*Printed and Published by:*

**TAYLOR & FRANCIS, LTD.**
RED LION COURT, FLEET STREET, LONDON, E.C.4.

# XXXVII. *Nuclear Transmutations Produced by Cosmic-Ray Particles of Great Energy.*—Part IV. *The Distribution in Energy, and the Secondary Interactions of the Particles Emitted from Stars.*

By U. Camerini, P. H. Fowler, W. O. Lock and H. Muirhead.
The H. H. Wills Physical Laboratory, University of Bristol*.

[Received March 20, 1950.]

[Plates IX.–XI.]

## Summary.

The measurements of "multiple scattering" and "grain density" discussed in Parts II. and III. of the present series of papers, have now been extended to include a total of 1000 tracks of particles associated with "stars". The method of measurement and the criteria for the selection of tracks were similar to those described previously (III.). The new material provides additional evidence in support of the view that most of the mesons ejected from nuclear explosions with kinetic energy less than 150 MeV. are $\pi$-particles.

The distribution in energy of the ejected mesons, protons, deuterons and tritons has been determined, and it is shown that the "spectrum" for the mesons is in good agreement with that calculated by Sands (1950). The mean free-path for nuclear interaction of the various types of particles in passing through the emulsion has been determined. The value obtained for mesons corresponds to a cross-section for the interaction equal to the "geometrical" value.

## Scattering Measurements.

The new measurements were made on plates coated with Ilford G5 emulsion, 400 $\mu$ thick and exposed in the balloon flight represented in curve *c* of fig. 2, Part II. Plates from the same batch were employed in the measurements described in Part III. (Fowler 1950).

The experimental results for 700 tracks, all with a grain density less than 50 grains per 50 $\mu$, are shown in fig. 1. The curves, $\mu$, $\pi$, P, D, T are the same as in the corresponding figure in Part III., and the value of the constant $k_2$ used (equation (3), Part III.) was 32·7. This particular value of $k$ has been chosen to give the best fit with the experimental distribution for those protons which produce tracks with values of the grain-density between 16 and 50 grains per 50 $\mu$. For higher values of the grain-density, there is a small departure of the experimental points for protons corresponding to a change in the value of $k$ of about 7 percent. This, however,

---

* Communicated by Professor C. F. Powell, F.R.S.

Fig. 1.

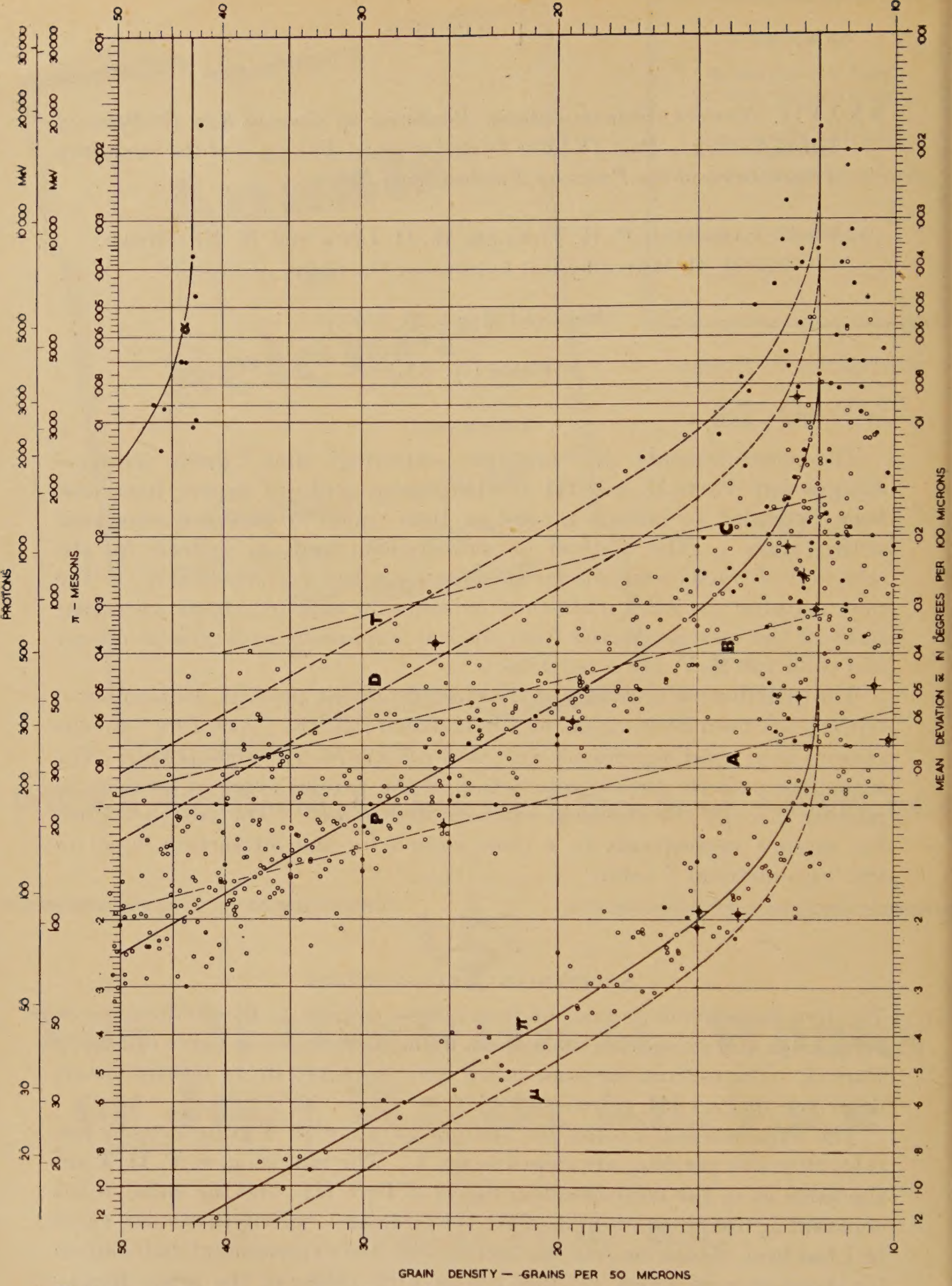

Relation between grain-density and $\bar{\alpha}^\circ$ ($100\,\mu$) for the tracks of 700 particles. " Primary " particles are shown thus • ; " Secondary " particles thus ○ ; and " interconnecting " particles thus -ϕ-.

The lines $\mu$ . $\pi$ . P, D, T are the same as in fig. 3 of Part III.

A, B and C are lines of constant momentum and correspond respectively to 500, 1000 and 2000 MeV./c.

Kinetic energy scales for $\pi$-mesons and protons are included at the top of the figure.

does not affect the measurements of the mass of the mesons, because a $\pi$-particle with a residual range of 3 mm. produces a track with a grain-density of approximately 45 grains per $50\mu$.

The mass spectrum of the particles has been obtained by the same method as that described in Part III., and is shown in fig. 2. The number of mesons suitable for measurement, and producing tracks with a grain density greater than 15 grains per $50\,\mu$ is 58, and the average value of the mass of these particles $283 \pm 7\ m_e$.

Fig. 2.

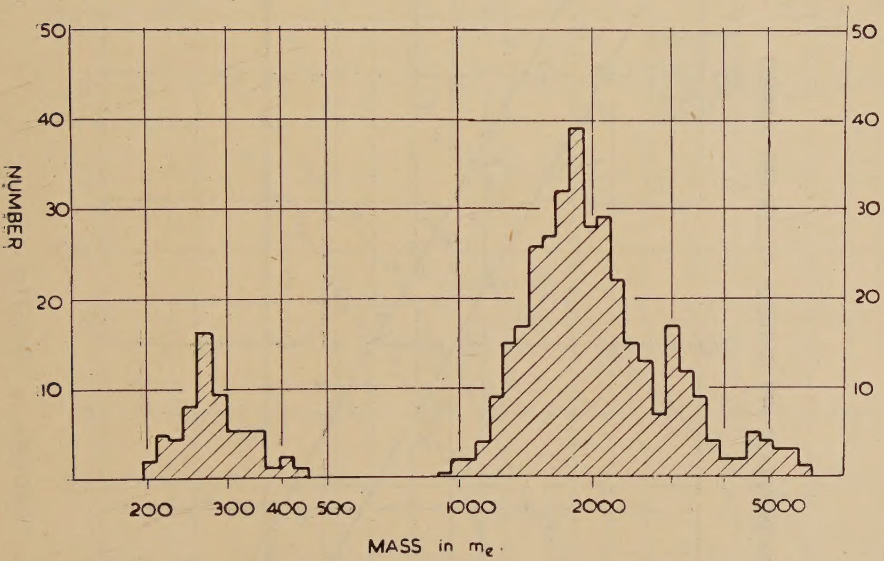

Distribution in mass of the particles of charge $/e/$ corresponding to the measurements represented in fig. 1.

In order to confirm the identity of these particles, we have made similar meaurements on the tracks of 22 $\pi$-mesons and 13 $\mu$-mesons of which the range in the emulsion was greater than 3 mm. The $\pi$-mesons were identified by their decay into a $\mu$-meson, or by the occurrence of a nuclear interaction at the end of the range ; and the $\mu$-mesons by the decay into an electron. The results of these measurements are displayed in fig. 3. We believe that these observations leave little doubt that all, or almost all, the mesons ejected from stars with kinetic energies less than 150 MeV. are indeed $\pi$-mesons.

The nature of particles with a kinetic energy between 150 MeV. and 1500 MeV., which produce tracks with values of the grain density less than 16 grains per $50\,\mu$, cannot be determined from these measurements

The work of Piccioni (1950), however, has shown that most of them are also $\pi$-mesons. Further, the possibility of the presence of a large proportion of electrons among the shower particles can be eliminated by the following observation :—Twenty of the 300 shower particles measured have had path lengths in the emulsion greater than 2 cm. Since the radiation length in the emulsion is 2·3 cm. (Carlson *et al.* 1950), a significant decrease in energy should have been observed in at least some of these tracks, had a considerable number of them been due to electrons.

Fig. 3.

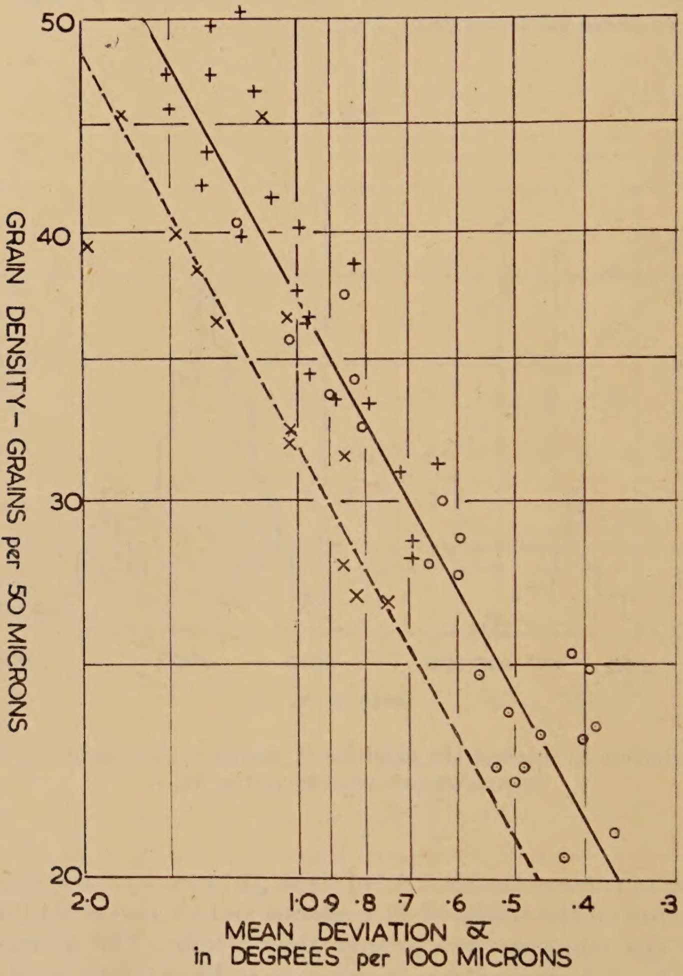

Relation between grain-density and $\bar{\alpha}^\circ$ (per 100 $\mu$). Mesons ejected from stars are shown thus ○, and are the same as those shown in the corresponding grain-density interval in fig. 1. Mesons, which, at the end of their ranges produce stars or $\pi$–$\mu$ decays are shown thus +; and mesons which decay into fast electrons at the end of their ranges are shown thus ×.

## THE DISTRIBUTION IN ENERGY OF THE PARTICLES EMITTED IN NUCLEAR DISINTEGRATIONS.

The results represented in fig. 1 allow us to determine the distribution in energy of the secondary particles, and fig. 4 shows the results for $\pi$-mesons, protons and for deuterons and tritons taken together without discrimination. The results are plotted on a logarithmic scale. The term $\pi$-mesons, in this instance, refers to all particles less massive than protons, but the arguments advanced above give us great confidence that the great majority of the points on or near curve $\pi$ (fig. 1), in the energy interval

Fig. 4.

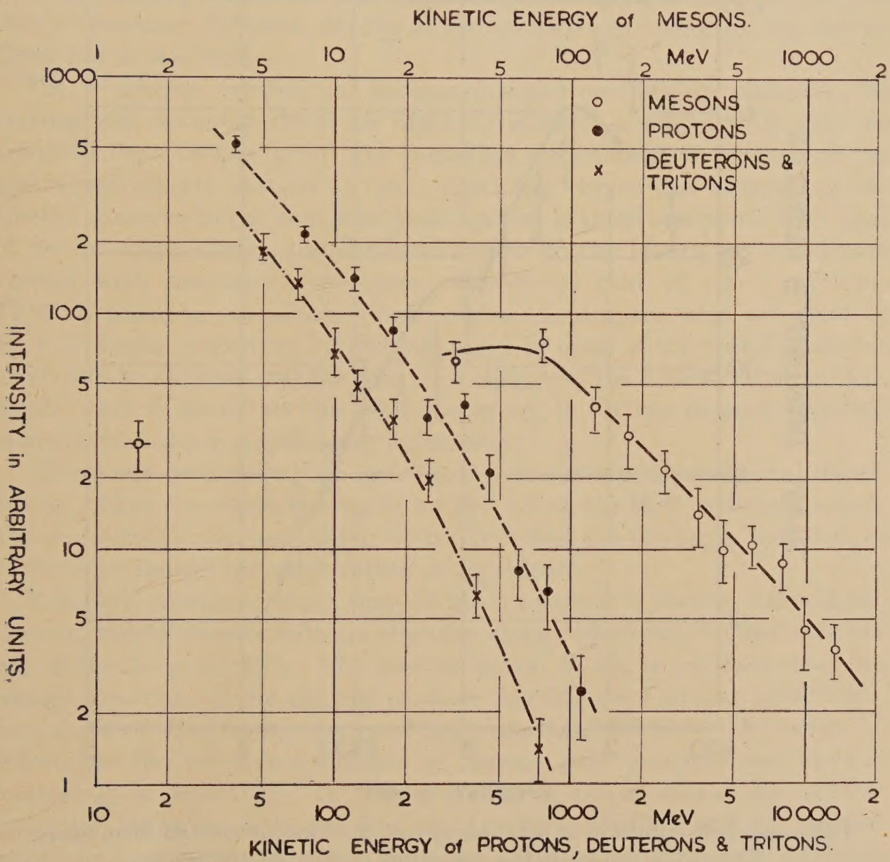

Differential distribution in kinetic energy for the various types of particles. The point at 1·6 MeV. for mesons, is for $\pi^-$-particles only and is calculated from the observed number of mesons which are ejected from stars and produce nuclear disintegrations at the end of their range. To obtain the number of particles per star per MeV. interval multiply by $\sim 2{\cdot}5 \, . \, 10^{-5}$.

from 150 to 1500 MeV., represent $\pi$-mesons. The point in fig. 4, corresponding to a $\pi$-meson of energy 1·6 Mev., is based upon the distribution in the values of the residual range of the slow ejected $\pi$-particles which reach the end of their range in the emulsion and produce "stars". In determining this point, allowance has been made for the fact that only 72 per cent of the $\pi^-$-mesons produce observable stars in photographic emulsions (Adelman and Jones 1949), and suitable geometrical corrections for "loss" have also been applied. The energy spectra have been "cut off" at energies corresponding to a mean angle of scattering of 0·022° per 100$\mu$, since the nature of the fastest "shower" particles is ambiguous.

Fig. 5.

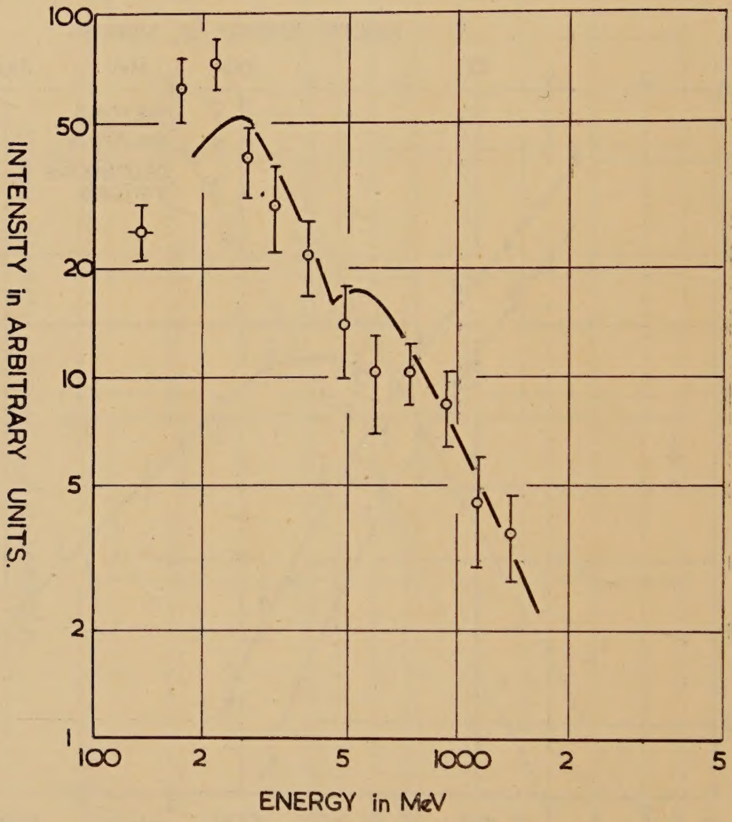

Differential distribution in total energy of the mesons ejected from stars. The curve drawn is the spectrum calculated by Sands.

In fig. 5, the data have been plotted in the form of a differential spectrum showing the total energy, E, of the $\pi$-mesons at their points of creation. The spectrum may be represented, to within the experimental errors, by a power law of the form $dE/E^{1\cdot5}$, in the energy region from 250 to 1400 MeV.

We have found no appreciable difference in the energy spectra of the mesons produced in stars with different numbers of heavy branches. This suggests that the energy spectrum does not depend strongly on the nature of the nucleus in which the mesons are created. It follows that the observed energy spectrum shown in fig. 5 is similar to that of the mesons created in the free atmosphere at a depth of 50 gm. cm.$^{-2}$. This altitude is near the main meson production layer of the atmosphere. It is therefore of interest to compare our observations with the results of Sands (1950) who has deduced the energy spectrum of the mesons at their points of production from (*a*), measurements of the intensity of the slow $\mu$-mesons at different depths in the atmosphere ; and (*b*), the energy spectrum at sea level.

The $\pi$-mesons created in nuclear interactions taking place in the atmosphere normally decay in flight to produce $\mu$-mesons. It may be assumed that, in the decay, the $\mu$-mesons are emitted at random in the spatial coordinate system of the $\pi$-particles. Since the velocity of the ejected $\mu$-meson in the centre of mass system is small compared with that of the moving $\pi$-meson, the $\mu$-mesons appear in the laboratory coordinate system with essentially the same velocity as that of the $\pi$-particles. Thus in order to transform Sands' curve to compare with our data in fig. 5, a simple correction for the difference in mass of the $\pi$ and $\mu$-mesons need only be applied, and the rest mass energy of the $\pi$-meson then added. Sands' data is shown by the solid line in fig. 5. It can be seen that two distributions are in satisfactory agreement.

There are indications of an arrest point in our experimental distribution which corresponds roughly to the dip at 450 MeV. in Sands' curve. The statistical errors associated with our values are too large, however, to allow us to regard the observation as significant.

At kinetic energies greater than 10 mc.$^2$, where $m$ is the rest-mass of the mesons, Sands' results indicate that the energy spectrum follows a power law of the form $d\mathrm{E}/\mathrm{E}^{2\cdot5}$. The results shown in fig. 4 indicate that the energy spectrum of the ejected protons also follows a similar power law, for values of the kinetic energy of the order of 1000 MeV. In order to determine the relative numbers of mesons and protons that have a scattering of less than $\cdot22^\circ/100\,\mu$, we have extrapolated the proton spectrum following a power law of the form $d\mathrm{E}/\mathrm{E}^{2\cdot5}$, and the meson spectrum from Sands' curve. There is a satisfactory agreement between the total number of particles expected on the basis of these extrapolations and the numbers observed.

The present results indicate that of the particles, with ionization less than four times the minimum value (44 grains per $50\mu$), which originate in nuclear disintegrations, $36\pm2\cdot5$ per cent are $\pi$-mesons, $51\pm2\cdot9$ per cent protons and $13\pm1\cdot5$ per cent deuterons or tritons. For "shower" particles with ionization less than 16 grains per $50\,\mu$, the figures are $79\pm6$ per cent, $17\pm3$ per cent and $4\cdot0\pm1\cdot3$ per cent respectively.

## NUCLEAR INTERACTIONS OF THE SHOWER PARTICLES.

It has been pointed out in Part II. that a shower particle, created in the disintegration of one of the atoms of the emulsion, is sometimes observed to make a nuclear collision. We call such phenomena double stars (Pls. IX., X. and XI.). It is possible to measure the mean free path for these interactions, and since it is now known that 80 per cent of the shower particles are mesons, almost certainly $\pi$-particles, observations of this type give important information about the strength of their interaction with nucleons.

### *Method I.*

The simplest approach is to make a direction comparison between the total length in the emulsion, $\Sigma L$, of the tracks of shower particles of length greater than 3000 $\mu$, and the number of nuclear interactions which they produce. We can thus confine attention to those shower particles which can be shown by scattering measurements to be mesons.

In an examination of 48 c.c. of emulsion, 241 mesons, ejected from stars with kinetic energies in the interval 150–1500 MeV., and each with a length of path in the emulsion greater than 3000 $\mu$ have been identified. The total length of the tracks is 200 cm., and six of them produce a second nuclear disintegration. A meson must, however, have travelled at least 3000 $\mu$ in the emulsion in order to be identified. If it makes a nuclear interaction before traversing this length it will be excluded from the statistics both of the nuclear interactions and of the number of tracks. The effective length we have to consider is therefore: $200-(241\times 0{\cdot}3)=128$ cm., and the average length of path per disintegration is $21\pm 9$ cm. This corresponds to the passage through a thickness of emulsion of mass $82\pm 35$ gm. cm.$^{-2}$, a value which may be compared with that to be expected if the atoms of the emulsion present a geometrical target area to the incident particle ; viz, 90 gm. cm.$^{-2}$. (George and Jason 1949.)

### *Method II.*

A similar calculation can be made for all "shower" particles of length greater than 400 $\mu$. This value of the minimum length allows the determination of the grain density of the interconnecting track to be made with an accuracy of at least 15 per cent. Figs. 6 and 7 show the distribution in values of the grain density of all interconnecting tracks. Tracks of a sufficient length to permit their identification are distinguished by cross marking. In some cases the identification was found to be possible even though the track was shorter than 3000 $\mu$. The corresponding distribution for all measured tracks arising from stars is shown reduced by a factor 10 in the same figures. The distributions in grain density for the tracks of particles of different types are given in fig. 8.

The mean free path for the shower particles may be calculated in the manner described in the Appendix. A value of $26\pm 7$ cm. was obtained for the mean thickness of emulsion traversed before a nuclear interaction occurred. This corresponds to a thickness of emulsion of mass $102 \pm 27$ gm. cm.$^{-2}$ and is also indistinguishable from that corresponding to the geometrical cross section.

Fig. 6.

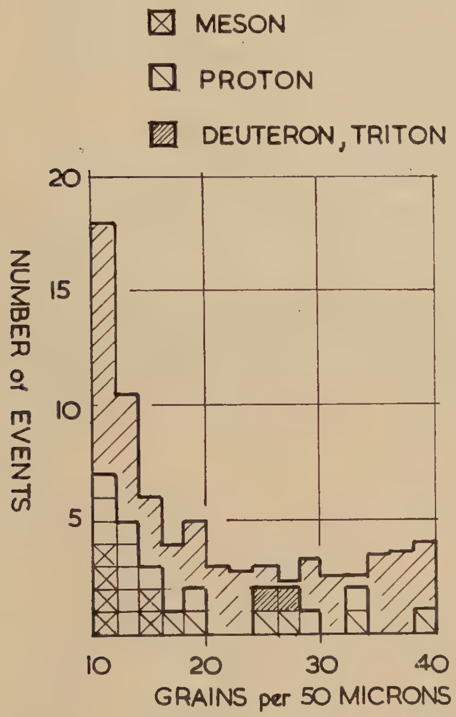

Fig. 7.

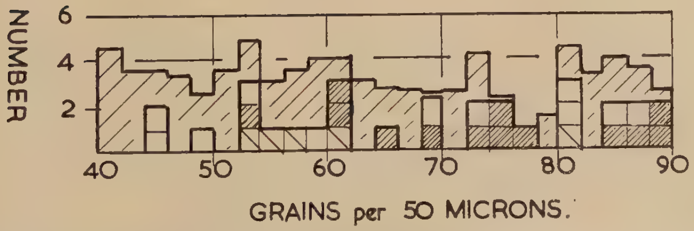

Distribution in grain-density of the tracks of particles causing secondary disintegrations. The corresponding distribution for all tracks ejected from stars is, reduced by a factor of 10, indicated by the shaded area.

We show, in a later section, that the cross section for protons with a kinetic energy between 100 and 600 MeV. is approximately geometrical. It is reasonable to assume that protons of higher energy, that is, those which are counted as shower particles, have a similar cross section. It therefore follows from the above result that the average cross section for $\pi$-mesons also corresponds to the geometrical value.

Fig. 8.

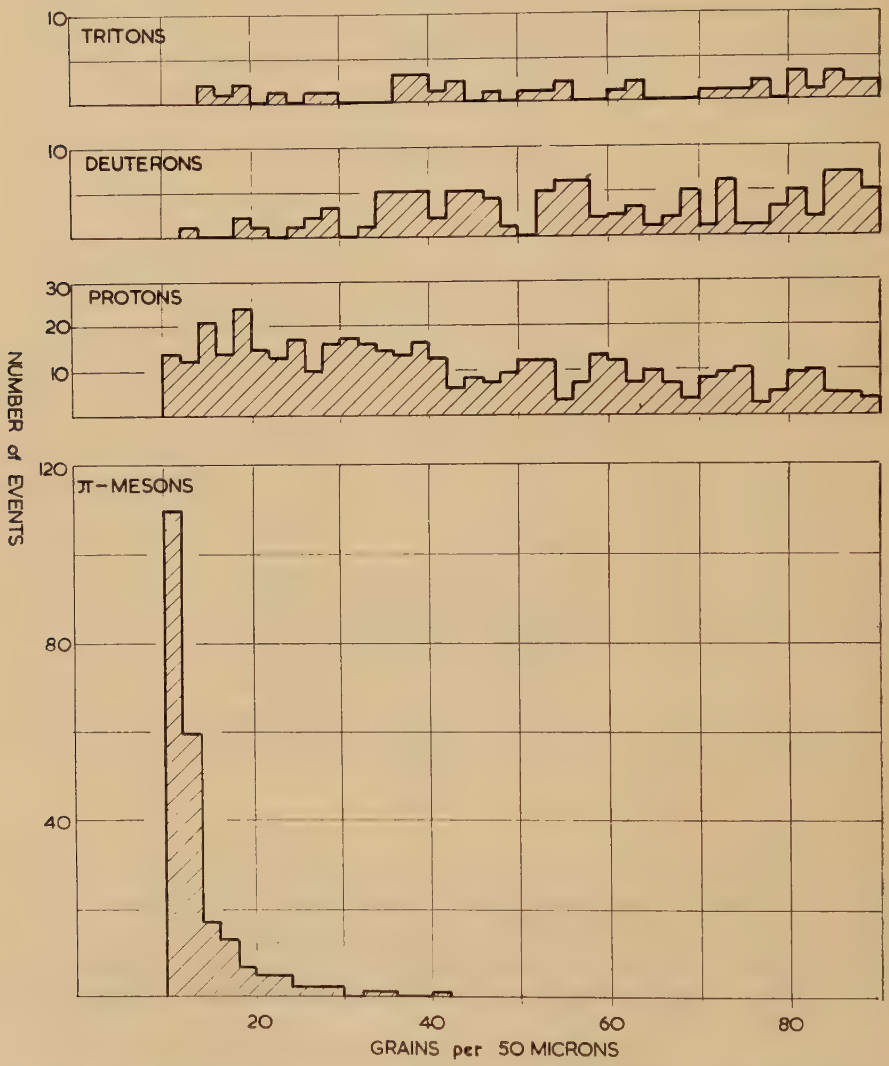

Distribution in grain-density of the tracks of various types of particles ejected from stars. To obtain the number of particles per star multiply by $\sim 1{\cdot}6 \, . \, 10^{-4}$.

### Comparison with Other Work.

The value given above for the collision mean free path of the shower particles, and therefore of $\pi$-mesons, is less than that obtained by other authors. A summary of their results is given in Table I. Since the interaction of shower particles has been studied in different materials, we include in the table the ratio of the observed mean free path to the geometrical value for each determination.

All the experiments with counters and cloud chambers, however, suffer from the defect that a shower particle cannot be followed and observed continuously. The work with cloud chambers has been carried out using lead plates of various thicknesses in the chambers. The majority of the values obtained for the collision mean free path have been corrected to allow for those nuclear interactions which are contained completely within the lead plates and thus escape observation.

TABLE I.

| Authors | Method | Result | Observed M.F.P. / Geom. value | Energy range (Mesons) |
|---|---|---|---|---|
| Piccioni | Counters at mountain altitudes | 1200 gm.cm.$^{-2}$ Fe | 14·0 | >400 MeV. |
| Fretter | Cloud chamber with Pb plates at mountain altitudes | 750 gm.cm.$^{-2}$ Pb<br>Uncorrected | 4·7 | >150 MeV.<br>$n_s \geqslant 2$ |
| Lovati, Mura, Salvini and Tagliaferri | Cloud chamber with Pb plates at mountain altitudes | 300±100 gm.cm.$^{-2}$ Pb<br>Corrected | 1·9 | >150 MeV.<br>$n_s \geqslant 2$ |
| Brown and McKay | Cloud chamber with Pb plates at mountain altitudes | 316±70 gm.cm.$^{-2}$ Pb<br>Corrected | 2·0 | >150 MeV. |
| Butler, Rosser and Barker | Cloud chamber with Pb plates at sea level | 400 gm.cm.$^{-2}$ Pb<br>Uncorrected<br>200 gm.cm.$^{-2}$ Pb<br>Corrected | 2·5<br>1·4 | Average energy of shower ~7000 MeV. |
| Harding and Perkins | Photographic plates exposed under ice | 120 gm.cm.$^{-2}$ Ice | 2·0 | >100 MeV. |
| Camerini, Fowler, Lock and Muirhead | Electron-sensitive plates exposed at high altitudes | 100 gm.cm.$^{-2}$ emulsion | 1·1 | >150 MeV. |

Table II. gives details of the type of star produced by the interaction of shower particles with the atoms of the emulsion. It can be seen that in general the stars produced are quite small, and this is confirmed by studies of the stars produced by identifiable fast π-mesons. We suggest therefore that the correction factors applied to the results of the cloud chamber work may in fact be too small. However, our results are not significantly different from the more recent results of Butler.

Table II.

| Primary star $N_H+N_S$ | Secondary star $N_H+N_S$ | Length of interconnecting track | Grain density in grains per 50 $\mu$ | $\bar{\alpha}^\circ$ per 100 $\mu$ | Nature of interacting particle |
|---|---|---|---|---|---|
| $10+1_p$ | $4+0_p$ | 3,800 $\mu$ | 14·9 | 0·191 | Meson |
| $17+5_p$ | $6+0_p$ | 700 $\mu$ | 13·3 | — | Unidentifiable |
| $14+1_p$ | $9+0_p$ | 4,600 $\mu$ | 10·1 | 0·025 | Meson |
| $16+1_p$ | $4+0_p$ | 750 $\mu$ | 14·5 | — | Unidentifiable |
| $8+2_n$ | $1+0_p$ | 3,000 $\mu$ | 15·0 | 0·21 | Meson |
| $3+4_p$ | $5+1_p$ | 10,600 $\mu$ | 12·2 | 0·0087 | Unidentifiable |
| *$18+5_n$ | $5+0_p$ | 10,600 $\mu$ | 10·4 | 0·049 | Meson |
| $6+5_n$ | $16+0_p$ | 5,800 $\mu$ | 12·4 | 0·0215 | Unidentifiable |
| $9+1_n$ | $5+0_p$ | 13,000 $\mu$ | 11·7 | 0·032 | Meson |
| $4+4_p$ | $4+0_p$ | 450 $\mu$ | 13·4 | — | Unidentifiable |
| † $0+7_p$ | $8+5_p$ | 1,200 $\mu$ | 11·7 | — | Unidentifiable |
| $6+6_p$ | $14+3_p$ | 1,500 $\mu$ | 12·1 | 0·017 | Unidentifiable |
| $18+15_p$ | $17+1_p$ | 1,700 $\mu$ | 11·4 | — | Unidentifiable |
| $9+1_p$ | $5+0_p$ | 1,750 $\mu$ | 10·0 | — | Unidentifiable |
| $8+1_p$ | $1+0_p$ | 11,200 $\mu$ | 10·1 | 0·068 | Meson |

* See Plate X. † See Plate XI.

## NUCLEAR INTERACTIONS OF PROTONS, DEUTERONS AND TRITONS.

The same method of analysis which has been applied above to shower particles may be used to obtain a value for the collision mean free path of protons, deuterons and tritons, within specific energy ranges. Fig. 9 shows the mass spectrum of particles with a grain density greater than 50 grains per 50$\mu$. It can be seen that it is possible to make a distinction between protons and deuterons, but not between deuterons and tritons.

The results obtained for the mean free path are summarized in Table III.* The figures given in column 6 of the table have been determined in the following way. We have determined the ratio of protons to deuterons plus tritons, in the different grain-density intervals, for the identified interconnecting tracks. The unidentified tracks have then been attributed to the different types of particle in accordance with this ratio. The fact that the mean free path for deuterons plus tritons is widely different from that obtained for protons, indicates that the distinction between protons and deuterons is in fact valid.

---

* The figures for shower particles are included for purposes of comparison.

Fig. 9.

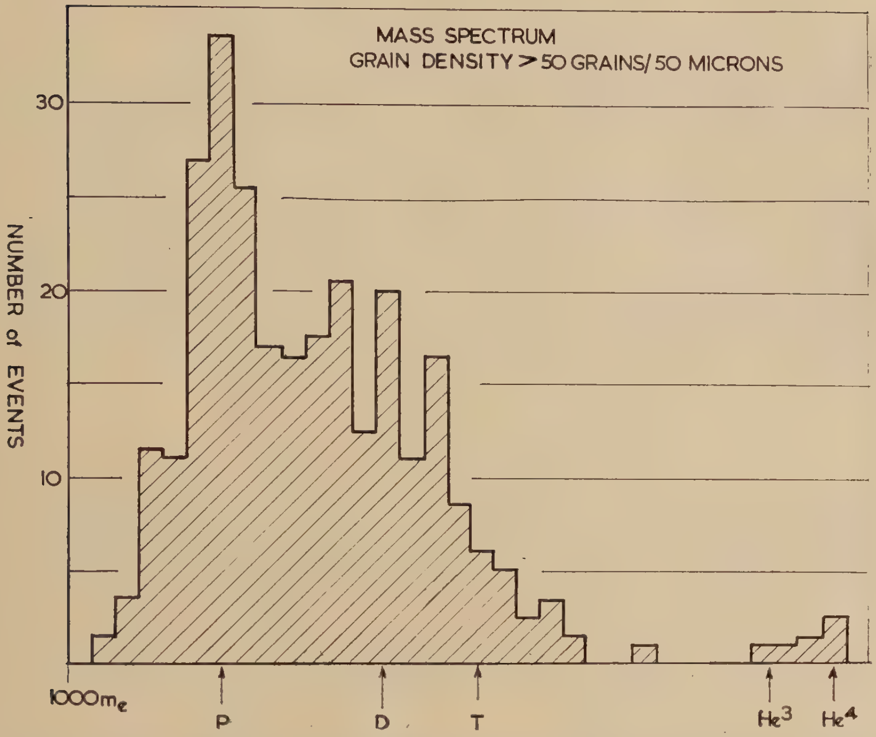

Distribution in mass of the particles ejected from stars with grain-density greater than 50.

Table III.

Mean free path of secondary particles for nuclear interaction.

| Type of particle | Energy range in MeV. | Grain density in grains per 50 $\mu$ | Effective path length considered | Number of interacting particles | Mean free path | Volume of emulsion examined |
|---|---|---|---|---|---|---|
| Identifiable Mesons | 150–1500 | 10–16 | 128 cm. | $6 \pm 2{\cdot}5$ | $21 \pm 9$ cm. | 48 c.cs. |
| Shower particles | 150–5000 (Mesons)<br>600–5000 (Protons) | 10–16 | 389 cm. | $15 \pm 4$ | $26 \pm 7$ cm. | 48 c.cs. |
| Protons | 40–100 | 40–66 | 174 cm. | $5{\cdot}5 \pm 2{\cdot}7$ | $32 \pm 16$ cm. | 87 c.cs. |
| Protons | 100–600 | 10–16 | 291 cm. | $9{\cdot}6 \pm 3{\cdot}3$ | $30 \pm 10$ cm. | 48 c.cs. |
| Deuterons plus tritons | 75–250 | 40–76 | 127 cm. | $10{\cdot}7 \pm 3{\cdot}9$ | $12 \pm 4{\cdot}5$ cm. | 87 c.cs. |

## APPENDIX.

The determination of the mean free path in the emulsion between nuclear collisions of particles of different types can be made in the following way. Observations on the directions of motion of the shower particles show that they are distributed nearly isotropically in the lower hemisphere (Davies *et al.* 1950). We assume, as a sufficient approximation, that the distribution is truly isotropic, and that the same is true for protons, deuterons and tritons. The tracks can be regarded as rectilinear and it is then easily shown that the number $N(L)dL$ of which the true length in the emulsion lies between L and $L+dL$ is given by

$$N(L)\,dL = N_0 \frac{D}{2L^2} dL \quad \text{for} \quad L>D, \quad . \quad . \quad . \quad . \quad . \quad (1)$$

where $N_0$ is the total number of particles ejected from stars, within the energy interval under consideration, and D is the thickness of the emulsion. The average length in the emulsion $\bar{L}$ of the tracks for which the values L lie between the limits $L_1$ and $L_2$ is given by :

$$\bar{L} = \frac{\log_e L_2/L_1}{1/L_1 - 1/L_2}$$

for $D=400\,\mu$, $L_1=400\,\mu$ and $L_2=20{,}000\,\mu$ this yields $\bar{L}=1596\,\mu$. We have imposed an upper limit of 20,000 μ for convenience of analysis.

In 48 c.c. of emulsion the number of tracks, of grain-density less than 16 grains per 50 μ, and with a length in the emulsion greater than 3000 μ, which have been measured, is 349. The calculated total number $N_0$ is then 5235 and the number greater than 400 μ in length is half this value, namely 2617·5.

From (1) the number greater than 20,000 μ in length is

$$\frac{N_0 D}{2 \times 20{,}000} = 52{\cdot}35.$$

Thus the number between 400 μ and 20,000 μ in length is 2565 and the average effective length is $1596-400=1196\,\mu$, since the first 400 μ are not included in the analysis. To this we must add the contribution up to 20,000 μ for those tracks which have a length greater than this value. This is given by $52{\cdot}35 \times (2{\cdot}00 - 0{\cdot}04)$ cm. Further, we have assumed an emulsion infinite in extent in the above calculations. Simple geometrical considerations show that, for the plates used, the total path length must therefore be reduced by 5 per cent. Thus the total effective path length $=\Sigma L = [(2565 \times 0{\cdot}1196) + (52{\cdot}35 \times 1{\cdot}96)]0{\cdot}95 = 389$ cm. The corresponding number of shower particles observed to make a nuclear disintegration is 15. Thus the collision mean free path of shower particles is $26 \pm 7$ cm.

## ACKNOWLEDGMENTS.

We wish to thank Professor C. F. Powell, F.R.S., for his continued interest and encouragement in the course of the work ; Dr. H. Heitler for the diagrams ; Mr. A. R. Gattiker and Miss P. Dyer for the photographs ; Miss M. Stott, Miss A. Cole and Mr. M. J. Harris for assistance with the measurements ; and the team of microscope observers of this laboratory.

## ERRATA.

In a previous paper (II.) an incorrect figure of 0·06 was given for the number of mesons produced per star. Our latest results indicate that this figure is 0·6±0·1. It was further stated that a large fraction of the mesons were emitted with kinetic energies of less than 60 MeV. Our latest data shows that this fraction is actually 0·1.

## REFERENCES.

ADELMAN and JONES, 1949, *Phys. Rev.*, **75,** 1468 (A).
BUTLER, ROSSER and BARKER, 1950, *Proc. Phys. Soc.*, **63,** 145 ; BUTLER 1950, Harwell Conference.
BROWN and MCKAY, 1950, *Phys. Rev.*, **77,** 342.
CAMERINI, COOR, DAVIES, FOWLER, LOCK, MUIRHEAD and TOBIN, 1949 *Phil. Mag.*, **40,** 1073 (II.).
CARLSON, HOOPER and KING, 1950, *Phil. Mag.* (in course of publication).
DAVIES, FRANZINETTI and PERKINS, 1950, *Phil. Mag.* (in course of publication).
FOWLER, 1950, *Phil. Mag.*, **41,** 169 (III.).
FRETTER, 1949, *Phys. Rev.*, **76,** 511.
GEORGE and JASON, 1949, *Cosmic Radiation* (Colston Papers), 31.
HARDING and PERKINS, 1949, *Nature*, **164,** 285.
LOVATI, MURA, SALVINI and TAGLIAFERRI, 1949, *Nature*, **163,** 1003 ; 1950, *Phys. Rev.*, **77,** 284.
PICCIONI, 1950, *Phys. Rev.*, **77,** 1, 6.
SANDS, 1950, *Phys. Rev.*, **77,** 180.

## EXPLANATION OF THE PLATES.

### PLATE IX.

A shower particle ejected from a $7+8_p$ star is observed to produce a second nuclear disintegration of the type $3+3_p$. The interconnecting track (5) has minimum grain-density and cannot be identified owing to its short length. Track (2) of the primary star is due to a meson ($\bar{\alpha}=0{\cdot}15°$ per 100 $\mu$; grain-density=12·9 grains per 50 $\mu$); the track ($a$) in the secondary star is also due to a meson. ($\bar{\alpha}=0{\cdot}03°/100\ \mu$; grain-density=12·1 grains/50 $\mu$).

Observer: Miss B. Hulbert.

### PLATE X.

A shower particle ejected from a $18+5_n$ star is observed to produce a second nuclear disintegration of the type $5+0_p$; the interconnecting track is 10,600 $\mu$ long and can be identified as due to a meson ($\bar{\alpha}=0{\cdot}049°$ per 100 $\mu$; grain-density=10·4 grains per 50 $\mu$).

Observer: Mrs. J. Cowie.

### PLATE XI.

A shower particle ejected from a shower of type $0+7_p$ originating at A produces a second shower of type $8+5_p$ at B. The event was observed in the corner of a plate, and the emulsion was too distorted to allow scattering measurements to be made.

Observer: Miss R. Mitchell.

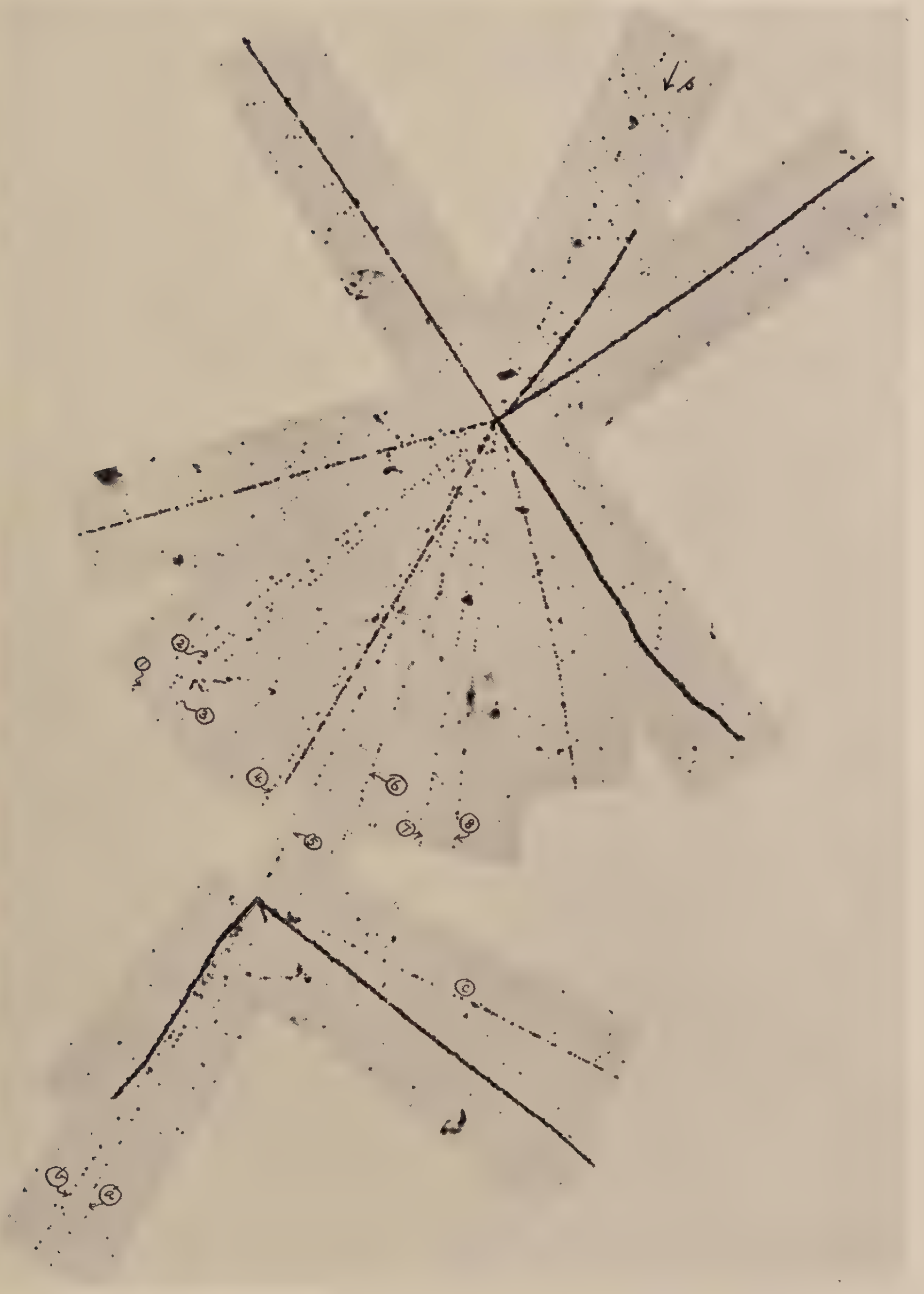

Observer: Miss B. Hulbert.

*To face page* 428

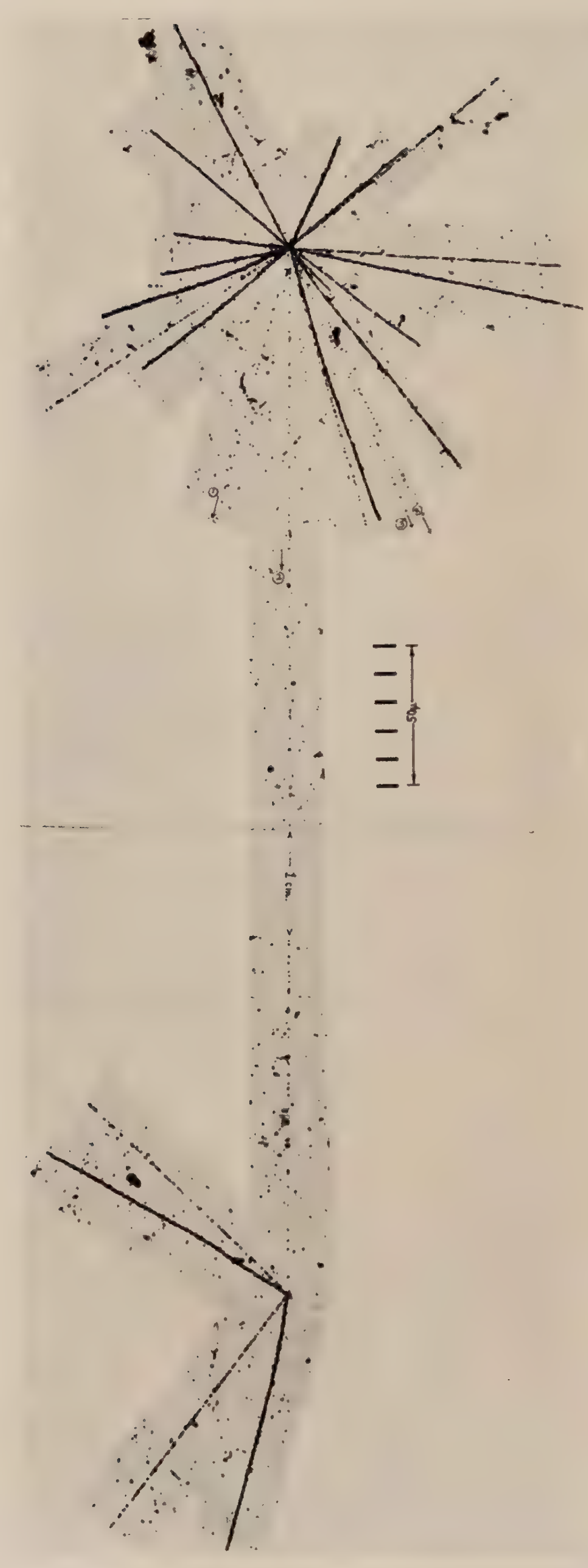

Observer:
Mrs. J. Cowie

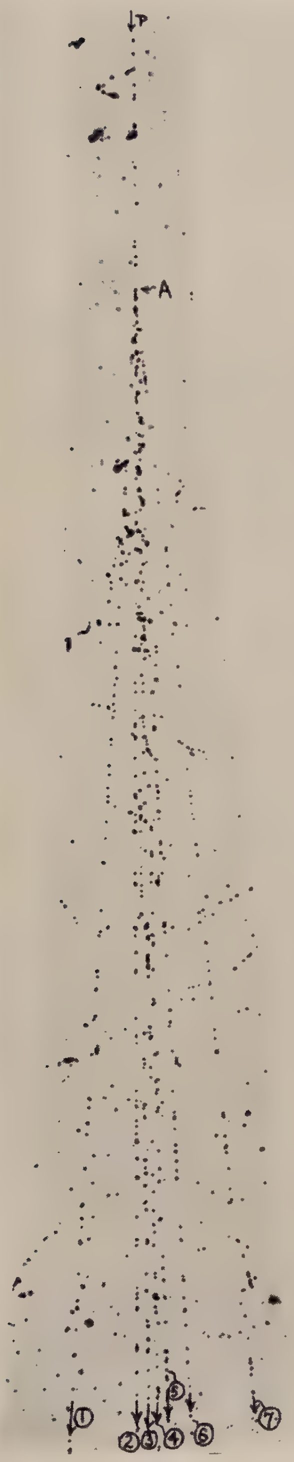

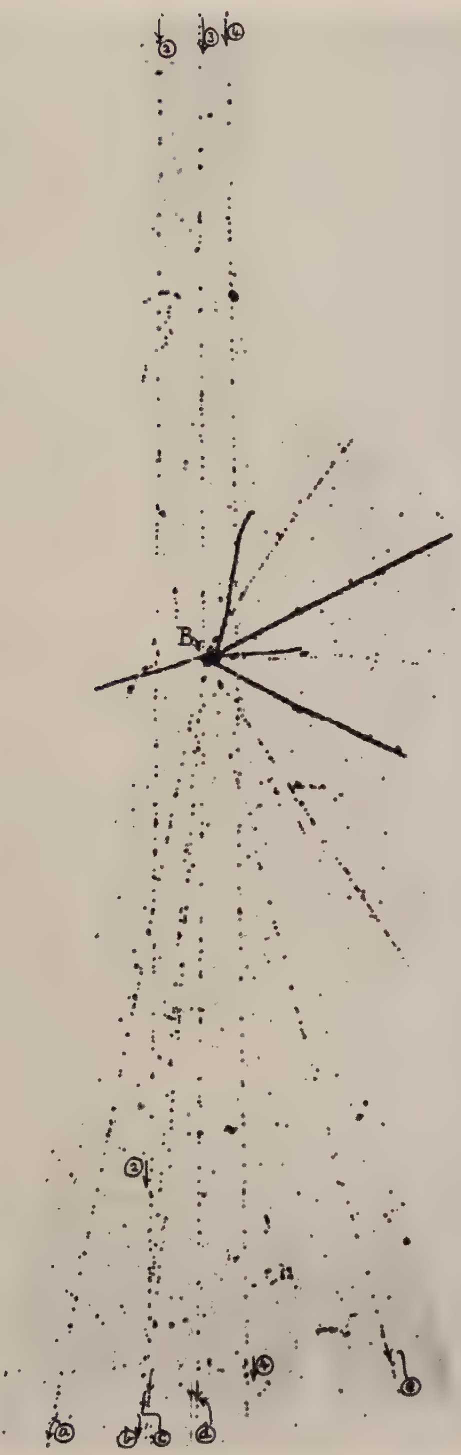

Observer: Miss R. Mitchell.

# XXXVIII. *Energy Spectrum of Fragments from the Spontaneous Fission of Natural Uranium.*

By W. J. WHITEHOUSE and W. GALBRAITH*.

[Received January 31, 1950.]

## ABSTRACT.

A direct comparison is made between the energy spectrum of fission fragments from the spontaneous fission and from the thermal neutron induced fission in the same foils of natural uranium. The results show that, within the limits of the experiment, the two distributions are not significantly different from one another. Calculations are made which indicate the magnitude of the distortion of the energy spectrum to be expected, and the theory is found to agree satisfactorily with experiment.

As a subsidiary result to the main experiment the rate for the spontaneous fission of natural uranium is found to be $24{\cdot}2 \pm 1{\cdot}5$ per hour per gram.

## § 1. INTRODUCTION.

THE possibility of the spontaneous fission of the heavy elements was forecast by Bohr and Wheeler (1939) who estimated a mean life for Uranium of the order of $10^{22}$ years. The phenomenon was first observed experimentally by Flerov and Petrzhak (1940, 1941). They used a multi-plate ionization chamber with active foils of $U_3O_8$ and obtained a value for the half-life (based on the assumption that all the spontaneous fissions were due to the $U^{238}$ isotope) of $10^{16}$–$10^{17}$ years. This corresponds to between 2·1 and 21 fissions per hour per gram of Uranium.

Shortly after this discovery, as a result of the war, the publication of experimental results on this subject was seriously interrupted, and a review of the literature is further complicated for the present authors by the difficulty in obtaining translations of Russian papers. There have, however, been a number of studies of the neutrons emitted in spontaneous fission (Maurer and Pose 1943, Pose 1943, Chatterjee 1945, Scharff-Goldhaber and Klaiber 1946). Pose obtained a nominal half-life for uranium, with respect to neutron emission, of $3{\cdot}1 \times 10^{15}$ years, corresponding to the emission of about 65 neutrons per hour per gram.

N. A. Perfilov (1947) measured the spontaneous fission rates of Uranium and Thorium using the method of track counting in photographic emulsions which had been exposed to the fragments at a depth of 50 metres below the surface of the earth. An oxidizing agent was employed to remove the tracks of alpha-particles from the emulsion. The value obtained for the half-life of Uranium with respect to spontaneous fission was $(1{\cdot}3 \pm 0{\cdot}2) \times 10^{16}$ years, (16±2 fissions per hour per gram). Perfilov also measured the ranges of the residual tracks, after oxidation, of the fragments from spontaneous fission, and from slow neutron-induced fission in Uranium, and in each case obtained a distribution with a single peak at about 1·0 cm. air equivalent. As he points out the fission tracks are much reduced in length by the oxidation. For this reason his results are not of any use in determining the amount of asymmetry in spontaneous fission.

---

* Communicated by the Authors.

A figure of 20 spontaneous fissions per hour per gram has been given for the spontaneous fission rate of $U^{238}$ (*The Science and Engineering of Nuclear Power* 1947), but without any account of the method of measurement. It is evident, therefore, that the rate for Uranium is nearer the upper of the original limits given by Flerov and Petrzak.

It was felt that a knowledge of the distribution in energy of the fragments from spontaneous fission of uranium, as distinct from the rate at which the phenomenon occurs, would be useful in the formulation of theories of fission and it was with this object in view that the present work was undertaken.

The experiment consists essentially of a direct comparison of the energy distributions of the fragments from the spontaneous fission of uranium and from the slow neutron induced fission of $U^{235}$, which forms a convenient standard of comparison, under identical conditions. The latter distribution has been investigated by a number of workers (Kanner and Barschall 1940 ; Flammersfeld, Jensen and Gentner 1943 ; Jentschke 1943) but the experiments of Fowler and Rosen (1947), Deutsch and Ramsey (1945) and Brunton and Hanna (1949, 1950) * are particularly suitable for comparison with the present results, since all of them used gridded ionization chambers similar to ours.†

Brunton and Hanna give in their paper a summary of the results obtained by themselves and five previous experimenters on the distribution for $U^{235}$. In each case two rather broad peaks are observed. That for the light group of fragments has a most probable energy of about 92 MeV., and a width at half maximum of 12–15 MeV., while that for the heavy group of fragments has a most probable value of about 60 MeV. and a width at half-maximum of 20–25 MeV.‡ The two peaks overlap slightly, and the height of the minimum between them is approximately 1/7 to 1/10 of the higher peak (see fig. 5, curve I.).

---

* The results of the latter paper were kindly communicated to us before publication.

† In the last two experiments the energies of the two fragments were measured simultaneously, but results were also obtained when only one fragment was observed, and it is these which are used for comparison.

‡ Brunton and Hanna point out that there is a correction to be applied in their experiment for energy loss in the foil and collimator.

The difficulties associated with a similar measurement of the energies of spontaneous fission fragments arise from the very slow rate of fission. We have used a large cylindrical ionization chamber with uranium foils of total area 675 square centimetres on the inner surface of the outer electrode. Even so, in order to obtain a counting rate of about 1·4 fissions per hour, we have had to use foils of approximately 0·1 mg./cm.$^2$ thickness. This distorts the observed energy distribution considerably, in a manner which will be discussed in § 3.1. Another difficulty associated with the slow counting rate is that of maintaining constant conditions in the ionization chamber itself, and in the electronic amplifiers and recording apparatus. We have overcome the difficulty associated with the chamber by using pure argon as the gas filling instead of the more usual argon–carbon dioxide mixture, and purifying it continuously, throughout the course of the experiment, by convective flow over hot calcium turnings. Our purifier worked on the same principle as that mentioned by Rossi and Staub (1949) but was simpler in design. This practice results in a longer collection time for the electrons, but does not appear to have led to any noticeable errors. The electronic apparatus was calibrated daily with a signal generator and we have good reason to believe that the error caused by random variations in the sensitivity of the chamber, amplifier and recording apparatus was not greater than ±3 per cent during the experiment. Other possible sources of error will be discussed in § 3.

In order to compare the two energy distributions under identical conditions, we simply removed part of the cadmiun shielding at different times (see § 2.2) and placed a neutron source near the chamber to induce fissions in the $U^{235}$ present in the foils. In this way we measured approximately 1000 neutron induced fissions in three groups over a period of a week, the number of spontaneous fissions recorded during a week being about 200. This procedure was repeated during subsequent weeks until in the end some 5000 neutron induced and 1000 spontaneous fissions were obtained.

## § 2. APPARATUS

### 2.1. *The Ionization Chamber.*

A cylindrical form for the ionization chamber was chosen, as it eased a number of mechanical problems, particularly the construction of the grid (see fig. 1). The outer electrode is 25 cm. in diameter and 20 cm. high and is supported on porcelain insulators. The uranium foils are carried on the inner surface of this electrode and are approximately 10 cm. across, ensuring that no ionization track left the active volume of the chamber. The inner electrode consists of a cylinder 20 cm. high and 11·5 cm. diameter, and is supported on insulators consisting of perspex rings. The grid which has diameter of 15 cm. consists of 64 beryllium copper wires (24 S.W.G.) of length 25 cm. supported on half-rings of brass attached to the same insulator system as the inner electrode. It is easily demountable and quite robust. There are two guard rings to prevent transient discharges along the insulators between the grid and the inner electrode. The system of electrical connections is shown in fig. 1.

The distance between the outer electrode and the grid is about 5 cm., which is considerably longer than the track length in argon at one atmosphere of either the fission fragments or the alpha particles from uranium. The distance from the grid to the inner electrode is about 1·7 cm.

In a chamber designed to measure spontaneous fission pulses the background either from gamma rays or alpha contamination is unimportant, and no attempt has been made to minimize it.

The theory of a planar grid chamber has been given by Bunemann, Cranshaw and Harvey (1949). Their formulæ have been used to calculate the dimensions of our grid, using the following transformations between electrically equivalent cylindrical and plane chambers.

Fig. 1.

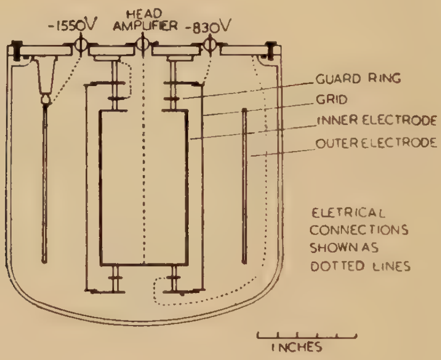

Diagram of ionization chamber.

If $R_P$ is the radius of the inner electrode,
$R_G$ is the radius of the grid,
$R_A$ is the radius of the outer electrode,

then the dimensions of the electrically equivalent plane chamber are given by (see fig. 2):

$p^1 = R_G \log_e R_G/R_P$ where $p^1$ is the distance from the anode to the central plane of the grid.

$a^1 = R_G \log_e R_A/R_G$ where $a^1$ is the distance from the central plane of grid to the outer electrode.

When this system of transformation is used the physical dimensions of the grid are the same in both chambers.

One important quantity to be calculated is the charge induced on the collecting electrode by the positive ions which, after each fission, are left in the neighbourhood of the outer electrode. The dimensions of the grid were so chosen that this was, theoretically, less than 2 per cent of the charge carried to the collecting electrode by the electrons. This rather low efficiency of the grid is tolerable because the accuracy of the measurements of the energies required in this experiment is much lower than that usually required in the measurement of alpha particle energies.

The other important condition to be satisfied is that none of the electrons should be collected on the grid wires. With our dimensions this requires that the voltages on the outer electrode ($V_A$), grid ($V_G$) and collector ($V_P$) should obey the relation

$$\frac{V_P - V_G}{V_G - V_A} \geqslant 0{\cdot}88. \qquad \dots\dots\dots \quad (1)$$

The chamber was filled with argon (99·8 per cent pure), to a pressure of about 1·25 atmospheres, and this was continuously purified by convective flow over calcium turnings at about 400° C. The volume of the chamber is approximately 30 litres, and the rate of flow of gas was about 40 c.c. per second, so that the chamber gas was frequently renewed. After the purifier had been switched on, the conditions in the chamber, as judged from the energy and resolution of the uranium alpha-peaks, improved for about fifteen hours, and then remained constant, within our limits of accuracy, for the three months during which preliminary work and the actual counting were carried out*.

Fig. 2.

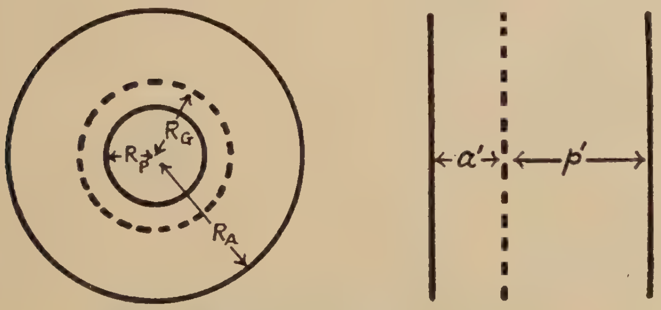

Electrically equivalent cylindrical and plane ionization chambers.

The voltages for the outer electrode and the grid were supplied by dry batteries, through simple resistance-capacity filters.

---

* We were unfortunate enough to have three failures in the power supply, early in the experiment, which resulted in some loss in gas pressure, due to the contraction of the seals of the purifier on cooling down. Apart from this there is no reason to suppose that the chamber and purifier could not have been operated continuously for a year.

### 2.2. *The Neutron Shield for the Chamber.*

The chamber was surrounded by a cadmium shield (0·5 mm. thickness) around which was a paraffin shield of approximately 25 cm. thickness. A hole was cut in one of the paraffin blocks in which a neutron source could be placed. By removing a section of the cadmium shield and inserting the neutron source a satisfactory rate of neutron induced fissions could be obtained.

### 2.3. *The Uranium Foils.*

Eight uranium foils each 9·2 cm. square were prepared by evaporation under vacuum on to platinum. No small scale irregularities were seen when the foils were viewed under a low power microscope. The uniformity over any one foil was checked by counting the alpha-particles from sections of the foils and was constant to within ±15 per cent. The total weight of the deposit, which is presumably oxidized, and of which the chemical composition is unknown, is 71 mg., which corresponds to an average surface density of 0·1 mg./cm². The separate foils were found, by weighing, to have average surface density per foil between 0·09 and 0·12 mg./cm². The total weight of uranium present, estimated by alpha-counting, is 57±3 mg. indicating either that the films are completely oxidized or that there is some impurity present. It is fortunately not important in this experiment to have a very exact knowledge of the weight of uranium in the foils.

Fig. 3.

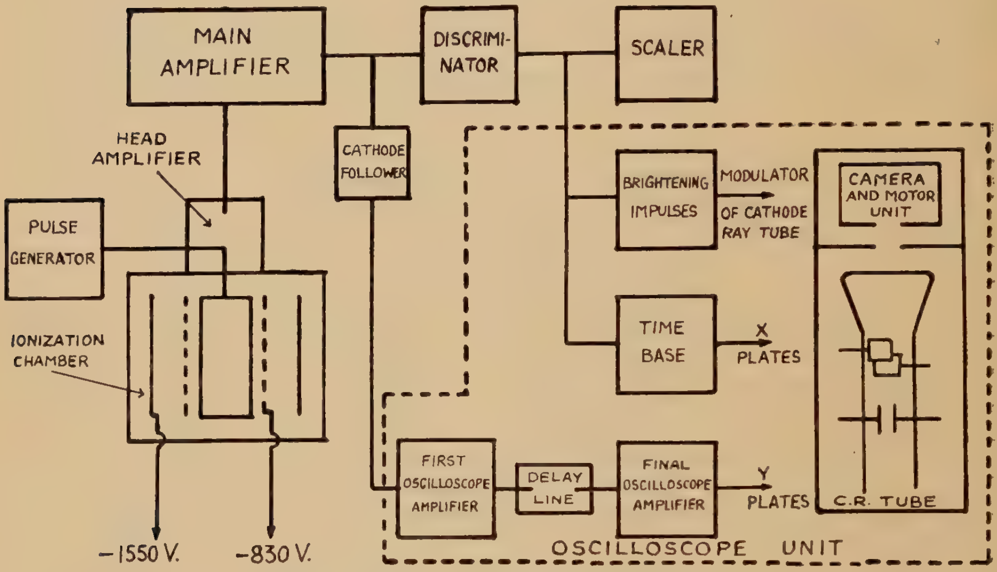

Block diagram of electronic apparatus.

### 2.4. *Amplifiers, Recorder, and other Electronic Apparatus.*

A block diagram of the apparatus is given in fig. 3. The head amplifier consists of one so-called " ring of three " circuit and the main amplifier of two such circuits. The circuits contained no electrolytic condensers, as these had been found to generate spurious pulses, and the grid bias voltages for the valves were derived from a resistance chain in the negative H.T. line. This modification increased the hum level of the amplifier, but not sufficiently to prevent an accurate determination of the position of the $U^{234}$ alpha-peak. At the gain setting used for measuring the fission pulses the hum is negligible. The band width of the amplifier is controlled by " differentiating " and " integrating " condenser–resistance networks with time constants which can be varied in steps from 0·08 $\mu$S to 8 $\mu$S. The gain is controlled by attenuators made up from high stability components.

The discriminator was a standard instrument (A.E.R.E. Type 1028). It was set at a level corresponding to an energy of 20 MeV.

The fission pulses were recorded by photographing an oscilloscope trace on 16 mm. film, and the times at which they occurred recorded by photographing a clock. All resistors in the oscilloscope amplifiers were high stability types. The fission pulses were passed through a 6$\mu$ second delay line in order to allow the time base and brightening circuits of the oscilloscope to operate. After each pulse the film was automatically moved on one frame. The interval between successive spontaneous fission pulses was sometimes several hours, in which case some fogging of the film occurred due mainly to the residual light from the filament of the cathode ray tube. This, however, was not serious.

The traces of the fission pulses were projected on to a screen for measurement.

The pulse generator, which was not a precision instrument, was coupled to the head amplifier through a small capacitor of about 1 $\mu\mu$F. It was used for intercalibrations between the discriminator setting and the cathode ray tube deflections, and also for checks on the linearity of the main linear amplifiers, and the amplifiers associated with the cathode ray tube.

It was essential to have a mains supply free from fluctuations which would have generated spurious pulses in the amplifiers. All the apparatus, except the heater for the gas purifier, was therefore supplied from a separate motor driven single phase alternator.

## § 3. ERRORS.

It is instructive to consider what limitations are imposed on the accuracy of the results by the conditions of the experiment.

### 3.1. *Energy loss of Fragments—Distortion of Energy Distribution Curve.*

#### (a) *Foil thickness.*

The distribution of the paths which the fission fragments traverse inside the foil can be shown to have the form given in fig. 4 provided that the thickness of the foil is small compared with the maximum range of the fragment in the foil. If T is the path length in the foil and $X_0$ is the thickness of the foil, and $t=T/X_0$, the distribution is a straight horizontal line with $N(t)=\frac{1}{2}$ for values of $t \leqslant 1$, and falls off for $t>1$ according to the formula

$$N(t)\,dt=\frac{1}{2}\frac{dt}{t^2}. \qquad (2)$$

The numerical constant $\frac{1}{2}$ is introduced to make the integral of $N(t)$ from $t=0$ to $t=\infty$ equal to unity, which corresponds with the fact that for every fission one fragment will emerge from the upper surface of the foil.

Fig. 4.

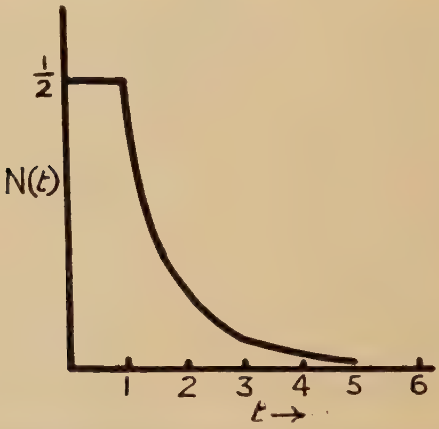

Distribution of particles originating in a foil as a function of their length of path in the foil.

The energy lost by the fragment near the beginning of its path can be calculated from the approximate formula of Bohr (1941, 1948) according to which the velocity of the fragment is

$$v=v_0(1-T/R_F), \qquad (3)$$

where $v_0$ is its initial velocity, T is the distance it has travelled, and $R_F$ is an extrapolated fission range which is nearly the same as the actual range of the fragment. We have therefore

$$\epsilon=E_0\left(\frac{2T}{R_F}-\frac{T^2}{R_F{}^2}\right). \qquad (4)$$

Where $\epsilon$ is the energy lost by the fragment in traversing a path T; $E_0$ is the initial energy of the fragment.

The value of $R_F$ can be calculated from the range of an alpha-particle with the same initial velocity as the fragment (Bohr 1941).

We have calculated values of $R_F$ in $U_3O_8$ for the light and heavy fission fragments using a relative stopping power of 4 mg./cm.$^2$ $U_3O_8$ equivalent to 1 cm. of air (Bøggild *et al.* 1947) and have found the initial energy losses ($d\epsilon/dT$ for $T=0$) of the two fragments, in terms of the path expressed in mg./cm.$^2$. For the light fragment this is 19 MeV. per unit of path and for the heavy it is 17 MeV. This agrees reasonably well with the measurements of West (1948) who found that the fragments lose 6·5 MeV. per mm. of nitrogen, corresponding to 16 MeV./mg./cm.$^2$ of $U_3O_8$.

In order to estimate, roughly, the distortion to be expected in our curve, we have taken the following round figures (*a*) an initial energy loss $d\epsilon/dT$ of 20 MeV. for each mg./cm$^2$ of film for all the fragments whether heavy or light, (*b*) a film of thickness 0·1 mg./cm$^2$. Thus all the fragments are assumed to lose 2 MeV. if they traverse the whole depth of the film in a direction normal to its surface.

Fig. 5.

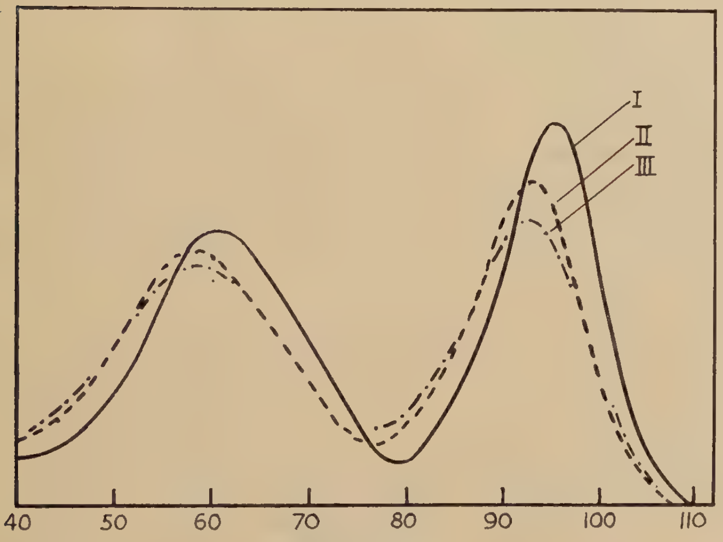

Corrections to be applied to the energy distribution of fission fragments.
Curve I. Energy distribution of fission fragments from thermal neutron induced fission of $U^{235}$ (after Brunton and Hanna).
Curve II. Curve after correction is made for energy loss in foil.
Curve III. Curve after correction both for energy loss and gain variation.

By combining equations (2), (3) and (4) and taking terms as far as the fourth power it is possible to show that the number of particles losing an energy $\eta$ is given by

$$\left.\begin{array}{l} n(\eta)=\tfrac{1}{2} \text{ for } \eta\leqslant 1, \\ n(\eta)\,d\eta=\tfrac{1}{2}\,d\eta/\eta^2\{1-1/16(\epsilon_0/E_0)^2\eta^2\} \text{ for } \eta>1 \end{array}\right\} \quad . \quad . \quad . \quad (5)$$

Where $\eta=\epsilon/\epsilon_0$ and $\epsilon_0$ ($=2$ MeV.) is the energy lost in traversing the film in a direction normal to its surface. Thus to a close degree of approximation the expressions for the distribution according to path lengths and to energy loss are identical in form.

When this correction is applied, curve II. of fig. 5 is obtained.

It has become a common practice in measurements of this type to collimate the particles with a perforated metal sheet, thus eliminating those which lose a large amount of energy in passing obliquely through the film. The disadvantage of this practice in an experiment such as this, where the counting rate is low, is that the collimator stops a large proportion of the particles, and necessitates the use of a much thicker source. Calculations have been carried out (Howlett and Whitehouse 1950) which show that in this experiment the use of a collimator would have increased the energy lost by the particles in the film, and a plain foil has therefore been used.

(b) *Energy lost by Particles striking the Electrode.*

In a cylindrical chamber such as ours some of the fragments lose energy at the ends of their paths by striking the curved surface of the outer electrode. This affects less than 5 per cent of the fragments, and we have estimated that the average loss in energy from this cause is less than $\frac{1}{4}$ MeV., whereas the average energy loss in the film itself is about 4 MeV. We therefore have not applied any correction for this effect.

(c) *Effect of Variations in the gain of the Amplifier and Recording Apparatus.*

Curve III. of fig. 5 shows the effect which might be expected from a random variation of the sensitivity of the apparatus. In order to simplify the computation we have assumed that the measurements for all the fragments regardless of their initial energy are subject to a random error with a standard deviation of $\pm 3$ MeV.

This figure has been chosen as the most probable value of the spread in our results as a result of the combination of the drift of the apparatus over a period of time (§ 3.2) and of the differential sensitivity to pulses of different rise time (§ 3.3).

Owing to the rough nature of the corrections described above we do not invite detailed comparison between our results and the theoretically distorted curves of fig. 5. In fig. 6, however, we plot our experimental results for $U^{235}$ along with curve III. of fig. 5. Our approximate energy calibration shows our results for the energies of the two peaks to be within experimental error of those given in the introduction, but in drawing fig. 6, we have adjusted the curves so that the total number of fissions is the same in each, and the positions of the minima between the peaks coincide.

It will be seen that the two main sources of error in the experiment do provide an adequate explanation for the difference between the shape of our curve and that of Brunton and Hanna.

### 3.2. *The Drift in Gain.*

A daily check was made of the linearity of the amplifiers and their overall gain, by means of the signal generator and the zero error of the discriminator was determined at the same time. It was decided to use the discriminator voltage as a standard and to refer all the pulse heights to it.

We have two independent checks of the constancy of the apparatus :

(*a*) the height of the $U^{234}$ alpha-peak. This was measured every second day using, of course, a different gain setting on the amplifier, and found to be nearly constant on the discriminator scale. The greatest deviation from the mean value, over three months was $\pm 2{\cdot}2$ per cent.

Fig. 6.

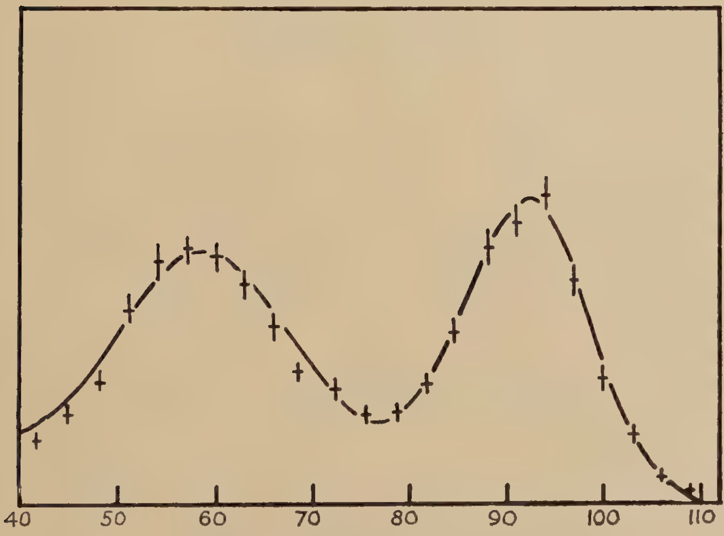

Approximate energy scale (MeV.).

Comparison of present results for fission fragments from thermal neutron induced fission of $U^{235}$ with corrected curve.

(*b*) It is also possible to maintain a general check on the steadiness of the apparatus from the average of the heights of the fission pulses.

If we regard the high energy peak alone as a statistical population, and apply simple sampling theory (neglecting the difference between the shape of the observed peak and the normal error curve) we can assume that the mean energy of $n$ fissions will have had a standard deviation of approximately $\sigma/\sqrt{(n)}$, where $\sigma$ is the standard deviation of the whole population. The value of $\sigma$ is of the order of 10–15 MeV ; consequently the mean energy of any hundred consecutive fission pulses in the high energy group should have a standard deviation of about 1 to $1{\cdot}5$ MeV. If the error due to slow drift in the apparatus is much greater than this, it will show up in the mean energies of groups of fragments. Exactly similar considerations apply to the mean energies of the fissions in the low energy group.

We have calculated the mean energies of the high and low energy fragments in groups of five-hundred for neutron induced fissions and of two hundred for spontaneous fissions. We find in both cases that the standard deviation of the mean of the groups is about 2 MeV., indicating that the error due to random slow drift could not have been larger than this.

### 3.3. *The Electron Collection time and the Resolving time of the Amplifier.*

Owing to the comparatively slow rate of electron drift in pure argon, the large dimensions of the chamber, and the moderate collecting voltages applied, it was considered necessary to check that the resolving time of the amplifier (8 $\mu$S) was sufficient to allow complete collection of the electron pulses. This was done by experiments on the $U^{234}$ alpha-peaks and on the energy distribution of fission fragments from neutron induced fission of $U^{235}$.

(*a*) It was found that it was necessary to reduce the time-constant of the amplifier from eight to five microseconds before there was any observable diminution of the $\alpha$-pulse height.

(*b*) The outer electrode potential could be reduced from $-1550$ volts to $-830$ volts, and the grid voltage from $-830$ volts to $-450$ volts, without any diminution in the height of the $\alpha$-pulse.

(*c*) With the reduced electrode voltages given above, the energy distribution of some 240 neutron induced fission pulses from $U^{235}$ showed no significant difference from that obtained with the chosen operation voltages. We concluded then that the resolving time of the amplifier was adequate.

Another small effect of the electron collection time, quite unconnected with the resolving time of the main amplifier, has been noticed.

By direct calibration with voltage pulses fed into the head amplifier we have found that the amplifier pulse height measured at the discriminator is proportional to the original voltage, and is not noticeably affected by the time of rise of the pulse within quite wide limits.

The heights of the traces on the oscilloscope do, however, decrease by about 3 per cent when the rise time is reduced from 3 $\mu$s. to a fraction of a microsecond, an effect which we attribute to the delay line. Since the collection time of electrons in our chamber depends upon the angle of the track, a slight spread in the measured energy values of fission fragments will be introduced, in addition to that caused by random drift in the gain of the apparatus.

### 3.4. *The background Rate of Real or Spurious Pulses.*

The neutron induced fission rate, with the Ra-$\alpha$-Be source in position, was about one hundred per hour, while the spontaneous fission rate was about 1·4 per hour. It follows that the background of spontaneous fissions during a period of measurement on neutron-induced fissions was too small to affect the observed distribution of pulse sizes.

By placing the neutron source outside the paraffin and comparing the count rates with and without the cadmium we were able to show that the percentage of spontaneous fissions which could be ascribed to neutrons penetrating the shield is probably negligible. Even if an unfavourable interpretation is placed upon the statistics of the results, the percentage would not be greater than of the order of 2 per cent.

Wheeler (1949) has pointed out that the capture of a negative $\mu$ meson by a uranium atom will in almost every case lead to the fission of the uranium nucleus, but that the number of fissions so induced will be negligible in comparison with the spontaneous rate.

The background of spurious counts was very low in comparison to the observed spontaneous fission rate. When the foils were removed from the chamber only two counts were recorded in 160 hours, and both these were too small to have been confused with fission pulses.

### 3.5. *Coincidences of Alpha-particles and Fission Pulses.*

Examination of the photographs of the trace of the cathode ray tube reveals the alpha-particles as small pulses along the time base. It is possible to make a fairly close estimate of how close the alpha-particle and the main fission pulse would have to be before it became impossible to distinguish them from each other. In this way we estimate that less than 1 per cent of the fission pulses are in effective coincidence with alpha-particles.

The chance of sufficient alpha-particles coinciding with each other to give an alpha build-up pulse which might be mistaken for a fission is negligible.

## § 4. RESULTS.

The results of the experiment are presented in fig. 7. The full line is the energy distribution curve for neutron-induced fissions, which, as has been explained, is consistent with the results of other observers, providing that allowance is made for absorption in the foil, and for some random variation in the recording apparatus. About 4700 neutron-induced fissions were used in the preparation of this curve, and the standard errors of the points are shown.

The energy distribution of 960 spontaneous fissions is shown by the histogram. The errors indicated are the square roots of the numbers of events in each cell of the histogram. The curve and the histogram have been adjusted to have the same area.

The energy scale on the diagram, derived from the height of the $U^{234}$ alpha peak, is approximate and, in view of the errors involved in its derivation, we would not expect it to be accurate to better than 5 per cent. However, it suffices to show that our observed values for the most probable energies of the fission fragments are not inconsistent with those of other workers. An accurate absolute energy determination was not attempted, since the present experiment consists of a direct comparison between the distributions for the two types of fission.

There is no significant difference between the observed distributions for neutron-induced fissions in $U^{235}$ and for spontaneous fissions, according to the standard $\chi^2$ test for goodness of fit (0·05 criterion)*.

It is too much to hope, with the small number of spontaneous fissions observed, that detailed differences in the shape of the two distribution curves would be revealed, but it might be thought possible to observe some difference in the positions of the peaks representing the most probable energies for the fragments. We have carried out a simple test of this point by moving a tracing of the continuous curve along the energy axis, over the histogram, and carrying out $\chi^2$ tests for different positions. We find that we get the best fit if we assume that the whole distribution for the spontaneous fissions is about 1·5 MeV. below that for the neutron-induced fissions. The $\chi^2$ test shows, however, that the two curves are consistent for any downward displacement of the spontaneous fission distribution between 0 and 3 MeV.

Fig. 7.

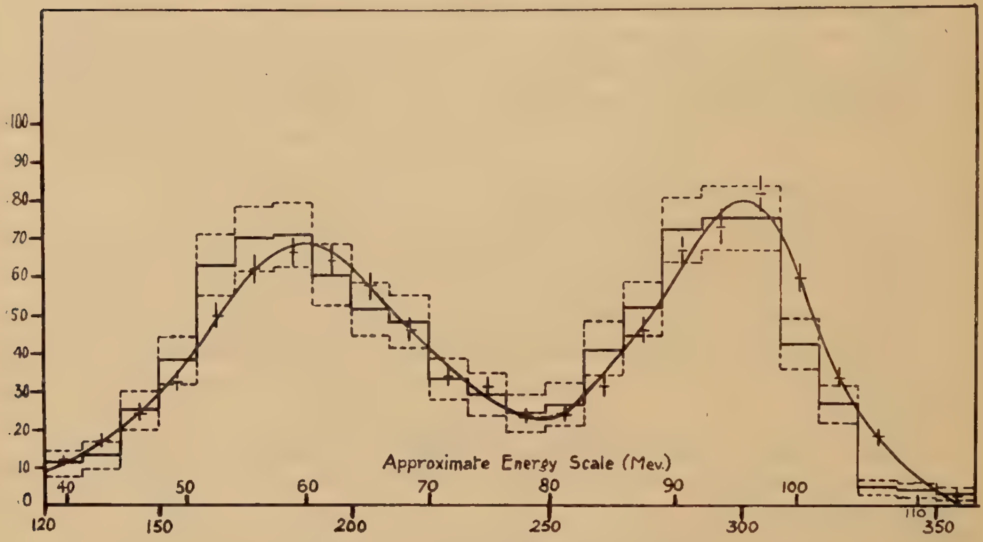

Arbitrary scale proportional to energy.

Comparison of thermal neutron induced fission pulses of $U^{235}$, and spontaneous fission pulses of natural uranium.

Full line curve—$U^{235}$ fission with thermal neutrons.

Histogram—spontaneous fission.

---

* This means that the probability of the difference between the two distributions being due to chance is greater than 0·05.

The present experiment is not particularly well adapted to an accurate measurement of the spontaneous fission rate but a combination of the observed frequency of the spontaneous fissions ($1{\cdot}38 \pm 0{\cdot}04$ per hour) and the mass of uranium in the foils ($57 \pm 3$ mg.) gives a figure of $24{\cdot}2 \pm 1{\cdot}5$ per gram of natural uranium per hour.

## ACKNOWLEDGMENTS.

This work is published by permission of the Director of the Atomic Energy Research Establishment. The authors wish to express their thanks to Messrs. Wells and Godfrey who designed and constructed the oscilloscope unit, to Messrs. Kandiah and Gillespie for the design and modification of the head and main amplifier circuits, to Mr. Robins and his group for the preparation of the uranium foils, and to Dr. E. Bretscher, Head of the Nuclear Physics Division at A.E.R.E.

## REFERENCES.

BØGGILD *et al.*, 1947, *Phys. Rev.*, **71**, 281.
BOHR, N., 1941, *Phys. Rev.*, **59**, 270; 1948, *Det. Kgl. Danske Vidensk Selsk., Mat. Fys. Medd*, 18, No. 8.
BOHR and WHEELER, 1939, *Phys. Rev.*, **56**, 426.
BRUNTON and HANNA, 1949, *Phys. Rev.*, **75**, 990; *Can. Journ. Res.* A. In press.
BUNEMANN, CRANSHAW and HARVEY, 1949, *Can. Journ. Res.*, A **27**, 191.
CHATTERJEE, 1945, *Indian Journal of Physics*, **19**, 211.
DEUTSCH and RAMSEY, 1945, LADC. 257.
FLAMMERSFELD, JENSEN and GENTNER, 1943, *Zeit f. Physik*, **120**, 450.
FLEROV and PETRZAK, 1940, *J. Phys. U.S.S.R.*, No. 4–5, **3**, 275; 1941, *Ibid.*, No. 3, **4**, 283.
FOWLER and ROSEN, 1947, *Phys. Rev.*, **72**, 926.
HOWLETT and WHITEHOUSE, 1950, A.E.R.E. Report N/R. 473.
JENTSCHKE, 1943, *Zeit. f. Physik*, **120**, 165.
KANNER and BARSCHALL, 1940, *Phys. Rev.*, **57**, 372.
MAURER and POSE, 1943, *Zeit. f. Physik*, **121**, 285.
PERFILOV, 1947, *J. Expt. Theor. Phys. U.S.S.R.*, **17**, 476; *J. Phys. U.S.S.R.*, No. 3, **11**.
POSE, 1943, *Zeit. f. Physik*, **121**, 293.
ROSSI and STAUB, 1949, *Ionization Chambers and Counters*, McGraw-Hill, p. 109.
SCHARFF-GOLDHABER and KLAIBER, 1946, *Phys. Rev.*, **70**, 229.
*Science and Engineering of Nuclear Power*, 1947, Addison Wesley Press, pp. 80 and 358.
WHEELER, 1949, *Rev. Mod. Phys.*, **21**, 133.
WEST, D., 1948, *Can. J. Res.* A, **26**, 115.

# XXXIX. *Scattering of* 90 *MeV. Neutrons by Alpha-Particles.*

By J. HEIDMANN,
Ecole Polytechnique, Paris*.

[Received January 2, 1950].

## §1. INTRODUCTION.

THE purpose of this note is to report calculations of the scattering of 90 MeV. neutrons by alpha-particles, which could be useful for the investigation of collisions between nucleons and nuclei built up of $\alpha$-particles. Using the Born approximation and the nucleon–nucleon interaction introduced by R. Serber, we have calculated :

(i.) The inelastic scattering, especially for the collision in which a deuteron is produced by stripping.
(ii.) The elastic scattering, estimating the errors due to the Born approximation.

No measurements being available on scattering of 90 MeV. neutrons by helium, we attempt to deduce values for comparison with our calculations from measurements on neutron-carbon and neutron-oxygen collisions : this is done using the alpha-particle model for these nuclei.

## §2. CALCULATIONS AND RESULTS.

As it is likely that all the nuclei produced by the collisions are formed in their ground state, the following cases arise :

(i.) Elastic scattering.
(ii.) Stripping scattering in which one neutron or one proton is stripped off.
(iii.) Formation of a deuteron plus a triton
(iv.) Scattering in which the alpha-particle is broken into two deuterons.
(v.) Scattering in which in addition one of these deuterons is disintegrated.
(vi.) Complete disintegration.

As cases (iv.)–(vi.) require more energy to be given up by the incident particle, they will be less probable ; we shall thus deal only with the three first cases. Let us begin with case (iii.)

---

* Communicated by the Author.

### (A) *Production of Deuterons in Neutron-α Particle Collisions.*

### (a). *Calculation.*

Let 1, 2 refer to the protons, 3 and 4 to the neutrons of the alpha-particle, 5 to the incoming neutron, and suppose that in the final state the deuteron (1, 5) and the triton (2, 3, 4) are formed. The Hamiltonian can be written, in the centre of mass system,

$$-\frac{\hbar^2}{2M}\frac{5}{6}\Delta_R+H_T+H_D+H'_{TD}=E, \quad . \quad . \quad . \quad . \quad (1)$$

where **R** is the distance between the centre of mass of the deuteron and the triton, $H_D$ and $H_T$ the Hamiltonians of the deuteron and of the triton, and $H'_{TD}$ the interaction terms which we shall treat as a perturbation.

We can expand the antisymmetric wave function of the system $\psi_a$ in terms of the eigenfunctions of $H_D$ and $H_T$,

$$\psi_a=\sum_{\epsilon\epsilon'}\psi_{T\epsilon}\psi_{D\epsilon'}F_{\epsilon\epsilon'}(\mathbf{R}).$$

Then from (1) we get

$$\sum_{\epsilon\epsilon'}\psi_{T\epsilon}\psi_{D\epsilon'}\left(\frac{-\hbar^2}{2M}\frac{5}{6}\Delta_R+\epsilon+\epsilon'-E\right)F_{\epsilon\epsilon'}=-H'_{TD}\psi_a. \quad . \quad . \quad (2)$$

Taking the scalar product of both sides of (2) with $\psi_{T\epsilon}\psi_{D\epsilon'}$ we get for $F_{\epsilon\epsilon'}$ the equation

$$\left[\Delta_R+\frac{12M}{5\hbar^2}(E-\epsilon-\epsilon')\right]F_{\epsilon\epsilon'}=\frac{12M}{5\hbar^2}\sum_{\text{spin}}\int\psi^*_{T\epsilon}\psi^*_{D\epsilon'}H'_{TD}\psi_a\,d\mathbf{q},$$

where **q** represents all the internal coordinates. Using the Born approximation we replace $\psi_a$ by the initial wave function

$$(1-P_{35}-P_{45})\chi_l\phi_\alpha\exp(i\mathbf{k}\,.\,\mathbf{r}),$$

which is correctly antisymmetrized with the forms given later for $\phi_\alpha$ and $\chi_l$. Here $\phi_\alpha$ is the spatial part of the wave function of the ground state of the alpha-particle, $\chi_l$ the spin wave function, **r** the distance between the incoming neutron and the centre of mass of the alpha-particle and $P_{ij}$ the operator exchanging both spin and space coordinates of nucleons $i$ and $j$. The amplitude of the asymptotic form of $F_{\epsilon\epsilon'}$ is then

$$f_{\epsilon\epsilon'}(\theta,\phi)=-\frac{1}{4\pi}\frac{12M}{5\hbar^2}\sum\iint\exp(-i\mathbf{K}\,.\,\mathbf{R})\psi^*_{T\epsilon}\psi^*_{D\epsilon'}H'_{TD}(1-P_{35}-P_{45})$$
$$\exp(i\mathbf{k}\,.\,\mathbf{r})\chi_l\phi_\alpha\,d\mathbf{q}\,d\mathbf{r}, \quad . \quad . \quad . \quad . \quad . \quad . \quad (3)$$

where **K** is a vector, with polar angles $\theta\phi$ relative to **k** and of modulus

$$\sqrt{\{12M(E-\epsilon-\epsilon')/5\hbar^2\}}.$$

As spin functions of the triton we shall take

$$S_1=(\alpha_3\beta_4-\beta_3\alpha_4)\alpha_2/\sqrt{2}, \quad S_2=(\alpha_3\beta_4-\beta_3\alpha_4)\beta_2/\sqrt{2}.$$

For the deuteron

$$R_1=\alpha_1\alpha_5, \qquad R_2=\beta_1\beta_5, \qquad R_3=(\alpha_1\beta_5+\beta_1\alpha_5)/\sqrt{2},$$

and for the initial state

$$\chi_1=(\alpha_1\beta_2-\beta_1\alpha_2)(\alpha_3\beta_4-\beta_3\alpha_4)\alpha_5/2, \qquad \chi_2=(\alpha_1\beta_2-\beta_1\alpha_2)(\alpha_3\beta_4-\beta_3\alpha_4)\beta_5/2,$$

where $\alpha_i$ and $\beta_i$ are the spin wave functions belonging to values $\frac{1}{2}$ and $-\frac{1}{2}$ of the $z$-component of the spin of nucleon $i$.

As spatial wave functions for the deuteron, triton and alpha-particle we shall take gaussian functions of the type

$$\phi=A\exp\Big(-\nu\sum_{i<j}\mathbf{r}_{ij}^2\Big). \quad . \quad . \quad . \quad . \quad . \quad . \quad (4)$$

With such choices $\psi_a$ is correctly antisymmetrized.

As nucleon–nucleon potential we have

$$V_{ij}=-\tfrac{1}{2}(1+P_{ij}^{\chi})(1-g+gP_{ij}^{\sigma})V\exp(-\beta\mathbf{r}_{ij}^2),$$

which is charge-independant.

As there are no tensor forces in this potential, we can separate in (3) the integration over spin and over spatial coordinates. $P_{ij}^{\chi}$i s the operator exchanging space coordinates of nucleons $i$ and $j$, while $P_{ij}^{\sigma}$ is exchanging spin coordinates.

In order to make a part of the calculations applicable to the other scattering cases dealt with later, we shall write $H'_{TD}$ as

$$H'_{TD}=\sum_{n=1}^{4}V_{5n}+\sum_{n=2}^{5}V_{1n}-2V_{51}.$$

Then decomposing $(1-P_{35}-P_{45})\exp(i\mathbf{k}\,.\,\mathbf{r})\chi_l\phi_\alpha$ in symmetric and antisymmetric functions of spin and space coordinates, we get for $f_{\varepsilon\varepsilon'}$ the expression, with $l$, $im$ referring to spin states

$$f_{l,\,im}(\theta,\phi)=-\frac{1}{4\pi}\frac{12M}{5\hbar^2}A_TA_DA_\alpha V(l,\,im)$$

with

$$(l,im)=-(S_iR_m,\,\chi_l)[3(1-g)J_1+\tfrac{1}{2}(1-3g)(I_2+I_4)-2(2-3g)I_5],$$

$$J_1=(\phi_F,\,U_{12}\phi_I), \qquad I_2=(\phi_F,\,U_{52}\phi_I), \qquad I_4=(\phi_F,\,U_{52}P_{52}^{\chi}\phi_I),$$

$$I_5=(\phi_F,\,U_{52}P_{53}^{\chi}\phi_I),$$

where we put for convenience

$$U_{ij}=\exp(-\beta\mathbf{r}_{ij}^2),$$

$$\phi_I=\exp(i\mathbf{k}\,.\,\mathbf{r})\phi_\alpha/A_\alpha,$$

$$\phi_F=\exp(i\mathbf{K}\,.\,\mathbf{R})\phi_T\phi_D/A_TA_D.$$

The differential cross section is then

$$\frac{d\sigma}{d\Omega}=\frac{2\mathrm{K}}{3k}\sum_{i,\,m}|f_{1,im}|^2,$$

that is to say,

$$\frac{d\sigma}{d\Omega}=\Gamma\tfrac{3}{4}\,|\,3(1-g)\mathrm{J}_1+\tfrac{1}{2}(1-3g)(\mathrm{I}_2+\mathrm{I}_4)-2(2-3g)\mathrm{I}_5\,|^2,$$

with

$$\Gamma=\frac{2\mathrm{K}}{3k}\cdot\frac{144}{16\times25}\cdot\frac{\mathrm{M}^2}{\pi^2\hbar^4}\cdot\mathrm{A}_\mathrm{T}^2\mathrm{A}_\mathrm{D}^2\mathrm{A}_\alpha^2\mathrm{V}^2.$$

The parameters of the potential were adjusted to the low energy proton–proton scattering experiments and to the binding energy of the deuteron (Hoisington *et al.* 1939) :

$$g=0{\cdot}211,\qquad \mathrm{V}=45\ \mathrm{MeV.},\qquad \beta=0{\cdot}266\ 10^{26}\ \mathrm{cm.}^{-2}.$$

The parameters of the wave functions of the deuteron, triton and alpha particle have been determined so as to give the best binding energy for these nuclei (Gerjuoy and Schwinger 1942) :

$$\nu_\mathrm{D}=0{\cdot}0716,\qquad \nu_\mathrm{T}=0{\cdot}0517,\qquad \nu_\alpha=0{\cdot}0517\ 10^{26}\mathrm{cm.}^{-2}$$

(we made the permissible approximation $\nu_\mathrm{T}=\nu_\alpha$).
Hence

$$\mathrm{A}_\mathrm{D}=3{\cdot}12\ 10^{18},\qquad \mathrm{A}_\mathrm{T}=1{\cdot}47\ 10^{37},\qquad \mathrm{A}_\alpha=1{\cdot}17\ 10^{56}\ \mathrm{c.g.s.}$$

For 90 MeV. neutrons we get

$$k=1{\cdot}68,\qquad \mathrm{K}=1{\cdot}78\ 10^{13}\mathrm{cm.}^{-1}.$$

(b). *Results.*

There is a small backwards scattering of the order of 0·1 per cent of the forwards one ; the differential cross section can then be fairly well approximated by a gaussion function

$$\frac{d\sigma}{d\Omega}=0{\cdot}76\exp\left(-15{\cdot}1\,\theta^2\right)\times10^{-25}\ \mathrm{cm.}^2.$$

in the centre of mass system (see fig. 1, curve (*b*)).

The total cross section is then

$$\sigma_\mathrm{D}=0{\cdot}16\ 10^{-25}\mathrm{cm.}^2.$$

Transforming to the laboratory system we see that the angular distribution of the deuterons has a half-half-width $\Gamma_0$ equal to 8·4 degrees. Their energy spectrum consists of a sharp line at ~70 MeV. with an half-width of about 0·6 MeV.

## (B). *Elastic Scattering.*

### (a). *Results.*

Using essentially the same formalism we get

$$\frac{d\sigma}{d\Omega}=\frac{9M^2}{25\pi^2\hbar^4}A_\alpha^4V^2(1-g)^2\,|\,I_1+I_2-2I_3\,|^2$$

with

$$I_1=(\phi_F, U_{51}\phi_I), \qquad I_2=(\phi_F, U_{51}P^{\chi}_{51}\phi_I), \qquad I_3=(\phi_F, U_{52}P^{\chi}_{51}\phi_I), \quad . \; . \; . \quad (6)$$

where $U_{ij}$ and $\phi_I$ have the same meaning as in (5) and $\phi_F=\exp(i\mathbf{K}\,.\,\mathbf{r})\phi/_\alpha A_\alpha$. The backwards scattering is small, being of the order of 0·3 per cent of the forward one ; then the differential cross section can be written, in the centre of mass system,

$$\frac{d\sigma}{d\Omega}=4{\cdot}50\exp(-7{\cdot}86\,\theta^2)\times10^{-25}\text{ cm.}^2$$

Fig. 1.

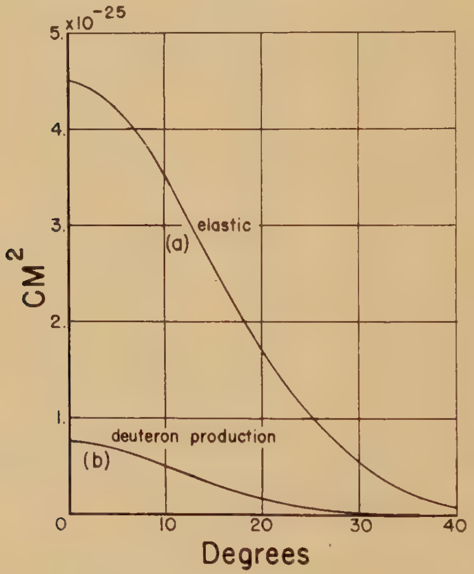

(see fig. 1, curve (*a*)). The total cross section is

$$\sigma_{el}=1{\cdot}80\times10^{-25}\text{cm.}^2.$$

### (b). *Correction to the Born Approximation.*

Consider the expansion in Legendre polynomials, of the scattered amplitude obtained in the Born approximation

$$\sqrt{\frac{d\sigma}{d\Omega}}=k^{-1}\sum_{l=0}^{\infty}(2l+1)\eta_lP_l(\cos\theta). \quad . \; . \; . \; . \; . \quad (7)$$

We may hope to get a better approximation than Born's by replacing in (7) the approximate expression $\eta_l$ of the contribution of the phases $\eta_l$ by the exact expression (Mott and Massey 1933):

$$(\exp(2i\eta_l)-1)/2i.$$

When using Gaussian functions, as we did for the wave functions and the radial part of the potential, the integrals defined by (6) take the simple form

$$I_n = a_n \exp(b_n \cos\theta).$$

It is then possible to get for the phases $\eta_l$ the formula

$$\eta_l = k\sqrt{\frac{\pi}{2}} \sum_{n=1}^{3} \frac{a_n}{\sqrt{b_n}}\, i^{-(l+\frac{1}{2})} J_{l+\frac{1}{2}}(ib_n),$$

where the functions $J_{l+\frac{1}{2}}$ are Bessel functions. The numerical calculation gives

$$\eta_0 = 0{\cdot}761, \qquad \eta_1 = 0{\cdot}733, \qquad \eta_2 = 0{\cdot}452.$$

For $l>2$ the phases are small enough for it to be possible to write

$$(\exp(2i\eta_l)-1)/2i \sim \eta_l.$$

Then the corrected cross section is

$$\tilde{\sigma}_{el} = \sigma_{el} - \frac{4\pi}{k^2}\sum_{l=0}^{2}(2l+1)(\eta_l^2 - \sin^2\eta_l) = 1{\cdot}60\times10^{-25}\ \text{cm.}^2.$$

## (C). *Stripping Scattering.*

### (a). *Stripping Scattering of a Proton.*

We shall first consider the case in which the stripped nucleon is a proton.

#### (1). *Calculation.*

Let I be that proton, and denote by $\hbar\mathbf{k}'$ the momentum of the stripped proton in the alpha-particle centre of mass system, $\hbar\mathbf{k}$ and $\hbar\mathbf{K}$ the initial and final momenta of the neutron 5 in the five nucleons' centre of mass system.

The final wave function can be written

$$\psi_F = (2\pi)^{-3/2} T_i \phi_T \exp(i\mathbf{k}'\,.\,\mathbf{R}), \qquad . \quad . \quad . \quad . \quad . \quad (8)$$

where $\mathbf{R}$ is the distance between the proton 1 and the centre of mass of the triton (2, 3, 4) and $\phi_T$ is defined as in (4), and $T_i$ is the spin wave function.

Using the same formalism as in paragraph 2, ((A) (a)), we get for the scattered intensity the expression

$$I = \frac{9M^2}{25\pi^2\hbar^4}(2\pi)^{-3}A_T^2A_\alpha^2V^2(1-g)^2\,|I_1+I_2-2I_3|^2, \qquad . \quad . \quad . \quad (9)$$

with $I_1$, $I_2$, $I_3$ as given in (6) but with $\phi_F$ replaced by

$$\phi_F = \exp(i\mathbf{K}\,.\,\mathbf{r})\exp(i\mathbf{k}'\,.\,\mathbf{R})\phi_T/A_T.$$

$I_3$ can be shown to be a delta function, which we can omit. I is a function of the momentum of the scattered neutron and of the momentum of the remaining triton, for example, related by the energy conservation condition. Then if we wish to get, for instance, the angular and energy distribution of the triton we have to integrate over the two parameters describing the scattered neutron.

We shall carry out this integration in the laboratory system, in which the momentum of the triton will be denoted by $\hbar\mathbf{k}_0$.

Expressing $\mathbf{k}'$ as a function of $\mathbf{k}_0$, $\mathbf{k}$ and $\mathbf{K}$, we get for the differential cross section

$$d\sigma = \mathrm{I}\frac{\mathrm{K}}{k}\,d\mathbf{k}_0\,d\Omega_{\mathrm{K}},$$

$d\Omega_{\mathrm{K}}$ can be replaced by $d\mathbf{K}\,\mathrm{K}^{-2}\delta(\mathbf{K}-\gamma)$ where $\gamma$ is such that for $\mathrm{K}=\gamma$ the energy conservation relation is satisfied. Furthermore we have

$$\delta(\mathrm{K}-\gamma) = 2\mathrm{K}\delta(\mathrm{K}^2-\gamma^2)$$

and for the energy of the system,

$$\mathrm{E} = \frac{5\hbar^2}{8\mathrm{M}}\mathrm{K}^2 + \text{ terms which are independent of } \mathbf{K}.$$

Then

$$d\sigma = \mathrm{I}\frac{\mathrm{K}}{k}\,d\mathbf{k}_0\,d\mathbf{K}\,\mathrm{K}^{-2}2\mathrm{K}\delta\left[\frac{8\mathrm{M}}{5\hbar^2}(\mathrm{E}-\epsilon_0)\right],$$

where $\epsilon_0$ is the initial energy.

Putting $\mathbf{W}=\mathbf{K}+\frac{1}{2}(\mathbf{k}\ -\frac{3}{4}\mathbf{k})$, the modulus of $\mathbf{W}$ being a constant on account of the energy conservation relation, $d\sigma$ can be written

$$d\sigma = \frac{5}{8}\mathrm{I}\frac{\mathrm{W}}{k}\,d\mathbf{k}_0\,d\Omega_{\mathrm{W}}\frac{8\mathrm{M}}{5\hbar^2}d\mathrm{E}\delta\left[\frac{8\mathrm{M}}{5\hbar^2}(\mathrm{E}-\epsilon_0)\right]$$

and integrating over E,

$$d\sigma = \frac{5}{8}\mathrm{I}\frac{\mathrm{W}}{k}\,d\mathbf{k}_0\,d\Omega_{\mathrm{W}}.$$

I is of the form $\sum_{i=1}^{3} f_i(\mathbf{k},\mathbf{k}_0)\exp\left[\mathbf{W}\,.\,\mathbf{V}_i(\mathbf{k},\mathbf{k}_0)\right]$, so that the integration over $d\Omega_{\mathrm{W}}$ is direct, and finally we get

$$\left(\frac{d\sigma}{d\Omega}\right)_0 = \frac{\mathrm{W}}{k}\mathrm{k}_0\sum_{i=1}^{3}\Gamma_i\frac{\sinh \mathrm{WV}_i}{\mathrm{WV}_i}\exp\left(\mathbf{A}_i\,.\,\mathbf{B}_i\right)d\mathrm{E}_0,$$

where $\mathbf{V}_i$, $\mathbf{A}_i$ and $\mathbf{B}_i$ are vector linear functions of $\mathbf{k}$ and $\mathbf{k}_0$ with coefficients obtained from the expressions for $\mathrm{I}_1$ and $\mathrm{I}_2$. $\Gamma_i$ are coefficients and $\mathrm{E}_0$ the energy of the triton.

(2). *Results.*

The result of the numerical calculation is shown in fig. 2 which gives $2\pi \sin \theta_0 (d\sigma/d\Omega)_0$/MeV., the angular and energy distribution of the remaining triton in the laboratory system when a proton has been stripped off by the incoming neutron.

It is seen that these tritons are of low energy, 2 MeV. on the average, and that they are distributed almost isotropically ; this is seen more easily in fig. 3 where $(d\sigma/d\Omega_0)$/MeV. is plotted for four various energies of the triton.

Fig. 2.

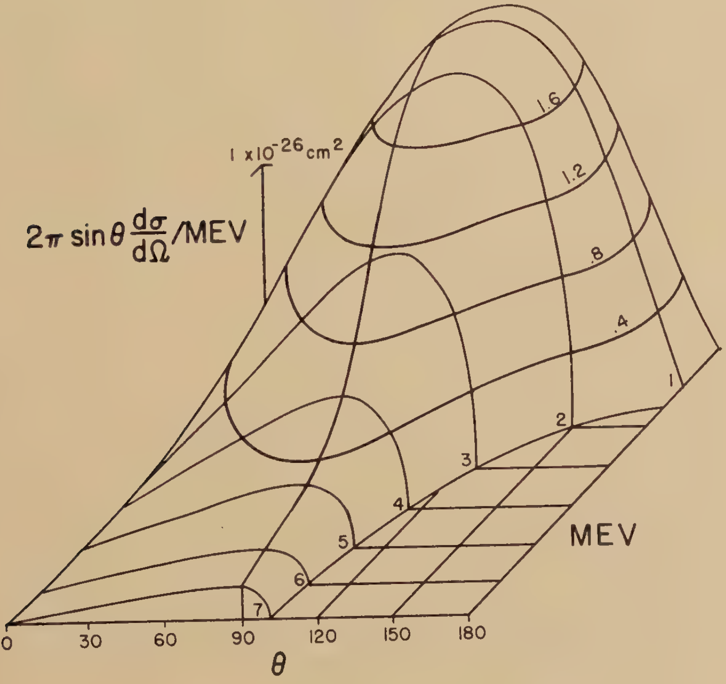

A graphical estimation of the total cross section for stripping of a proton gives

$$\sigma_P = (0{\cdot}63 \pm 0{\cdot}10) \times 10^{-25} \text{ cm.}^2.$$

(b) *Stripping Scattering of a Neutron.*

We have to perform the same calculations with $\psi_F$ in (8) replaced by

$$P^{\sigma}_{13} P^{\sigma}_{24} P^{\chi}_{13} \psi_F.$$

But instead of two integrals as in (9) we are left with six of them, since the symmetry of this case is less than in the case of the stripping of a proton. As the subsequent integration over $d\Omega_W$ would be rather tedious we shall estimate the total cross section by the following argument : with the chosen potential between nucleons the neutron–neutron interaction takes non-zero values only in singlet states ; it can then be estimated to be $\frac{\frac{1}{4}}{\frac{1}{4}+\frac{3}{4}}\cdot\left(\frac{V_S}{V_T}\right)^2=$ one tenth of the neutron–proton interaction (Chew 1948). Assuming that the stripping of a nucleon off an alpha-particle is a process of the first order, we can say that the cross section for stripping of a neutron would be about

$$\sigma_N=0{\cdot}06\times10^{-25}\text{ cm.}^2.$$

Fig. 3.

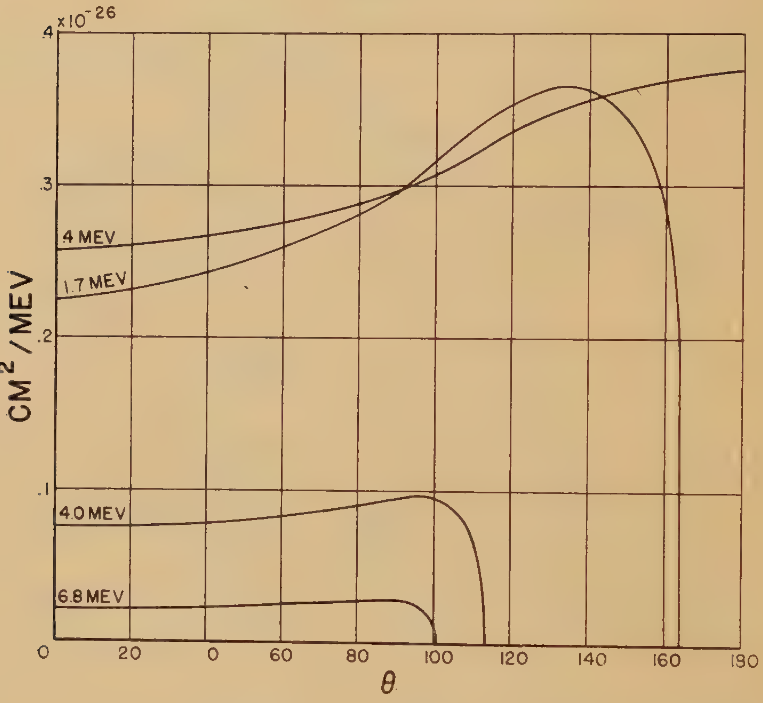

## 3. Comparison with Experiments.

There are no experiments on 90 MeV. neutron–He scattering ; therefore we have to compare our calculations with experiments on other nuclei, especially the nuclei of carbon and oxygen, which may be considered as built of α-particles.

### (A). *Total Cross Section.*

From the previous analysis we found for the total cross section for 90 MeV. neutron–He scattering the value

$$\sigma_\alpha=(2{\cdot}45\pm0{\cdot}10)\times10^{-25}\text{ cm.}^2$$

if we neglect the processes (iv.)–(vi.). In fact we think the cross sections for these processes to be very small, through the following estimate: let P be the probability for the incoming neutron to strip off a proton and N for stripping of a neutron, and S the probability for the incoming neutron to stick to a stripped proton. These three numbers can be estimated from the previous calculations. Then the cross section for process (v.) for instance. could be estimated to be 1 per cent the elastic cross section $\sigma_{(V)}=PN\sigma_{el}$.

Experimental data about the total cross section can be obtained from the measurements performed on the nuclei H, D, Li, Be, C, N, O . . . (Cook *et al.* 1949). If we draw a curve plotting the experimental values of $\sigma$ as a function of the atomic mass, we see that the value for He would be about 2·0 $10^{-25}$ cm.$^2$ (fig. 4).

Fig. 4.

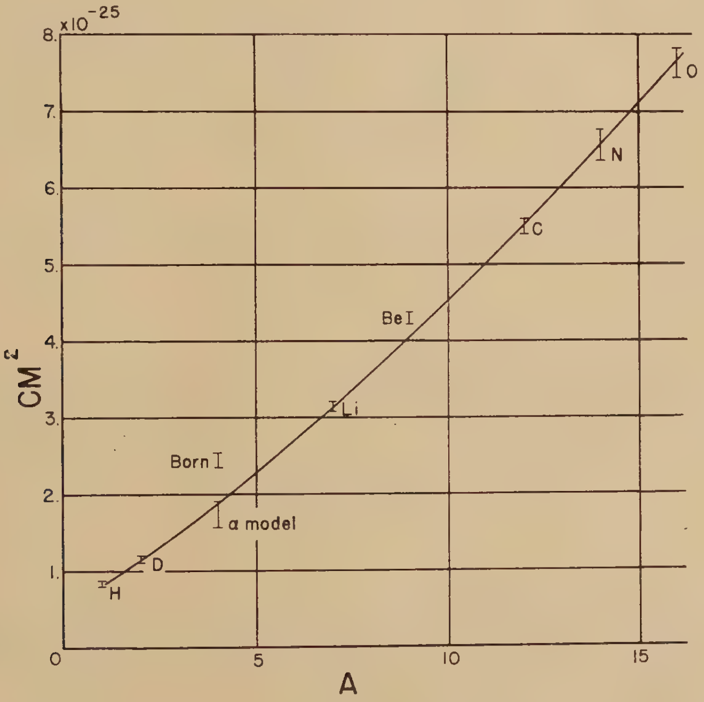

In order to check this estimation we shall use the following argument: Let us consider the carbon and oxygen nuclei as a triangle and a tetrahedron of side $s$, which we can reasonably assume to be the same in C and O, (Wheeler 1937) with weakly bound alpha particles at the corners; then we can, with the Born approximation, calculate their cross sections from that of He as a function of $s$; conversely from the experimental values of the cross sections of C and O, we can calculate $s$ and $\sigma_\alpha$. We find

$$\sigma_c=3(1+2y)\sigma_\alpha, \qquad \sigma_0=4(1+3y)\sigma_\alpha,$$

with

$$y = \sin ks/ks$$

and, comparing these values of $\sigma_c$, $\sigma_0$ with the experimental values, we get

$$s = (1{\cdot}79 \pm 0{\cdot}08) \times 10^{-13} \text{ cm.}, \qquad \sigma_\alpha = (1{\cdot}70 \pm 0{\cdot}17) \times 10^{-25} \text{ cm.}^2.$$

This value for $\sigma_\alpha$ can be said to be in good agreement with the value we calculated, in view of the fact that our calculations are crude for the following reasons: (i.) use of Born approximation, (ii.) use of the plane wave approximation as made in (8), (iii.) use of gaussian functions for the radial part of the potential and for the wave functions, especially for the deuteron one (Chew 1948).

Nevertheless if one makes a better calculation for neutron–He scattering, the He cross section as deduced from these for the carbon and oxygen should be considered more carefully:

(i.) We have not taken into account, using the Born approximation, the influence of double scattering. A measure of this effect is given by the amplitude of the wave, scattered by a single α-particle, at the distance $s$ from it; this we can write approximately from our previous calculations

$$4 \exp(-4\theta^2).$$

The average value of this is 0·25.

Then the correction will be proportional to the number of ways in which a pair of alpha particles can be chosen in C and O nuclei, *i. e.* 3 and 6. We can write

$$\sigma_c' = 3(1+2y')\sigma_\alpha' + 3\Sigma, \qquad \sigma_0' = 4(1+3y')\sigma_\alpha' + 6\Sigma,$$

where $\Sigma$ is the correction term due to double scattering, and $y'$ is defined in the same way as $y$ but for a new value $s'$ of $s$. As an estimate we can write

$$\Sigma \sim (0{\cdot}25)^2 \tfrac{1}{2}\sigma_\alpha,$$

hence

$$y' \sim y(1 - 0{\cdot}015).$$

For the value of the cross section of He the correction has a coefficient small compared with unity; thus we can say that $\sigma_\alpha$ is not influenced appreciably.

(ii.) We have not taken into account the binding energy of the alpha particles, which is 2·4 MeV. per bond. This binding will not affect our estimate of the elastic cross section of the alpha particles in C and O, nor the cross section for production of deuterons, as follows from inspection of their spectrum.

But the stripping cross section will be reduced: the nucleus of mass 3, which received on a small energy, will almost never be ejected; then both of the other nucleons have to receive an energy greater than $0{\cdot}6l$ MeV., with $l=2$ or 3, in order that the stripping scattering should be possible. As an estimate we can take, for the differential cross section for the scattering of one of these two nucleons, the experimental Berkeley curve (Hadley *et al.* 1948) and find that the stripping cross section has to be multiplied by $(1-0{\cdot}035\,l)$.

As the stripping cross section is about one quarter of the total one, we get

$$\sigma_c'=3(1+2y')(1-\tfrac{1}{4}0{\cdot}035\times 2)\sigma_\alpha',$$

$$\sigma_0'=4(1+3y')(1-\tfrac{1}{4}0{\cdot}035\times 3)\sigma_\alpha',$$

hence

$$y'\sim y(1-0{\cdot}017),\qquad \sigma_\alpha'\sim\sigma_\alpha(1+0{\cdot}017).$$

This correction will increase $\sigma_\alpha$.

(iii.) We have not taken into account the fact that in the expansion of the exact wave the probability of finding the nuclei C or O in the state described above is less than 1, as the alpha particles are always exchanging nucleons, decomposing, reforming, . . . (Wheeler 1937). The most probable state after the one we used should be that in which one of the alpha particles is decomposed in lighter elements ; the probability of such an event is proportional to the number of alpha particles in C and O, *i. e.* 3 and 4.

If one of the alpha particles is decomposed we can write

$$\sigma_c=[2(1+y)+\rho]\sigma_\alpha,$$

$$\sigma_0=[3(1+2y)+\rho]\sigma_\alpha,$$

where $\rho\sigma_\alpha$ is the cross section of the decomposed alpha particle, together with interference terms which we shall neglect as is suggested from the preceding analysis by the small value of the correction on $y$ ; then we can assume that $\rho$ is the same for C and O. Then

$$\sigma_c'=3[1+2y'+q(\rho-1-4y')]\sigma_\alpha',$$

$$\sigma_0'=4[1+3y'+q(\rho-1-6y')]\sigma_\alpha'.$$

$q$ being the probability that an alpha-particle is decomposed. $q$ being small, we get

$$y'\sim y-qy'(1+\rho),\qquad \sigma_\alpha'\sim\sigma_\alpha[1+q(1-\rho)],$$

$\sigma_\alpha$ will be increased or decreased according as $\rho\lesssim 1$.

We can evaluate $\rho$ as follows : the general slope of the curve of fig. 4 shows that the cross section of a light nucleus is less than the sum of the cross sections of the nuclei into which it could be decomposed. Assuming this to be true also for the alpha particle, we can write

$$\sigma_{\alpha d}>\sigma_\alpha,$$

where $\sigma_{\alpha d}$ denotes the cross section of the decomposed $\alpha$-particle. Furthermore, since the elements into which an alpha particle could be decomposed have atomic masses in the range 1 to 3, we can say that the binding energy of the nucleons of these elements per nucleon will be in the range 0 to 2·8 MeV., while in the alpha particle it has the value 7·05 MeV., which is much larger. Then we can consider these elements as almost free nucleons, that is to say that the most important part of their cross section will be the elastic one. Under these circumstances the reduction of the cross section of these elements due to their being bound in C or O will be very small ; we can then write

$$\sigma_{\alpha d} \text{ in C or O} \sim \sigma_{\alpha d}.$$

Furthermore, we remark that the most probable decomposition of the $\alpha$-particle should be the one into one nucleon+one nucleus of mass 3. Then, from the curve fig. 4, we get

$$\rho \sim 1{\cdot}2.$$

The cross section of He is then

$$\sigma'_\alpha \sim \sigma_\alpha(1-0{\cdot}2q),$$

$q$ being small we can neglect this correction and estimate, in the light of this discussion,

$$\sigma_\alpha=(1{\cdot}74\pm0{\cdot}17)\times10^{-25}\text{ cm.}^2.$$

## (B) *Production of Deuterons.*

In paragraph 2((A)(*b*)) we found for the cross section for production of fast ($\sim$70 MeV.) deuterons in neutron–alpha particle collisions the value

$$\sigma_{\mathrm{D},\alpha}=0{\cdot}16\ 10^{-25}\text{ cm.}^2.$$

Experiments have been performed mainly on carbon nuclei (Brueckner 1949, York 1949). York gives the estimate

$$\sigma_{\mathrm{D,C}}=\text{a few hundredths of a barn},$$

which certainly includes deuterons of energy smaller than say 60 MeV. Bruecker's value for deuterons of energy larger than 60 MeV. can be obtained from his Table II. and fig. 1 :

$$\sigma_{\mathrm{D,C}}=(0{\cdot}02\pm0{\cdot}01)\ 10^{-25}\text{ cm.}^2.$$

In order to compare our value for the Helium nucleus with these experimental values on the carbon nucleus it would be necessary to take into account the fact that, when formed by interaction of the incoming neutron with one of the alpha particles of carbon nucleus, the deuteron has some probability of being disintegrated by interaction with the two other alpha particles of the carbon nucleus. Nevertheless, we think it is safe to say that the cross section for production of fast deuterons on carbon should be of the order of two to three times $\sigma_{D,\alpha}$. In view of the crudeness of our calculations as mentioned above, we can say that our result is in agreement with both of these experimental values.

### (C) *Percentage of Inelastic Scattering.*

Our calculations show that the ratio of the inelastic to the total cross section is 0·35. The experimental value measured on various nuclei, He excepted, lies in the range 0·4 to 0·5 (Knable *et al.* 1949). The low value for He could be explained by the absence of small binding energies in He.

This work was performed in the Wills Physics Laboratory, Bristol. I would like to thank Professor N. F. Mott for valuable discussions, Miss J. Littleton for a large part of the numerical calculations, R. H. Dalitz for friendly advice and criticisms and the British Council whose scholarship enabled me to spend one academic year in Bristol University.

I would like to thank too Professor H. A. Bethe for criticisms.

### REFERENCES.

BRUECKNER *et al.*, 1949, *Phys. Rev.*, **75**, 1274.
CHEW, 1848, *Phys. Rev.*, **74**, 809.
COOK, *et al.*, 1949, *Phys. Rev.*, **75**, 7.
GERJUOY and SCHWINGER, 1942, *Phys. Rev.*, **61**, 138.
HADLEY, *et al.*, 1948, *Phys. Rev.*, **73**, 1114.
HOISINGTON, *et al.*, 1939, *Phys. Rev.*, **56**, 884.
KNABLE, *et al.*, 1949, *Phys. Rev.*, **75**, 1470.
MOTT and MASSEY, 1933, *Theory of Atomic Collisions*, p. 25.
WHEELER, 1937, *Phys. Rev.*, **52**, 1083, 1107.
YORK, 1949, *Phys. Rev.*, **75**, 1467.

# XL. *Relaxation Methods applied to Problems of Plastic Flow.*—II.

By J. A. Jacobs, M.A., Ph.D., A.F.R.Ae.S.,
Royal Holloway College, University of London *.

[Received January 11, 1950.]

## Summary.

As in Part I., this paper considers the consequence of a particular hypothesis regarding plastic strain, viz. the Mises-Hencky criterion, and, by application of a numerical method due to Allen and Southwell, traces the effect of plastic straining. Two problems are considered here :

(i.) a sharp ended bar under specified edge tractions,

(ii.) the uniform compression of a block between two smooth rigid plates, which do not overlap it.

The general theory is not discussed, the reader being referred back to Part I.

Fig. 1.

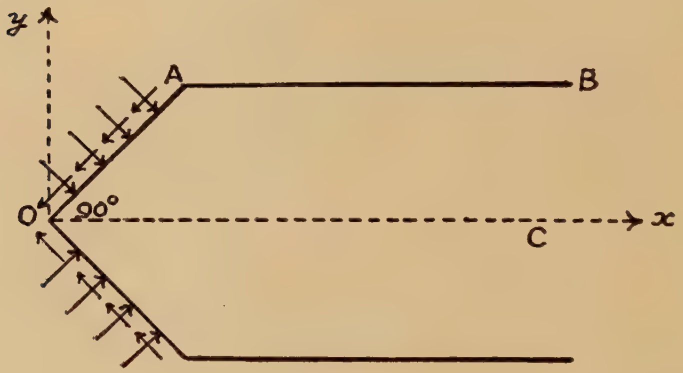

## 1. Stress Distribution in a Sharp-ended Bar under Specified Edge Tractions.

Fig. 1 illustrates the sharp-ended bar subject to specified edge tractions, in which the normal and shearing forces over the nose are of equal magnitude. From symmetry it will be sufficient to consider one half the bar, BAOC. The bar was taken sufficiently long so that points sufficiently far from the nose are sensibly stress free. Thus the length of the nose AO is immaterial. As in Part I. (Jacobs 1950) dimensional factors are eliminated and in the subsequent analysis, the symbols stand for purely numerical quantities. Thus $N_\nu$ was taken equal to 960, and $N_s$ equal to $-960$. (See fig. 2.)

---

* Communicated by the Author.

The boundary conditions give, along OA,

$$N_\nu \cos\frac{\pi}{4} + N_s \sin\frac{\pi}{4} = X_\nu = \frac{\partial}{\partial s}\left(\frac{\partial \chi}{\partial y}\right),$$

*i. e.*

$$\frac{\partial}{\partial s}\left(\frac{\partial \chi}{\partial y}\right) = 0 \quad \text{or} \quad \frac{\partial \chi}{dy} = \text{constant}, \qquad (1)$$

and

$$-N_\nu \sin\frac{\pi}{4} + N_s \cos\frac{\pi}{4} = Y_\nu = -\frac{\partial}{\partial s}\left(\frac{\partial \chi}{\partial x}\right),$$

or

$$960\sqrt{(2)} = \frac{\partial}{\partial s}\left(\frac{\partial \chi}{\partial x}\right)$$

Fig. 2.

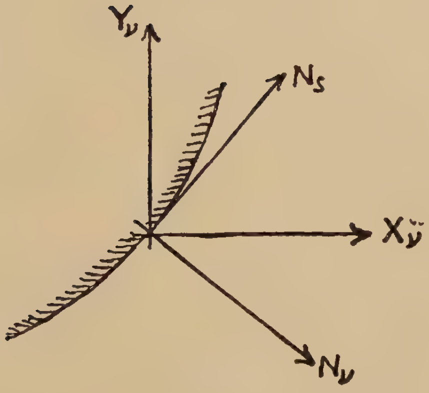

which gives

$$960\sqrt{(2)}s + C = \frac{\partial \chi}{\partial x},$$

where C is a constant. Along OA, $s = x\sqrt{(2)}$, so that

$$1920x + C = \frac{\partial \chi}{\partial x}. \qquad (2)$$

Along AB, $N_\nu = 0 = N_s$. Hence

$$\frac{\partial \chi}{\partial y} \quad \text{and} \quad \frac{\partial \chi}{\partial x} \quad \text{are both constants.} \qquad (3)$$

If we take $\frac{\partial \chi}{\partial y} = 0$ at O, then $\frac{\partial \chi}{\partial y} = 0$ along OA and AB, and if $\frac{\partial \chi}{\partial x} = 0$ at A, then from (2),

$$1920+C=0 \quad i.e. \quad C=-1920, \quad \text{since at A,} \quad x=y=1.$$

Hence along OA,

$$\frac{\partial\chi}{\partial x}=1920(x-1) \quad \text{and along} \quad \text{AB,}\ \frac{\partial\chi}{\partial x}=0. \quad . \quad . \quad . \quad (4)$$

Finally along OA, $\chi=960(x-1)^2+\text{constant}$.

Taking $\chi=0$ at A$(x=1)$, the constant is zero, so that

$$\chi=960(x-1)^2. \quad . \quad . \quad . \quad . \quad . \quad . \quad . \quad . \quad . \quad (5)$$

Since both $\frac{\partial\chi}{\partial x}$ and $\frac{\partial\chi}{\partial y}$ are zero along AB,

$$\begin{aligned}\chi&=\text{constant along AB}\\&=\text{value of } \chi \text{ at A}=0.\end{aligned}$$

The problem was first solved for the elastic case, the values of the principal stress difference being given in fig. 3. It was found that the same maximum values of the Mises-Hencky equivalent stress were attained at all mesh points long a line at right angles to the centre line, so that the result of plastic straining is evident at once from the contours of fig. 3. A plastic enclave starts on the centre line at H (fig. 4) and quickly extends outwards towards the faces of the bar. The growth is extremely rapid, and it would appear that once plastic flow has started in a region around H, it would very soon reach across the bar, isolating a small elastic core at the nose.

This problem was undertaken as a preliminary investigation into some of the problems that occur in sheet extrusion and sheet drawing, and which are discussed in detail by Hill (1948). One of the problems raised by Hill involves the reverse procedure to that considered here, viz. that of unloading from an initial plastic state. That problem, however, is not the same as loading an initially unstressed body of the same shape up to the final external stress system. In the practical problem raised by Hill, the material is unloading from an initial plastic state at the left hand end (the nose), and the material at the right hand end (at a great distance from the nose) is in a state of residual stress. It is these residual stresses which are of interest to the engineer. One must also consider the question as to whether the material immediately unloads or remains plastic for a time.

Assuming all the material to remain elastic during an unloading process, we can calculate the reversed stresses thereby induced, and superposing these on the stresses computed previously we have the stresses that will persist, unless plastic strain occurs in the process of unloading. It will do so, if in any region, these computed stresses violate the Mises-Hencky criterion, in which case adjustment will have to be made both in the stresses and in the strains.

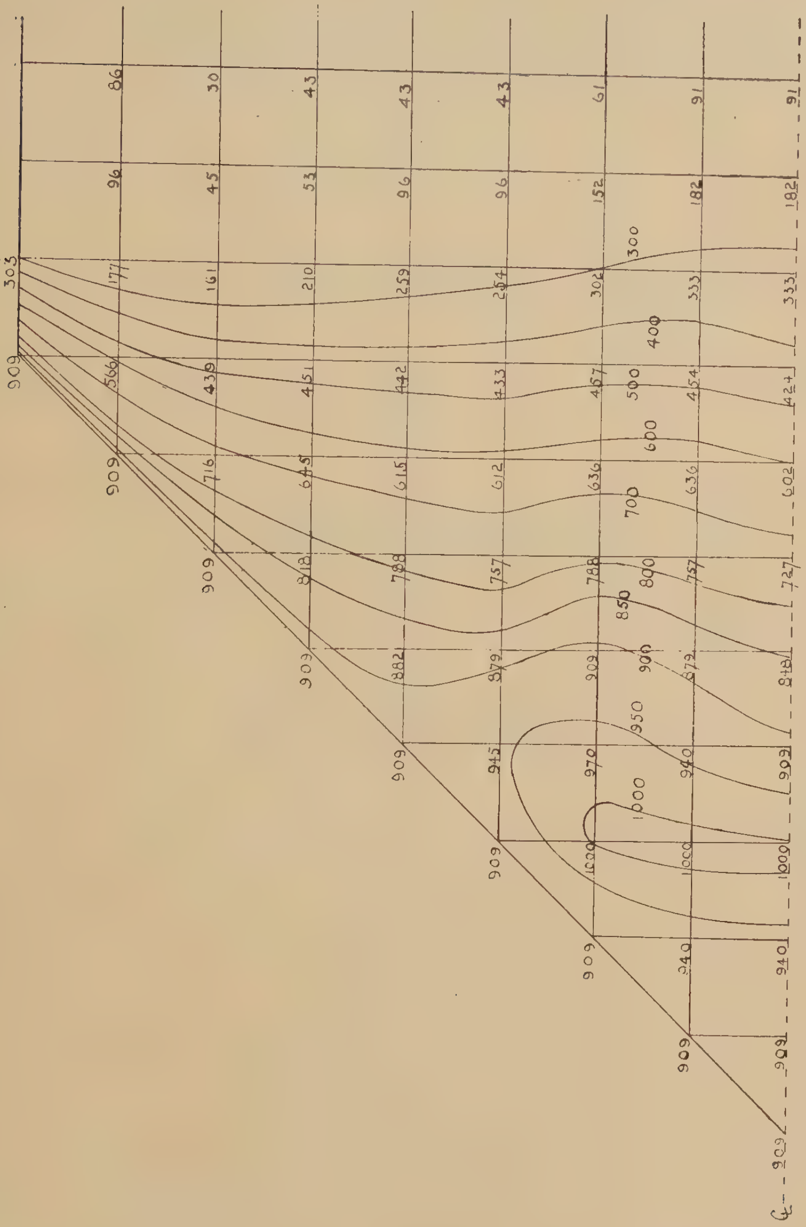

Fig. 3.

Values of the principal stress difference for the sharp ended bar under specified edge tractions.

## 2. UNIFORM COMPRESSION OF A BLOCK BETWEEN TWO SMOOTH RIGID PLATES, WHICH DO NOT OVERLAP IT.

Fig. 5 illustrates the block compressed between two smooth rigid plates which do not overlap it. The dimensions taken were

$$OD=DC=2CB.$$

The lengths of the plates were thus twice the block thickness. From symmetry it will be sufficient to consider the quadrant OABC, which is shown in fig. 6 re-orientated to compare with the problem of the notched

Fig. 4.

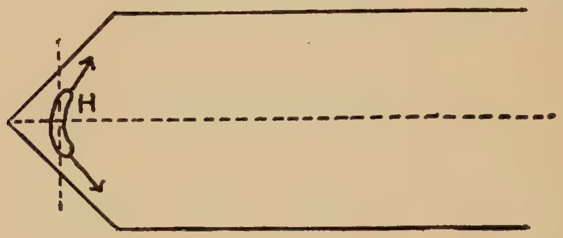

Fig. 5.

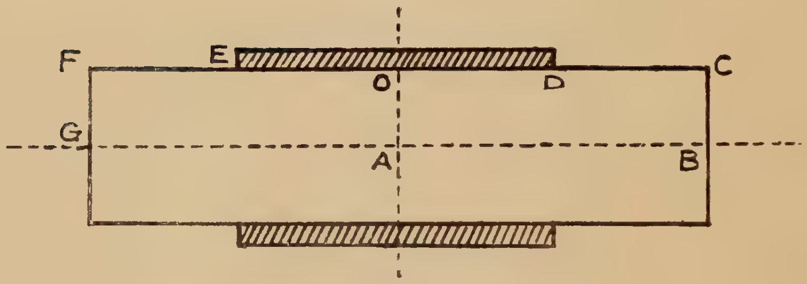

Fig. 6.

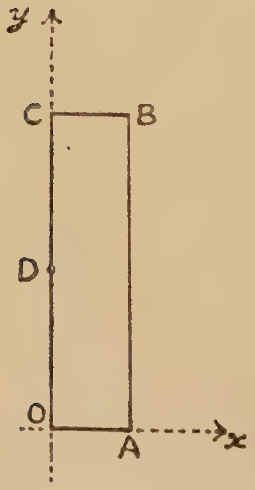

bar under tension discussed in Part I. (Jacobs 1950). This problem is, in fact, very similar to that of the notched bar, differing only in that the specimen is very much shorter in length (*i. e.* OA<AB, whereas before

OA>AB), and that a symmetry condition obtains at the right hand boundary AB, instead of a uniform tension there. As in the first two problems, dimensional factors are eliminated, and in the subsequent analysis, the symbols stand for purely numerical quantities.

The boundary conditions are

$$\left.\begin{array}{l}\text{(i.) BCD is stress free;}\\ \text{(ii.) symmetry exists across OA and AB;}\\ \text{(iii.) along OD, } X_y=0 \text{ (the plates are smooth) and}\\ \qquad u=\text{const. (uniform compression).}\end{array}\right\} \quad \ldots \quad (6)$$

From these last two conditions (iii.), we can deduce that, along OD,

$$\frac{\partial\chi}{\partial x}=0, \quad \text{and} \quad \frac{\partial^3\chi}{\partial x^3}=0.$$

Since BCD is stress free, both $\frac{\partial\chi}{\partial x}$ and $\frac{\partial\chi}{\partial y}$ are constant along it.

Owing to the symmetry condition, $\frac{\partial\chi}{\partial x}=0$ along AB.

Hence

$$\frac{\partial\chi}{\partial x}=0$$

along BC and CD. (7)

The constant value of $\frac{\partial\chi}{\partial y}$ along BC and CD was taken as 2000. Finally

$$\begin{aligned}\chi&=\int\left\{\frac{\partial\chi}{\partial x}\frac{dx}{ds}+\frac{\partial\chi}{\partial y}\frac{dy}{ds}\right\}ds\\ &=\int\left\{\frac{\partial\chi}{\partial y}\frac{dy}{ds}\right.ds \quad \text{along} \quad \text{BCD}\\ &=\int 2000\,dy\\ &=2000y+C.\end{aligned}$$

Taking $\chi=0$ at D ($y=\frac{1}{2}$), C$=-1000$, so that along BCD,

$$\chi=1000(2y-1). \quad \ldots\ldots\ldots \quad (8)$$

Actually along BC ($y=1$), $\chi=1000$, and along CD, $\chi=1000\ (2y-1)$.

The problem was first solved for the elastic case; the contours of principal stress difference compare favouably with the isochromatics obtained by Frocht (1947) who examined the stresses produced by a concentrated load acting through a rigid flat die (the load being applied so that the deflections under the die were constant).

Fig. 7.

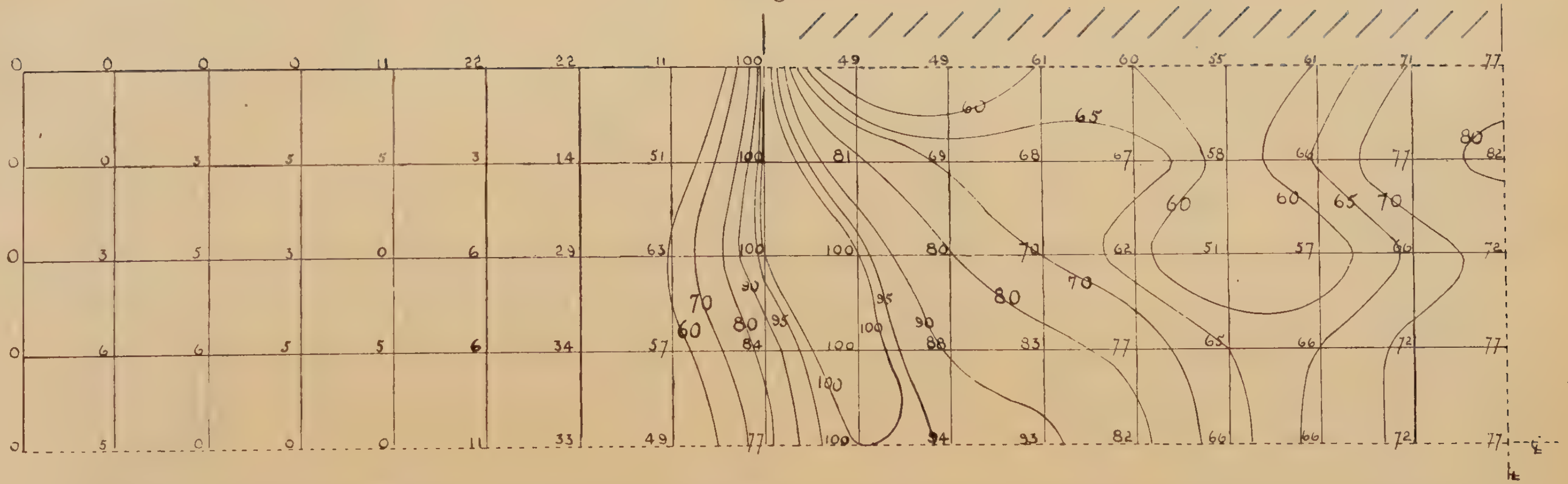

Values of the Mises-Hencky equivalent stress (taking 100 as its maximum value) when the plastic enclave has spread right across the block.

The elastic solution was modified by the methods already described and successive stages in the growth of the plastic enclave traced. Three distinct stages of plastic straining were obtained, and fig. 7 gives the values of the Mises-Hencky equivalent stress when the plastic enclave has spread until it extends right across the block. Fig. 8 summarizes these three stages, and illustrates the growth of the enclave as the compression is increased. In both these diagrams the upper left-hand quadrant is represented.

It was found that when the enclave had extended about 80 per cent of the way down the block, there was a strong tendency for it to spread towards the centre line OA as well as towards the other centre line GA. (Fig. 5.) It was not possible to obtain any records of this phenomenon owing to the extreme rapidity with which the enclave was spreading for quite small increases in the compressive load. This trend is illustrated, however, by the contours of values 90 and 80 of fig. 7 and was further confirmed by a preliminary investigation when all $\chi$ values were increased fourhold. As the enclave reached the centre-line GA, it spread out towards the centre-line OA, covering a distance approximately equal to $\frac{1}{2}$EO.

Fig. 8.

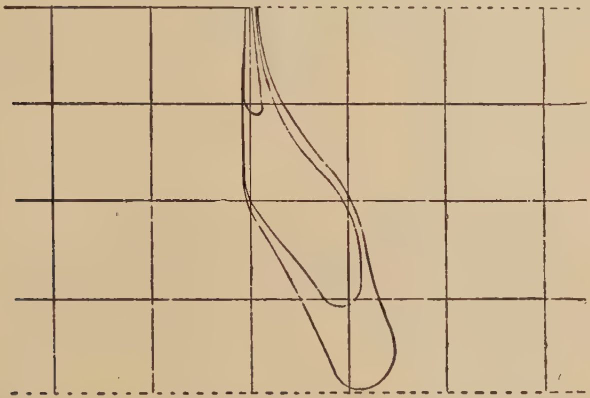

Diagram showing the progress of plastic straining (superposed plastic-elastic interfaces).

A feature of particular interest in this problem is the pressure distribution between the plates and the block, which is presented in fig. 9. The pressure falls off fairly rapidly from a maximum value at the ends of the plates, the decrease becoming less marked as we approach the centre of the plates, where it is interesting to note that the pressure intensity has risen again. The minimum pressure is about one third the maximum at the ends, whilst that at the centre is just under one half the maximum pressure. This pressure distribution was sensibly the same for the elastic case and all those of plastic straining, slight differences occurring only at the ends. The above distribution may be compared with the theoretical results of Sadowsky (1928), who showed that when a load is applied through a rigid flat die pressing on a semi-infinite plate so that the deflections under it are constant, the distribution of pressure under it is given by

$$p=\frac{\mathrm{P}}{\pi(a^2-y^2)^{\frac{1}{2}}}, \quad . \quad . \quad . \quad . \quad . \quad . \quad . \quad . \quad (9)$$

where P is the total applied load, and $2a$ the width of the plate. This gives $p=\mathrm{P}/\pi a$, a minimum at the centre ($y=0$), and makes $p$ infinite at the ends ($y=\pm a$).

Fig. 9.

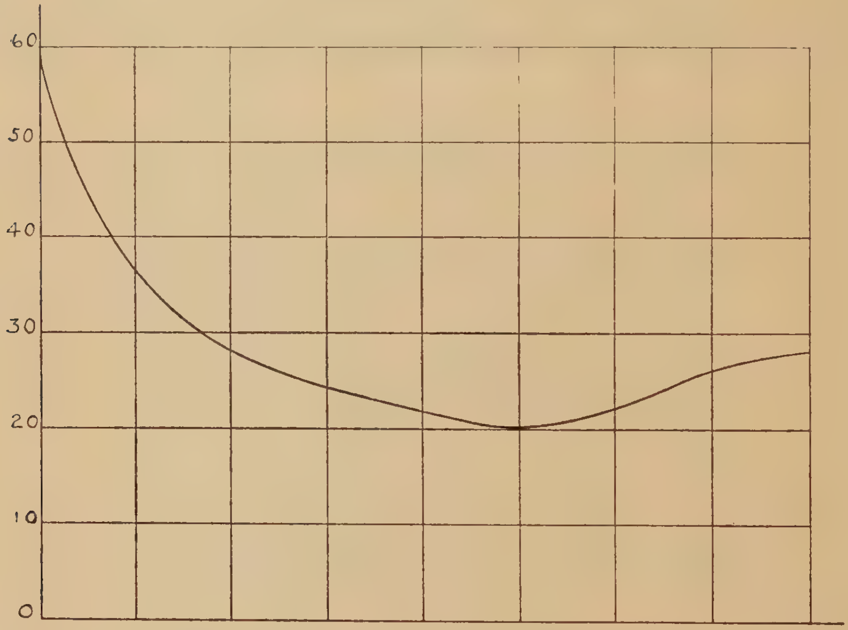

Pressure distribution between plate and block.

One of the reasons for the investigation of this problem was to compare the results obtained with the classical work of Prandtl on indentation. The problem of the indentation of a semi-infinite mass by a flat rigid-punch was first considered by Prandtl (1920), three years before Hencky (1923) published the general equations of the slip-line field. Hill (1949) has pointed out, however, that Prandtl does not seem to have fully appreciated the nature of the problem and the assumptions involved. "Prandtl did not realize the significance of the fact that the plastic boundary can only be determined by a calculation of the stresses in both plastic and elastic regions; nor was he aware of the condition determining the start of indentation, viz. that the plastic region should just include the slip lines from the centre O of the punch face to the free surface (since the slip lines are characteristics of the velocity equations)''. Unfortunately, owing to the extreme rapidity with which the plastic enclave develops after it has reached the centre-line of the block, it was impossible to determine with any great accuracy its further growth. It was not possible, therefore, to determine the plastic boundary when indentaton begins and so make direct comparison with Prandtl's work. The same difficulty, viz. that of determining the exact moment of indentation is also met with experimentally.

## REFERENCES.

FROCHT, M. M., 1947, *Photo elasticity*, 2, 73–74 (John Wiley and Sons, Inc., New York).

HENCKY, H., 1923, *Z. Angew. Math. Mech.*, **3**, 241–251.

HILL, R., 1948, *Journ. Iron and Steel Inst.*, **158**, 177.

HILL, R., and TUPPER, S. J., 1948, *Ibid.*, **159**, 353.

HILL, R., 1949, *Quart. Journ. Mech. and Applied Math.*, **2**, 40–52.

JACOBS, J. A., 1950, *Phil. Mag.*

PRANDTL, L., 1920, *Nachr. Ges. Wiss., Gottingen*, 74.

SADOWSKY, M. A., 1928, *Z. Angew Math. Mech.*, **8**, 107.

# XLI. *Some Extensions in the use of Resistance Thermometry in the Study of Gaseous Explosions.*

By A. Smeeton Leah, Ph.D., A.M.I.Mech.E.,
C. Rounthwaite, B.Sc., and D. Bradley, Ph.D.,
University of Leeds*.

[Received January 25, 1950.]

[Plate XII.]

## Summary.

1. A modified technique for recording resistance wire temperatures is described.

2. By using plain and quartz-coated wires as the resistance elements in explosions a possible method of investigating the course of the reactions occurring within the flame reaction zone is suggested.

3. The corrections to be applied to estimate the true flame gas temperature from the quartz-coated wire records are evaluated.

4. A method of determining the rate of catalytic heating on the plain wires is outlined and the results from a typical explosion of a 90 per cent $CO+10$ per cent $O_2$ mixture at 0·4 atmosphere initial pressure are shown.

5. The thickness of the reaction zone in the early stages of the explosion is estimated to be 4 cm.

## Introduction.

Of the known methods of measuring high temperatures in flame gases, particularly flame gases resulting from gaseous explosions, the resistance wire method has much to commend it. It is easy of application and can yield very reliable information when suitable precautions are taken and the necessary corrections applied. The fusing temperature of the wire used obviously sets a limit to the temperatures which can be recorded. David and co-workers(1) have consistently used this method for studying flame gas temperatures in closed-vessel explosions. The temperatures they have observed have generally been well below the flame temperatures measured by other methods for corresponding inflammable mixtures. Such discrepancies have led to a tendency in some quarters to discredit the method for general use(2). Yet it would appear to us that David(3) has explained qualitatively this seeming anomaly. Conditions in the flame gases resulting from explosions are very probably different from conditions above the inner zone in open flames. Still more convincing experimental proof of the substantial accuracy of the resistance method is afforded by experiments in which flame temperatures have been determined without introducing thermometers or other solid bodies into the flame gases(4). The mean translational temperature of the flame gases was determined by correlating photographically determined flame volumes with pressure rise. It was found that the wire resistance thermometer temperatures agreed very closely with the pressure-volume temperatures, if anything, being slightly on the high side.

---

* Communicated by the Authors.

The usual argument for assuming the resistance method to yield incorrect temperatures appears to be that the inevitable radiation losses from the wires used are excessive. David and co-workers attempted to minimize this by the use of exceedingly fine wires of 0·0005 in. diameter and by this means reduced the error to small proportions. The correction to be applied to the observed wire temperature is amenable to fairly accurate computation and has been calculated for the experiments now to be described.

Of far greater consequence, however, is the possibility of errors caused by surface reactions on the wires due to the diffusion in towards the surface of active particles or uncombined gases. David and co-workers recognized that catalytic reactions might well occur on platinum wires and they therefore used special quartz-coated platinum wires on which no catalysis could occur. By this means the phenomenon of abnormal dissociation in carbon-monoxide explosions was discovered. The use of these two types of wires suggested to us a possible method of studying reactions occurring in the flame gases which has not, hitherto, received much attention.

If two wires, one completely inert to surface reactions and the other having a high catalytic surface activity to any particular reaction, could be used as resistance elements in an explosion, any difference in the temperatures attained by the wires would be a measure of the degree of catalytic heating occurring on the active wire. This principle forms the basis of the method developed by Kondratieva and Kondratiev(5) for detecting H atoms in flame gases. Platinum appears to be particularly effective in catalysing atomic and radical combinations, for example, Smith(6) found a reaction probability of unity for H atom recombination. Quartz-coated wires, on the other hand, are most probably relatively inactive, at least to reactions in carbon-monoxide explosions since they yield temperatures very close to the true translational temperatures of the flame gases. These two types of wires may, therefore, be taken to approximate to the ideal condition.

The technique of David and co-workers was developed in order to study the steady temperatures reached by the flame gases left behind the flame front. But it is certain that the greatest concentration of possible reactants, atoms or radicals or uncombined gases is likely to occur within the narrow zone immediately behind the flame front. In order to study this region a new technique has been developed utilizing a Cathode Ray Oscillograph for recording the rapidly changing wire temperatures. In addition a method of deducing the rate of catalytic heating of the platinum wires based upon dimensional analysis and requiring basic experimental data on the energy required to heat the wires electrically has been developed. These new techniques are described in the present paper. A later paper will show how certain interesting conclusions concerning the presence of atomic oxygen in carbon-monoxide explosions can be deduced from this type of experiment.

## APPARATUS.

A spherical steel explosion vessel of 18 in. internal diameter and equipped with a centrally placed spark gap was used to carry out the explosions. Further details of the explosion vessel and of the earlier technique of recording wire temperatures may be obtained from a paper by David and Jordan(1). The present technique of recording the wire temperatures differed somewhat from that of David and Jordan. A resistance bridge was again used but the bridge was supplied with a high frequency alternating current of 5 milliamps at 1500 cycles per second from an oscillator and the recording was effected by the use of a Cathode Ray Oscillograph (Cosser Model 1035) equipped with a recording camera. The out-of-balance voltage caused by resistance changes of the wires during heating were recorded from the trace on the oscillograph screen as the envelope of the carrier wave curves. The photographic records were measured very accurately by the use of a Cooke, Troughton and Simms toolroom microscope adapted for the purpose.

The wires used were of two types namely, plain platinum-rhodium (10 per cent) wires of 0·0005 in. diameter and quartz-coated platinum-rhodium (10 per cent) wires of 0·0005 in. outside diameter of 0·0002 in. diameter metal core. The wires were electrically welded on to 22 gauge platinum-rhodium leads, in the case of the quartz-coated wires after dissolving off the quartz at the ends with hydrofluoric acid. A length of approximately 1 in. of wire was used in all cases and the wires were positioned $\frac{3}{4}$ in. distance from the spark gap.

The wires were directly calibrated by introducing them quickly into a tubular electric furnace and recording the deflections on the oscillograph screen. The wires were found to attain the furnace temperature in less than two seconds after immersion, the lag being due to the air currents set up by the motion of the wire holder. All the calibrations were therefore carried out at the end of a two-second period. Any prolongation of the immersion beyond a few seconds was found to result in a distinct change in the resistance characteristics of the plain wires due possibly to volatilization of some of the rhodium.

The inflammable mixtures of carbon-monoxide and oxygen were made up in a large tank of 11 cu. ft. capacity and were allowed to mix intimately before use. Similar precautions in drying the gases were taken as in earlier work(7) and the gases used were also from the same source. The mixtures were ignited by means of a high tension electric spark provided by discharging a 3 microfarad condenser which had been previously charged to a sufficiently high voltage by a voltage generator. The apparatus used for determining the electrical energy required to heat up the wires was

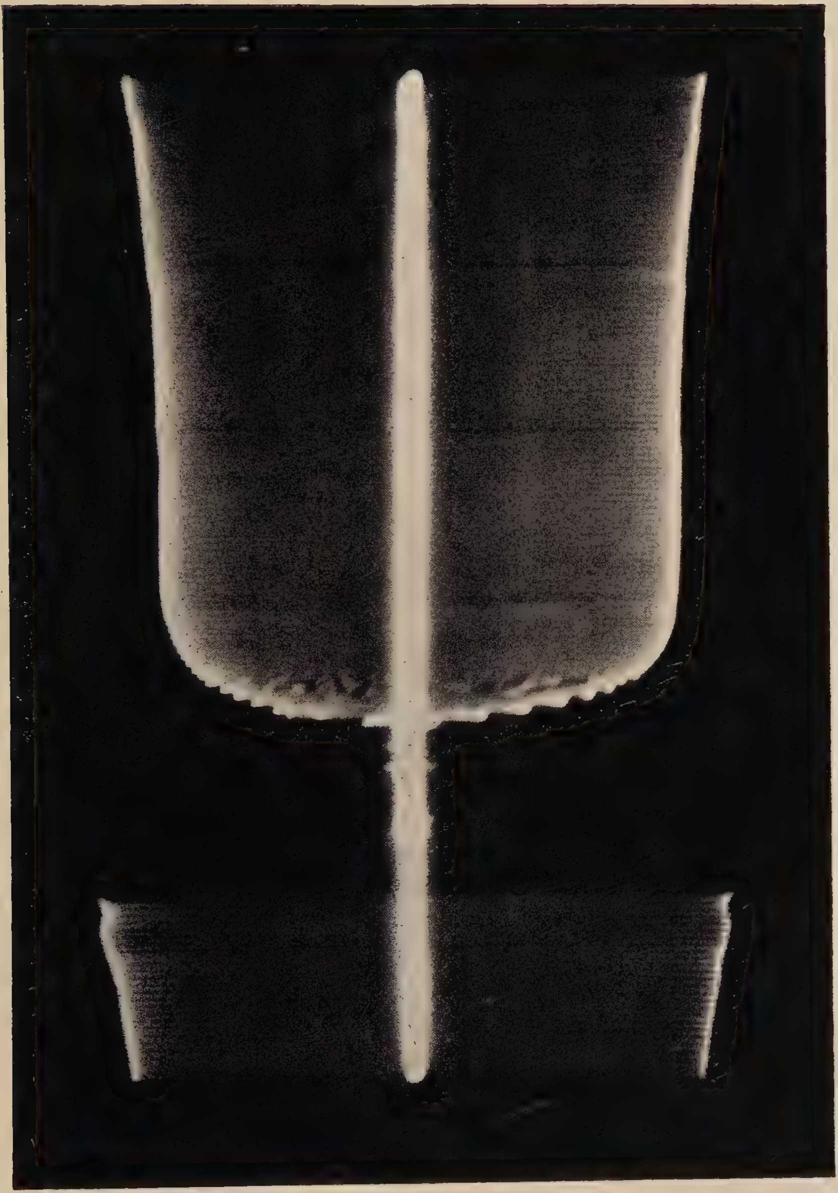

identical with that described by Davies(8). These experiments were undertaken to provide basic data on which to estimate the rates of catalytic heating on the plain wires.

An enlarged reproduction of a typical oscillograph record of wire temperature taken with a quartz-coated wire during an explosion is shown in Pl. XII.

## RESULTS OF EXPERIMENTS.

In a later paper it is hoped to give a comprehensive account of investigations with carbon-monoxide and oxygen explosions carried out at different initial pressures but for the present it would appear better to confine the attention to a single typical explosion for illustrative purposes only. A 90 per cent CO+10 per cent $O_2$ mixture explosion at an initial pressure of 0·4 atmosphere and an initial temperature of 15° C has been chosen for this purpose.

Fig. 1.

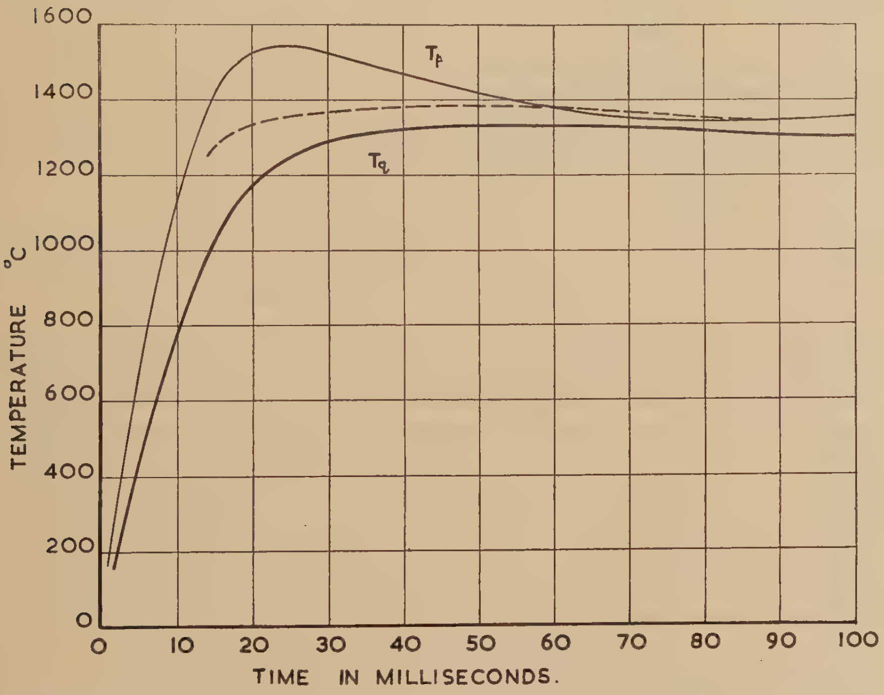

The plain and quartz covered wire temperature records are reproduced in fig. 1, the actual temperatures being plotted against the time from the commencement of the rise of temperature. The plain wire temperatures are given by the curve marked $T_p$ and the quartz-covered wire temperatures by the curve $T_q$. The " hump " on the plain wire curve, $T_p$, will be apparent and indicates that considerable catalytic heating of the wire has occurred. In our view, these records may be taken to represent the changes of temperature of the wires themselves within very close limits. In order to estimate the true translational temperature of the flame gases it will be assumed, for the reasons previously mentioned, that no catalytic surface reactions of any kind occur on the quartz-covered wires. Nevertheless certain corrections must be applied in order to ascertain the true gas temperatures and these will now be considered in detail.

In a general case, let a wire having a temperature T at time $t$ seconds be immersed in a gas maintained at a uniform temperature $T_g$ in an enclosure whose wall temperature is maintained at temperature $T_w$. The wire will be either gaining or losing heat by conduction and convection from the gas and will be gaining or losing heat from the walls of the enclosure by radiation. In addition, let the wire be receiving heat by some other means (*e. g.* by electrical heating or catalytic surface heating) at the rate of S watts per sq. cm.

If H = the rate of heat loss by conduction and convection in watts per sq. cm. of wire surface.
R = the rate of heat loss by radiation in watts per sq. cm.
$m$ = mass of wire in gm. per sq. cm. of surface.
$k$ = mean specific heat of wire in watt-sec. per gm. per °C.

the equation of heat flow for the wire will be :—

$$mk\frac{dT}{dt} = S - R - H. \qquad \qquad (1)$$

The function R is dependent only upon the temperature of the wire and that of the vessel walls. It is the same for a wire *in vacuo* as for a wire in a surrounding gas. The function H is dependent on the gas temperature and on the wire temperature. A method of determining these functions will be given shortly but first consider the curves of fig. 2 showing the functions R and H for a particular case, the function H being for a gas temperature $T_g = 1300°$ C.

For quartz-coated wires it has been assumed that there is no catalytic heating, thus S = 0. When the wire temperature has attained a steady value, $T_s$, the rate of heat accumulation $mk(dT/dt) = 0$, thus R + H = 0.

The wire temperature, $T_s$, will be given by the point A on the diagram where this condition is fulfilled, for there, the curve (H + R) cuts the temperature axis.

Alternatively, if $T_s$ is known the gas temperature $T_g$ may be found in the following manner. The function H is determined for various assumed values of $T_g$ and the corresponding (H + R) curves are plotted. They are found to be very nearly parallel curves as will be seen from the broken line curves of fig. 2 which refer to gas temperatures of 1110° C. and 900° C. If the wire temperature were raised to equal the gas temperature $T_g$, the conduction and convection heat transfer would be zero, or H = 0. The point B in fig. 2, therefore gives the gas temperature $T_g$ which is also given by the point of intersection, D, of the curve R and the curve (H + R)*.

---

* This principle forms the basis of the heated wire method of determining flame temperatures used by Schmidt (9) and Kohn (10).

Thus with $T_s$ known the point A is located and the (H+R) curve passing through this point is continued to intersect the curve R in D giving the gas temperature $T_g$. If the wire temperature is below the steady value the wire will be receiving heat at the rate :

$$mk\frac{dT}{dt} = -(H+R) \quad \text{(from equation (1))}.$$

Fig. 2.

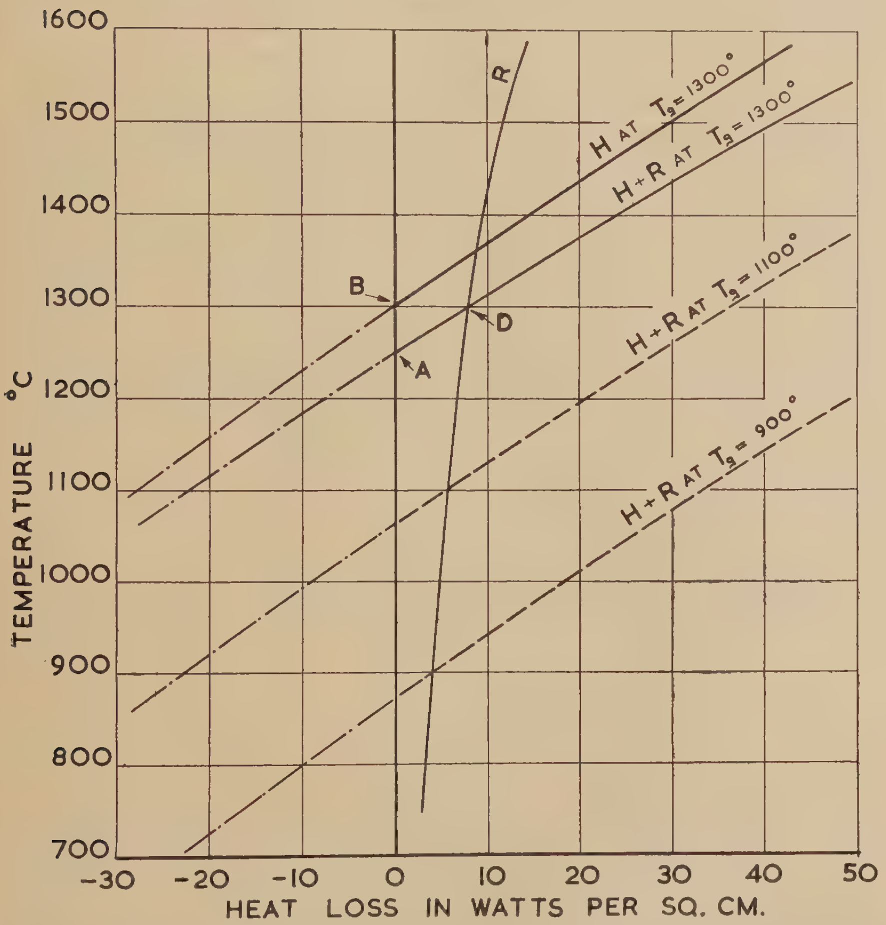

From the record of the temperature changes of the wire, $dT/dt$ may be determined at any time $t$ as well as the wire temperature T. The gas temperature may again be inferred from the curves of fig. 2 by marking a point with co-ordinates $-mk(dT/dt)$ and T and following the (H+R) curve passing through this point until it cuts the curve R in D giving the gas temperature $T_g$.

It will be evident, therefore, that providing the functions H and R can be determined the quartz-coated wire temperatures may be corrected to yield the flame gas temperatures.

The radiation loss R was determined by the use of the Stefan-Boltzman law using values for the emissivity of quartz surfaces given by Pirani(11) up to fairly high temperatures. Doubtless some of the radiation from the platinum-rhodium core will be transmitted through the quartz coating resulting in a effective emissivity somewhere between those for the two materials. But since the two emissivities are not appreciably different at high temperature little error will result from using the value for quartz. For the case of platinum-rhodium wires, which will be dealt with later, values for the emissivity were Hottel's values taken from Brown and Marco(12).

The determination of the rate of conductive and convective loss values, H, is a matter of some considerable difficulty. The flame gases in an explosion are in motion due to the adiabatic compression resulting from the rising pressure. This motion will set up a forced convection loss from the wires in addition to the natural convection loss. Fortunately, in the very early stages of an explosion, whilst the flame diameter is small in relation to the diameter of the explosion vessel, the pressure rise is so small that the gas velocities due to compression are small enough to be neglected in relation to the natural convection velocities. With this simplification it is possible to predict the conduction and natural convection losses from electrically heated wire experiments by means of dimensional analysis.

The rate of heat loss by conduction and convection, H per sq. cm. of wire surface will be dependent on the following factors :—

D, the diameter of the wire.

$T_g$, the temperature of the surrounding gas.

$T_d$, the temperature difference between the wire and the surrounding gas.

P, the pressure of the gas.

K, the thermal conductivity of the gas.

$\mu$, the viscosity of the gas.

$C_p$, the specific heat of the gas at constant pressure.

g, the acceleration due to gravity (to allow for the buoyancy of the gas undergoing natural convection).

Thus,

$$H=\phi[D, T_g, T_d, P, K, \mu, C_p, g].$$

This relation must be dimensionally homogeneous and can be expressed by a relation involving five dimensionless quantities, the most convenient for the present investigation being :

$$\frac{H}{D^{1/2}Pg^{1/2}}=\psi\left[\frac{T_d}{T_g}, \frac{KT_g}{D^{3/2}Pg^{1/2}}, \frac{C_p\mu}{K}, \frac{C_pT_g}{Dg}\right]. \quad . \quad . \quad . \quad (2)$$

The quantity $C_p\mu/K$, Prandtl's Number, is very nearly constant for all diatomic and triatomic gases and in addition, the wire diameter D is constant, thus equation (2) may be reduced to :

$$\frac{H}{P} = \psi'\left[\frac{T_d}{T_g}, \frac{KT_g}{P}, C_pT_g\right]. \quad \dots\dots \quad (3)$$

The relationship between the quantities in equation (3) was determined by measuring the power required to heat, electrically, in various quiescent gases at different pressures from 2·5 to 250 mm. Hg Abs., samples of the wires used in the explosion experiments. The wires were heated from atmospheric temperature up to about 400° C, and since the radiation losses are but a very small fraction of the conduction and natural convection losses at these low temperatures, the power input represents very closely the conduction and convection rate of loss. The results of these experiments are shown in fig. 3, values of H/P being plotted against $KT_g/P$ for different values of the ratio $T_d/T_g$ and for two gases, namely air and hydrogen, having widely different values of $C_pT_g$. It will be seen that the value of $C_pT_g$ has no effect at the lower values of $KT_g/P$ and only a slight effect at the higher values. For this reason little error will result in performing a linear interpolation between the extreme values of $C_pT_g$ for intermediate values. It may be mentioned that when the heating

Fig. 3.

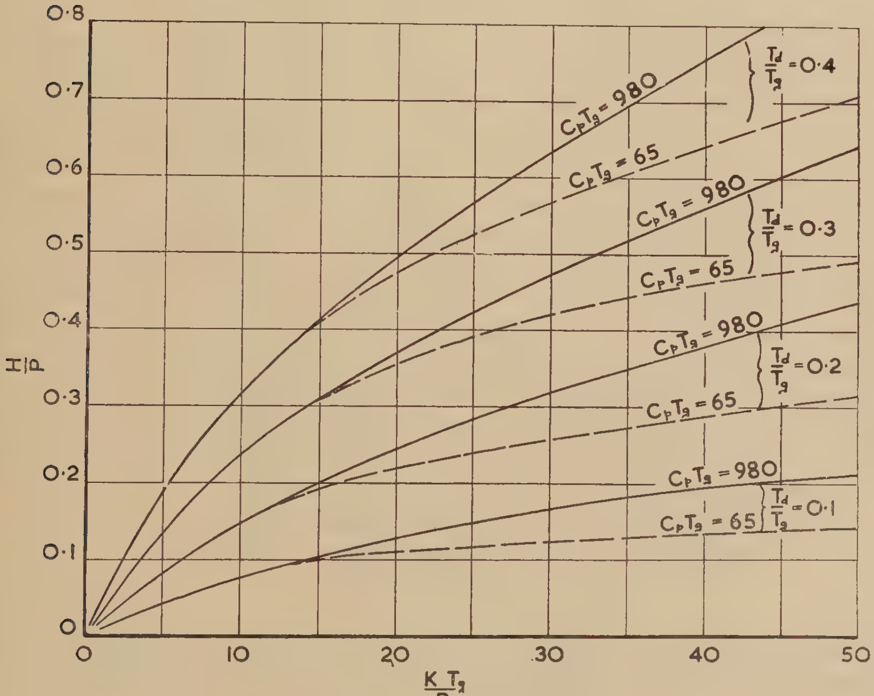

experiments were conducted with carbon-dioxide the resulting curves agreed identically with those for air in fig. 3 as was expected since the heat capacities of $CO_2$ and air per unit mass are very nearly the same.

In order to estimate the conduction and natural convection loss from a wire heated in any gas, the values of $KT_g/P$ and $C_pT_g$ are computed for the known temperature and pressure conditions of the gas. From the curves of fig. 3, the value of H/P is found for different values of the ratio $T_d/T_g$ and the corresponding values of H and $T_d$ yield the heat loss curve, H, shown in fig. 2 from which the (H+R) curve may be constructed. The values of H will only be obtained for positive values of $T_d$, (*i. e.* when the wire is above the gas temperature). Fortunately the H curves are very nearly straight lines and may safely be extrapolated to negative values of $T_d$, giving negative heat loss values. Such extropolated values are shown in fig. 2 by the chain-dotted part of the H curve. The corresponding portions of the (H+R) curves are also shown chain dotted.

The quartz coated wire temperatures of fig. 1 have been corrected for radiation and heat capacity in the manner described and the corrected curves are shown by the broken line in fig. 1. These corrected values will represent the true gas temperature providing no surface heating has occurred due to catalytic reactions, as we have assumed to be the case. Should it happen that catalytic reactions do occur, then the broken line curve of fig. 1 will give over-estimates of the true gas temperature.

Turning now to the plain wire temperature record of fig. 1, here it is apparent that catalytic surface reactions are occurring causing the wire temperature to exceed the gas temperature. At any instant the wire temperature $T=T_p$ is known, the gas temperature $T_g$ may be found from the corrected quartz-coated wire temperatures and the rate of rise of wire temperature $dT/dt$ is known. Thus from equation (1):

$$S=H+R+mk\frac{dT}{dt}.$$

Knowing the gas temperature $T_g$, the function H may be determined and the curve of H+R constructed as shown in fig. 2. The value of H+R at the wire temperature $T_p$ can be read off this curve and the rate of catalytic heat reception can then be directly computed.

Values of the rate of catalytic heating for the explosion under consideration are shown in fig. 4 plotted against the time from the commencement of the rise of temperature. As would be expected from the temperature curves of fig. 1, the rate of heating diminishes to zero after about 50 milliseconds from which it may be concluded that at this time after the passage of the flame front the reacting species have disappeared from the flame gases.

No attempt has been made in this work to measure the flame velocities by photographic, or other means. An estimate of the mean flame velocity can be found, however, from the time taken to reach maximum pressure after the passage of the igniting spark. The mean flame speed appears to be of the order of 80 cm. per sec. If the reaction zone in the advancing flame front is defined as that zone in which species exist which set up the catalytic surface reactions on the plain wires, its depth must be 0·05×80=4 cm. That is to say, the flame front will be 4 cm. beyond the wire when catalytic activity on the wire surfaces ceases. This is far and away above the thicknesses calculated by Lewis and von Elbe⁽¹³⁾ for ozone explosions but is not surprising in view of the much slower burning gas we have used, quite apart from the very different chain mechanism by which the flame is propagated.

Further discussion will be deferred and given in a subsequent paper.

Fig. 4.

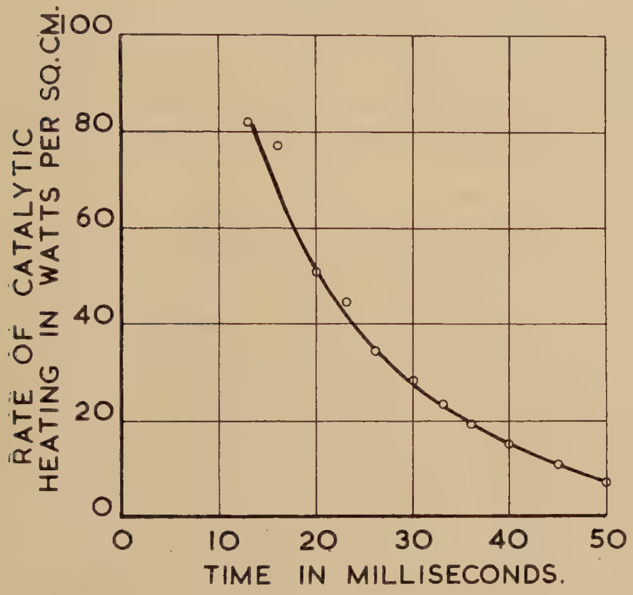

## References.

(1) David and Jordan, 1934 a, *Phil. Mag.*, **17**, 172 ; 1934 b, *Ibid.*, **18**, 228.
David, Leah, and Pugh, 1941, *Phil. Mag.*, **31**, 156.
(2) *Cf.* Lewis and von Elbe, 1935, *Engineering*, **139**, 168.
Ribaud, Laurie, and Gaudry, 1939, *J. Inst. Fuel*, **12**, 18.
(3) David, 1937, *Phil. Mag.*, **22**, 251.
David, Leah, and Pugh, 1937, *loc. cit.*
(4) Leah, 1943, *Phil. Mag.*, **34**, 795 ; *Ibid.*, 1947, **38**, 657.
(5) Kondratieva and Kondratiev, 1946, *Acta. Physicochimica, U.R.S.S.*, **21**, 1.
(6) Smith, 1943, *J. Chem. Phys.*, **2**, 110.
(7) Leah, 1947, *Phil. Mag.*, **38**, 657.
(8) Davies, 1934, *Phil. Mag.*, **17**, 233.
(9) Schmidt, 1909, *Ann. Physik*, **29**, 1027.
(10) Kohn, 1914, *Ann. Physik*, **44**, 749.
(11) Pirani, 1939, *J. Scientific Instruments*, **16**, 377.
(12) Brown and Marco, 1942, *Introduction to Heat Transfer*, McGraw-Hill.
(13) Lewis and von Elbe, 1938, *Combustion, Flames and Explosions of Gases*, Cambridge.

# XLII. *Atomic Oxygen in Carbon-Monoxide Explosions.*

By A. Smeeton Leah, Ph.D., A.M.I.Mech.E., C. Rounthwaite, B.Sc., and D. Bradley, Ph.D.,
University of Leeds †.

[Received March 2, 1950.]

## Summary.

Catalytic heating on plain platinum wires has been studied by a method described in a previous paper and has been ascribed to the presence of high concentrations of atomic oxygen within the reaction zone of 10 per cent $O_2+90$ per cent CO gaseous explosions carried out in a large spherical explosion vessel. The atomic oxygen quickly disappears in the flame gases according to an overall reaction process which gives an effective first order reaction constant. The atomic oxygen content of the flame gases is also shown to account for only a small part of the total " missing " energy in the explosions.

Contemporary theories of flame propagation in gaseous explosions recognize the important part played by the diffusion of active particles such as atoms or radicals into the unburnt gases ahead of the advancing flame front. These active particles being capable of initiating chain branching reactions in the unburnt gases multiply their concentration to a value far in excess of the equilibrium value as was shown by Jost and Müffling (1938) and more recently by Tanford (1947). Making certain simplifying assumptions Lewis and von Elbe (1934, 1938) were able to evolve a theoretical treatment allowing for the effects of diffusion which enabled them to calculate the flame speeds in ozone explosions with remarkable accuracy. Their analysis showed that the concentration of atomic oxygen in the reaction zone rises from the equilibrium value in the unburnt gases ahead of the flame front, passes through a maximum and reverts to the corresponding equilibrium value in the burnt gases behind the flame front when all reactions are completed. It is not yet possible to carry out analyses similar to that of Lewis and von Elbe for other gaseous inflammable mixtures as insufficient is known of the kinetics of the chain reactions involved in the combustion process. There is no doubt, however, that whatever inflammable mixture is used, the concentrations of the particular active species taking part in the reaction will pass through well defined maxima somewhere in the reaction zone. There is certainly some doubt about whether the concentrations of the active species rapidly attain the normal equilibrium values in the burnt gases left behind the flame front since electronically excited molecules, and possibly vibrationally excited molecules, remain in these gases for a long time, as evidenced by the long-sustained afterglow.

---

† Communicated by the Authors.

In the case of carbon-monoxide, oxygen explosions, although a theoretical analysis cannot yet be undertaken, it has become possible in certain cases to determine experimentally the concentration of atomic oxygen in the reaction zone by utilizing the technique of wire resistance thermometry described in a previous paper (Leah, Rounthwaite and Bradley, 1950), by which the rate of catalytic heating of platinum wires could be determined. Consider for a moment a general case ; if it were known that a particular active species would react catalytically on one type of resistance wire element with some other reactant present in large excess, whereas with some second type of resistance wire element no surface reactions at all could be sustained, then providing the reaction probability on the surface of the first type of wire were known, the observed rate of catalytic heating should be a direct measure of the rate of diffusion to the wire of the particular active species involved. From this an estimate could be made of the concentration of the active species in the surrounding gases. This principle has been utilized by Kondratieva and Kondratiev (1946) in their method of measuring the concentration of atomic hydrogen in the slow reaction flames of hydrogen–oxygen mixtures. They used two similar thermocouples, one coated with $ZnOCr_2O_3$ which has a high reaction probability towards hydrogen atom recombination and the other coated with KCl, which has a very low reaction probability, as was shown by Taylor and Lavin (1930) and W. V. Smith (1943).

In explosions of dry, hydrogen free, $CO–O_2$ mixtures it would appear that the only active species which are likely to be present in the flame gases are O atoms, excited oxygen molecules $O_2^*$ and excited carbon-dioxide molecules $CO_2^*$. Gaydon (1946) has demonstrated the presence of O atoms in $CO–O_2$ open flames by means of the nitric oxide test. Similarly Kondratjew (1937) has shown that low pressure flames of $CO–O_2$ mixtures contain a large concentration of $CO_2^*$. The presence of these active species in the explosion flame gases is, therefore, highly probable. Laidler (1949) has shown recently that $O_2^*$ is also present in flame gases resulting from the combustion of $CO–O_2$ mixtures containing excess $O_2$ but if the mixtures contain a large excess of CO then it seems unlikely that $O_2^*$ will be present in large amounts during explosions. In fact it would seem that with these mixtures the most probable active species will be O atoms and $CO_2^*$.

In any case, since the mixtures contain a large excess of CO, it is certain that any O atoms or normal $O_2$ molecules (or excited $O_2^*$ molecules if any are present) would react catalytically with the CO on plain platinum wires. The work of Langmuir (1921) indicates that the reaction probability would be very high on platinum and indeed Smith (1948) shows that platinum has a reaction probability of unity towards certain atomic and radical combinations. In addition, of course, there will be the possibility of recombination of O atoms taking place on the surface together with heating effects due to the normalizing of $CO_2^*$ on striking the wire. With quartz-coated wires, however, the catalytic surface reactions will be inhibited although the surface effects due to $CO_2^*$ and recombination of O atoms may still take place in some degree. If the heating due to these effects were substantial then the quartz-coated wires should record temperatures well in excess of the true translational temperature of the flame gases, due allowance being made for radiation losses from the wires. The quartz-coated wires, however, have been shown to yield values of gas temperatures which are not greatly in error (Leah 1943) and it must be concluded that only a relatively small surface heating occurs with these wires. But in any case it is reasonable to suppose that similar surface effects will occur on the plain platinum wires and hence, the differences in the temperatures observed with the two types of wires should still be a measure of the catalytic heating due to $O_2$ and O atom combination with CO on the plain wires.

Although it will not be possible to say what proportion of the observed catalytic heating of the plain platinum wires is due to O atoms or to $O_2$ molecules it is possible to prove that the heating is not due to the combination of $O_2$ with CO alone. Analysis shows that if it is assumed that the high rate of catalytic heating observed in the early stages of the explosions is due to $O_2$ alone, the concentration of the $O_2$ in the high temperature flame gases would require to be a very large proportion of that in the unburnt mixture, a condition which is obviously absurd. In fact it is evident that the catalytic heating must be due, in very large measure, to the combination of O atoms with CO on the platinum wires. Since the mixtures chosen contain a large excess of CO, and since it will be taken that the reaction probability of platinum for the O atom—CO reaction is unity, the rate of catalytic heating will be governed by the rate at which the O atoms diffuse to the wire surface from the surrounding gas.

As it is the object of the present work to estimate the concentration of the atomic oxygen in the flame gases well removed from the influence of the wires, it will be essential before proceeding further, to form some idea of the rate of reaction causing the disappearance of O atoms in the gas phase. In this connection the catalytic heating curve given in the previous paper, and reproduced later in fig. 3 of the present work, gives an indication of the rate of disappearance of the active species causing the catalytic heating of the wires irrespective of the particular identity of the species concerned. The rate of catalytic heating will be proportional to the rate of diffusion of the reacting species to the wire surface, and this in turn may be taken, as a first approximation, to be proportional to the concentration of the species in the surrounding flame gases. On plotting the logarithm of the rate of catalytic heating against time, as in fig. 1, the experimental points are seen to lie very nearly on a straight line. This indicates that the rate of reaction of the active species is given by the expression

$$\frac{d[x]}{dt}=g[x],$$

where $g$ is a constant, and $[x]$ the concentration of the species. If the species is wholly atomic oxygen, then it will be reasonable to infer that $d[\mathrm{O}]/dt=g[\mathrm{O}]$. An alternative argument leads to the same conclusion as follows :

The most probable reactions occurring in the reaction zone would appear to be those suggested by Semenov (1935) namely,

$$\mathrm{O}+\mathrm{CO}\rightarrow\mathrm{CO}_2^*, \quad . \; . \; . \; . \; . \; . \; . \; . \; . \; . \quad (1)$$

$$\mathrm{CO}_2^*+\mathrm{O}_2\rightarrow\mathrm{CO}_2+2\mathrm{O}, \quad . \; . \; . \; . \; . \; . \; . \; . \; . \quad (2)$$

$$\mathrm{O}+\mathrm{CO}+\mathrm{M}\rightarrow\mathrm{CO}_2+\mathrm{M} \quad . \; . \; . \; . \; . \; . \; . \; . \quad (3)$$

(where M is any third body).

Fig. 1.

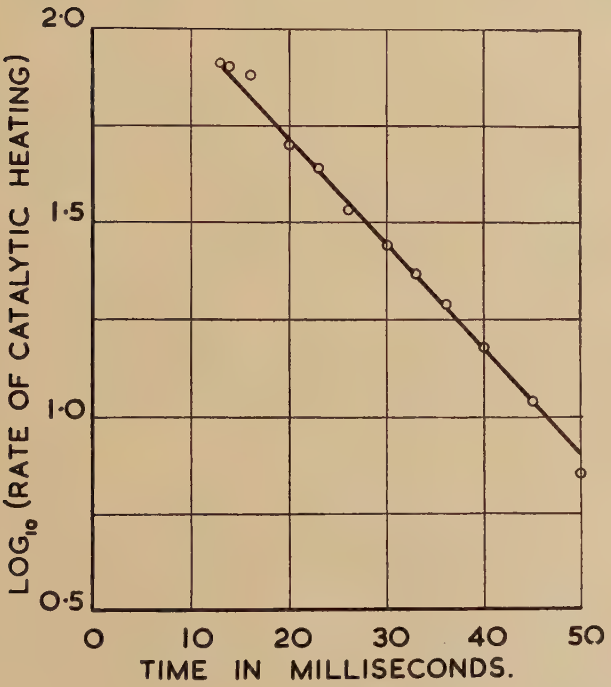

In addition there will be certain reactions involving $\mathrm{O}_3$ and probably the chain branching reaction suggested by Hinshelwood (1940),

$$\mathrm{O}+\mathrm{CO}+\mathrm{O}_2\rightarrow\mathrm{CO}_2+2\mathrm{O},$$

although Semenov (1935) has pointed out certain objections to this reaction. The explosion flames would appear to be propagated chiefly by the branching chain reactions (1) and (2) whereas the disappearance of O atoms from the reaction zone would seem to be most probably accounted for in large measure by the chain breaking reaction (3).

When the flame front has passed beyond the wires, the temperature of the plain wires rises very rapidly corresponding to the period of most intense chain branching in the reaction zone. After this stage, which is the period when the O atoms are disappearing and with which period the present work is mainly concerned, the reactions then proceeding will be dominated by those of a chain-breaking character. The rate of decay of the O atoms will be given by

$$\frac{d[\mathrm{O}]}{dt}=f([\mathrm{O}],[\mathrm{CO}],[\mathrm{O}_2],[\mathrm{O}_3],[\mathrm{CO}_2],[\mathrm{CO}_2^*]). \quad . \quad . \quad . \quad (4)$$

It would appear that the greatest contribution to the function (4) is likely to be that due to reaction (3), and since CO is present in large concentration during the later stages in the reaction zone, then, at any one pressure and temperature, we may write as a first approximation

$$\frac{d[\mathrm{O}]}{dt}=g[\mathrm{O}]. \quad . \quad . \quad . \quad . \quad . \quad . \quad . \quad . \quad (5)$$

Here $g$ is very nearly a constant at any one pressure and temperature, and it will be shown later that, during the period of the explosions we are concerned with, the pressure and temperature do remain substantially constant and equation (5) will then apply.

The concentration of the atomic oxygen in the flame gases may be determined from the catalytic heating curve by means of the following analysis :

Let $n'$=the concentration of atomic oxygen in the flame gases away from the influence of the wires at time $t$.

Then

$$\frac{dn'}{dt}=gn'. \quad . \quad . \quad . \quad . \quad . \quad . \quad . \quad . \quad . \quad (6)$$

Let $n$=the concentration of atomic oxygen at a distance $r$ from the centre of a plain platinum wire at time $t$,

$a$=radius of the wire,

D=diffusion coefficient for O atoms diffusing into the flame gases.

Neglecting the relatively small temperature gradient in the flame gases surrounding the wires the diffusion equation will be

$$\frac{dn}{dt}=\mathrm{D}\left\{\frac{\partial^2 n}{\partial r^2}+\frac{1}{r}\frac{\partial n}{\partial r}\right\}+gn. \quad . \quad . \quad . \quad . \quad . \quad . \quad (7)$$

Imagine the wire to be suddenly immersed in the gases at time $t=0$ and let it be assumed that $n=n'=n_0$ at $t=0$, an assumption which will be seen to be reasonably close in the later part of this paper.

Subsequently, since the reaction probability at the wire surface is unity $n=0$ at the wire surface at all times after $t=0$.

*i. e.* for $t>0$, $\quad n=0 \quad$ at $\quad r=a$.

In order to solve equation (7) let

$$n=n'(n''+1), \qquad (8)$$

where $n'$ is defined by equation (6) and is independent of $r$ and $n''$ is defined by

$$\frac{dn''}{dt}=\mathrm{D}\left\{\frac{\partial^2 n''}{\partial r^2}+\frac{1}{r}\frac{\partial n''}{\partial r}\right\}. \qquad (9)$$

It can easily be shown that relations (8) and (9) satisfy the diffusion equation (7). The boundary conditions will be :

At $t=0$, $n''=0$ for $r>a$

and also for $t>0$, $n''=-1$ at $r=a$.

Carslaw and Jaeger (1947) show the solution of (9) with these boundary conditions to be

$$n''=-1-\frac{2}{\pi}\int_0^\infty \exp\,(-\mathrm{D}u^2t)\,\frac{\mathrm{J}_0(ur)\mathrm{Y}_0(ua-)\mathrm{Y}_0(ur)\mathrm{J}_0(ua)}{\mathrm{J}_0^2(ua)+\mathrm{Y}_0^2(ua)}\,\frac{du}{u}$$

and also that

$$\left(\frac{\partial n''}{\partial r}\right)_{r=a}=\frac{4}{a\pi^2}\int_0^\infty \exp\,(-\mathrm{D}z^2t/a^2)\,\frac{dz}{z[\mathrm{J}_0^2(z)+\mathrm{Y}_0^2(z)]}, \qquad (10)$$

where $z=au$.

For large values of $\mathrm{D}t/a^2=x$, Carslaw and Jaeger give an approximation for the right hand side of (10)

$$\left(\frac{\partial n''}{\partial r}\right)_{r=a}=\frac{4}{a\pi^2}\left[\frac{\pi^2}{2}\left\{\frac{1}{\log_e(4x)-2\gamma}-\frac{\gamma}{(\log_e(4x)-2\gamma)^2}\right\}+\text{etc.}\right], \qquad (11)$$

where $\gamma$=Euler's constant=0·57722. From (8)

$$\left(\frac{\partial n}{\partial r}\right)_{r=a}=n'\left(\frac{\partial n''}{\partial r}\right)_{r=a}. \qquad (12)$$

Substituting (11) in (12) and multiplying through by D

$$\mathrm{D}\left(\frac{\partial n}{\partial r}\right)_{r=a}=\frac{2\mathrm{D}n'}{a}\left[\frac{1}{\log_e(4x)-2\gamma}-\frac{\gamma}{(\log_e(4x)-2\gamma)^2}+\text{etc.}\right]. \qquad (13)$$

The left hand side of (13) is the rate at which O atoms are striking the wire per unit surface and may be determined from the catalytic heating curves, at any time $t$, hence $n'$ can be found at this time $t$.

### *Explosions of a* 10 *per cent* $O_2$+90 *per cent* CO *Dry Mixture.*

These explosions were carried out in the same spherical explosion vessel of 18 in. internal diameter and utilizing the same technique of determining rates of catalytic heating on plain platinum–rhodium wires as was described in a previous paper (Leah, Rounthwaite and Bradley 1950). In fig. 2 (*a*) are shown the plain and quartz-coated wire temperatures attained in an explosion of a dry, hydrogen free mixture of 10 per cent

$O_2$+90 per cent CO at an initial pressure of 0·4 atmosphere and an initial temperature of 15° C. These curves are reproduced from the previous paper as also is the full line curve of fig. 3 showing the variation of the rate of catalytic heating deduced from the temperature records of fig. 2 (*a*). The flame gas temperature obtained by correcting the quartz-coated wire

Fig. 2.

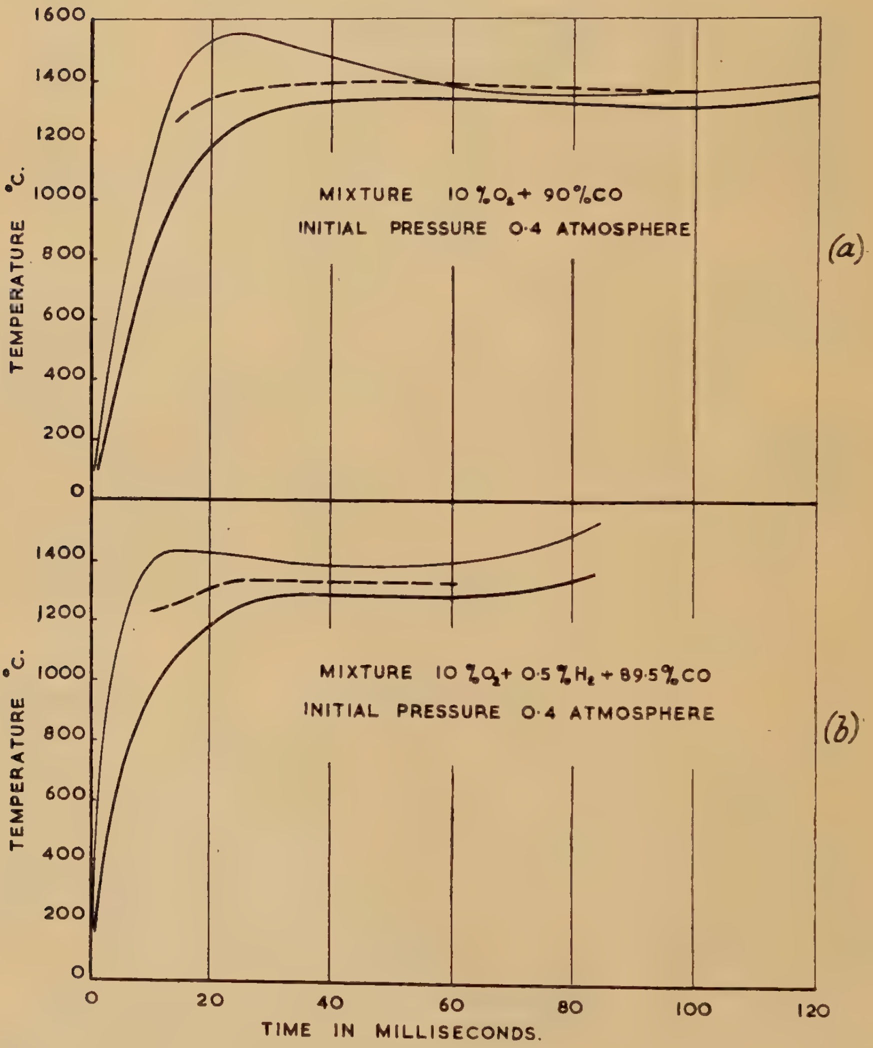

temperaure for radiation and heat capacity effects is shown in fig. 2 (*a*) by the broken line. It will be seen that the flame gas temperature is well below the ideal constant pressure temperature for this mixture, which is 1680° C., and that it remains reasonably constant, sufficiently so to be taken as constant in the subsequent diffusion analysis.

It is rather important to note that the temperature records are only of value in the present work during the early stages of the explosions whilst the gases are being burnt at very nearly constant pressure. After the so-called "pre-pressure" period the wire temperatures increase in consequence of the increase of flame gas temperature due to adiabatic compression resulting from the rising pressure. This temperature rise will be seen in the records reproduced in fig. 2 (*a*) and the portions of the curves beyond the point at which the rise commences have therefore been discarded in the subsequent analysis.

Taking the reaction $O+CO=CO_2+127$ kcals. to be proceeding exclusively on the plain wire it is possible to deduce the number of O atoms and CO molecules which must be reacting on the wire in order to release the amount of heat given by the curves of fig. 3.

Fig. 3.

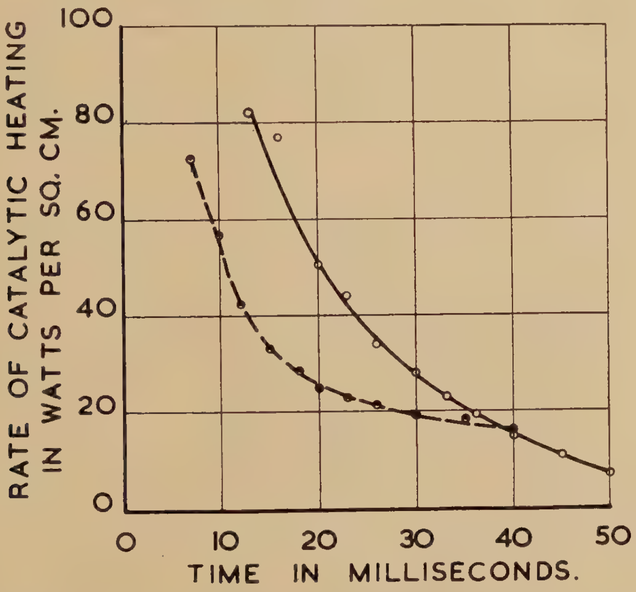

In accordance with the previous assumption that every atom of oxygen striking the wire reacts with CO the number of atoms reacting per sq. cm. per sec. is $D(\partial n/\partial r)_{r=a}$.

Thus, from equation (13), the concentration of O atoms, $n'$, in the gases beyond the influence of the wire may be obtained. These values are given in Table I. for various times from the initial rise of temperature of the platinum wire. It should be noted that $n'$ is the concentration of O atoms above the equilibrium concentration but as the latter is minute in the present explosions of mixtures containing excess CO, the values given may be taken to be the absolute concentrations. In using equation (13) the diffusion coefficient for the O atoms has been evaluated from the expressions of Chapman and Cowling (1939) using molecular data given by Rice (1940), and in the *Smithsonian Physical Tables* (1934).

TABLE I.

| Time in milliseconds | O-atom concentration atoms per c.c. $\times 10^{-16}$ | Percentage O-atoms by volume |
|---|---|---|
| 13 | 2·34 | 1·30 |
| 16 | 2·22 | 1·25 |
| 20 | 1·47 | 0·80 |
| 23 | 1·30 | 0·70 |
| 26 | 1·01 | 0·55 |
| 30 | 0·88 | 0·50 |
| 33 | 0·70 | 0·40 |
| 36 | 0·59 | 0·35 |
| 40 | 0·46 | 0·25 |
| 45 | 0·33 | 0·20 |
| 50 | 0·22 | 0·10 |

Fig. 4.

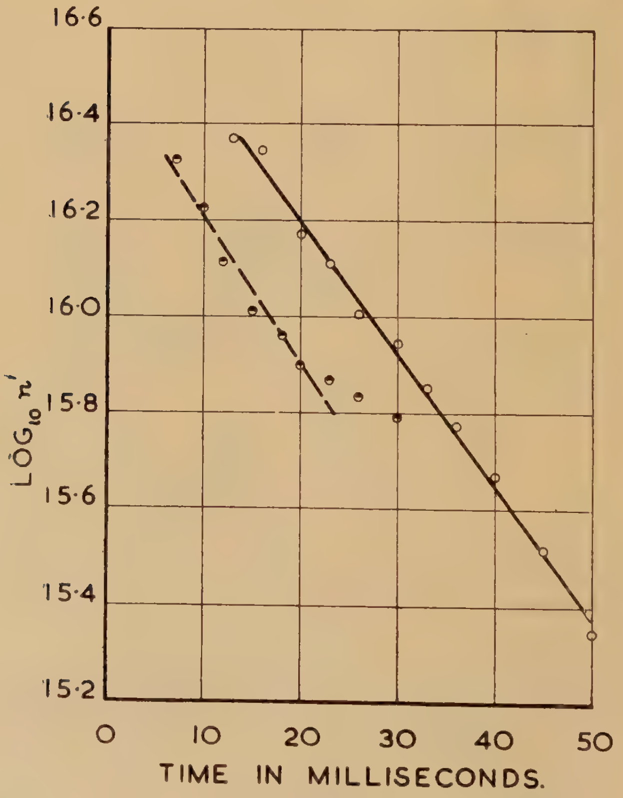

If the rate of decay of the O atom concentration in the gas phase is given reasonably closely by equation (6) then $\log_e n' = gt + a$ constant. Plotting $\log_{10} n'$ against $t$ for the explosion the full line curve of fig. 4

is obtained. It will be observed that for the greater part of the curve the experimental points lie very closely on a straight line, the slope of the line being proportional to $g$. The actual value of $g$ obtained is 61 $\text{sec.}^{-1}$ at a mean gas temperature of 1360° C. and at 0·4 atmosphere pressure. The fact that the relationship between log $n'$ and $t$ is linear seems to lend strong support to the assumption which was made that the rate of decay of the O atoms was given closely be equation (V).

Explosions of this same mixture at higher initial pressure, up to 1 atmosphere, also show similar effects, the relationship between log $n'$ and $t$ always being linear in the early stages. Unfortunately it was found impossible to ignite a dry 10 per cent $O_2+90$ per cent CO mixture at pressures very much below 0·4 atmosphere and even when the mixtures did ignite at slightly lower pressures the flame speed was so low that convective rise of the inflamed gases caused them to rise out of the field of the wires. For this reason it was felt that a little hydrogen should be added to the mixtures in order to facilitate ignition at the lower pressures and to effect more rapid combustion. A new series of experiments was therefore carried out with a mixture consisting of 10 per cent $O_2+0{\cdot}5$ per cent $H_2+89{\cdot}5$ per cent CO.

### *Explosions of a* 10 *per cent* $O_2+0{\cdot}5$ *per cent* $H_2+89{\cdot}5$ *per cent* CO *Dry Mixture.*

It was, of course, appreciated that the addition of hydrogen to the mixture must have a profound influence upon the reaction mechanism of the explosions. This case has been considered qualitatively by Semenov (1935), Hinshelwood (1940), Lewis and von Elbe (1934, 1938) and others. Additional reactions of the following types will be introduced :

$$\begin{gathered}
H+O_2\rightarrow OH+O,\\
O+H_2\rightarrow OH+H,\\
OH+H_2\rightarrow H_2O+H,\\
OH+CO\rightarrow CO_2+H,\\
H+O_2+M\rightarrow HO_2+M,\\
CO+HO_2\rightarrow CO_2+OH.
\end{gathered}$$

They have the effect of very materially increasing the rapidity of chain branching and the velocity of flame propagation but whether they should greatly effect the concentration of O atoms in the later stages of reaction it seemed impossible to predict. At the outset, therefore, explosions were carried out at an initial pressure of 0·4 atmosphere so that a direct comparison could be made with the hydrogen-free mixture previously used. The temperature records are shown in fig. 2 (*b*) together with the flame gas temperatures deduced from the quartz-coated wire temperatures. The corresponding catalytic heating curve is shown by the broken line of fig. 3. Comparison of fig. 2 (*b*) with fig. 2 (*a*), the latter referring to the hydrogen free mixture, and also comparison of the corresponding two curves of fig. 3, reveals that the rates of catalytic heating due to reactions on the plain wires are of the same order and decay in a similar manner in the two cases.

It is unlikely that the main catalytic reactions producing this heating of the plain wires can be due to any other reactions but those responsible for the heating with hydrogen free mixtures, for the hydrogen added is only present initially in small concentration. The possibility of H atom reactions on the wire surface cannot of course be excluded but it is felt that they play only a minor part in the catalytic heating of the wires. If these views are valid the analysis previously applied can once again be used to determine the atomic oxygen concentration in the gas phase. The results are shown on the $\log_{10} n'-t$ curve of fig. 4 by the broken line. The values of $g$ agree almost identically and from this it might be inferred that the hydrogen addition has had little effect on the rate of decay of the atomic oxygen.

The addition of the small amount of hydrogen has been found to have no appreciable effect on the atomic oxygen concentration at any explosion pressure from 0·4 up to 1 atmosphere. These mixtures, unlike the hydrogen free mixtures, can be ignited at initial pressure down to as low as 0·05 atmosphere without any disturbance of the wire temperature records due to convective rise of the flame gases. At the lower pressures, however, an electric spark of greater intensity than was necessary at 0·4 atmosphere initial pressure had to be used in order to ignite the mixtures.

The wire temperature records for explosions at 0·2, 0·15 and 0·05 atmosphere initial pressure are shown in figs. 5 (*a*), (*b*), (*c*) respectively, the flame gas temperature being shown in each case by the broken line. Inspection of these temperature records, together with those given in fig. 2 (*b*) for the 0·4 atmosphere explosion, shows that the difference between the plain and quartz-coated wire temperatures increases with reduction of initial pressure, at least down to 0·15 atmosphere. The curves of fig. 6 which give the actual rates of catalytic heating on the plain wires at the different initial pressures, show that the rate of catalytic heating is somewhat greater as the pressure is reduced.

At the lowest pressure of 0·05 atmosphere the heating curve is of rather different form to those at the higher pressures, the rate at first increasing and then falling away again as in the other cases. The explanation of this phenomenn is almost certainly that with reduction of pressure the rate of chain branching is reduced, due to the lower frequency of collisions, and this has the effect of making the maximum concentration of atomic oxygen occur further behind the flame front (*i. e.* a greater time after the passage of the flame front over the wire). This heating curve has an obvious similarity to the curve of atomic oxygen concentration in the reaction zone for ozone explosions derived theoretically by Lewis and von Elbe (1934, 1938). In fact it is quite certain that had our technique been

Fig. 5.

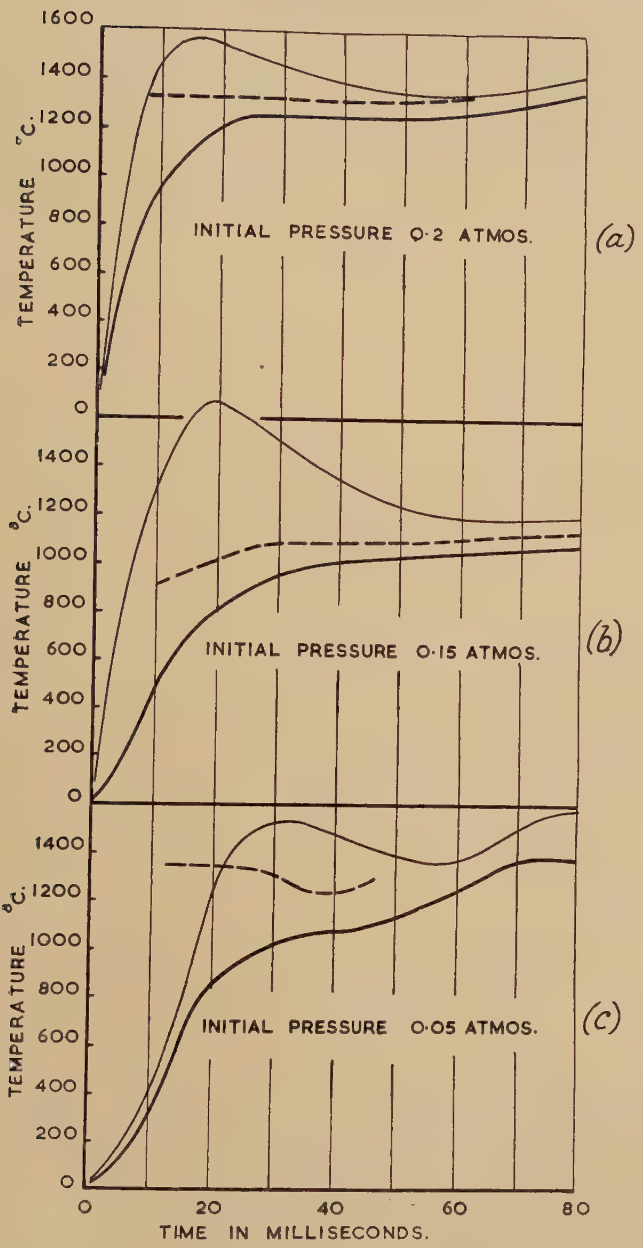

capable of recording the catalytic heating rates immediately after the passage of the flame front, all the curves shown in fig. 6 would have been found to pass through maxima and fall again as is observed at 0·05 atmosphere pressure.

From the diffusion equation the concentration of atomic oxygen at various times from the beginning of the rise in wire temperature has been calculated for each explosion pressure. The results obtained are given in Table II. being expressed in atoms per c.c. and also as percentages by volume of the total products of combustion. At each pressure the maximum concentration will be seen to be of the order of 2 per cent, a value which at these temperatures and pressures is far above the equilibrium value. For the explosion at 0·05 atmosphere initial pressure the values obtained may be considerably in error. This is because the chain branching reactions are so retarded at the low pressure that the maximum rate of catalytic heating on the wires does not occur in a very short time after the pasage of the flame front over the wire, as in the case of the higher pressure explosions. Thus the assumption made in deriving the expressions for calculating the concentration of O atoms, namely, that at time $t=0$, the concentration was a maximum in the gas phase and equal to $n_0$, will possibly introduce considerable errors. In addition, at 0·05 atmosphere initial pressure, the assumed rate of decay of the O atoms, $d[O]/dt=g[O]$, cannot be applicable during the earlier period as the rate of catalytic heating (and possibly the O atom concentration) is increasing.

Fig. 6.

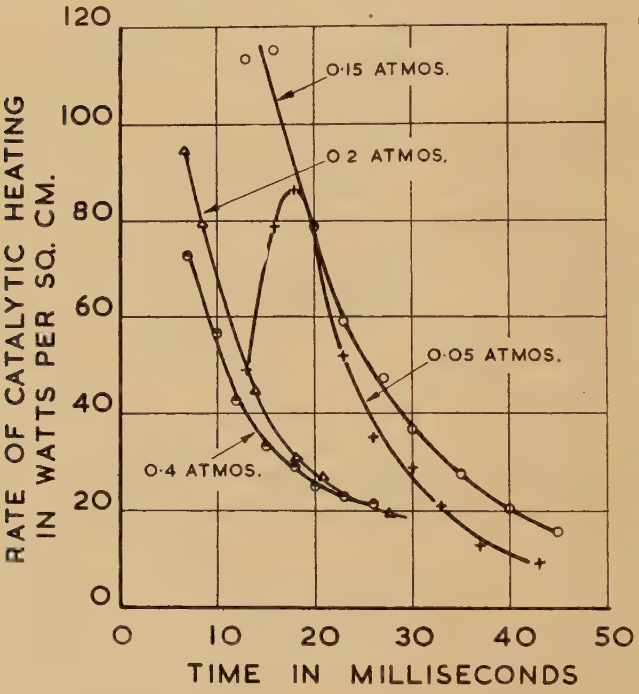

In Table II., therefore, the results of the calculations for 0·05 atmosphere conditions are given only for the period after the peak of the catalytic heating curve and are not to be interpreted as anything more than very rough approximations. Of course, this does not in any way invalidate the conclusions drawn from the curve of catalytic heating which is quite independent of any assumed reactions occurring on the wires. Inspection of the catalytic heating curves of fig. 6 will show, however, that no serious errors due to this assumption will result in the case of explosions at higher initial pressures.

Table II.

| Time in milli-seconds | Initial pressure in atmospheres | | | | | | | |
|---|---|---|---|---|---|---|---|---|
| | 0·4 | | 0·2 | | 0·15 | | 0·05 | |
| | O-atoms per c.c. $\times 10^{-16}$ | Per cent O-atoms by vol. | O-atoms per c.c. $\times 10^{-16}$ | Per cent O-atoms by vol. | O-atoms per c.c. $\times 10^{-16}$ | Per cent O-atoms by vol. | O-atoms per c.c. $\times 10^{-15}$ | Per cent O-atoms by vol. |
| 7 | 2·10 | 1·10 | 1·33 | 1·45 | | | | |
| 10 | 1·69 | 0·90 | 1·00 | 1·10 | | | | |
| 12 | 1·28 | 0 65 | 0·81 | 0·90 | | | | |
| 15 | 1·03 | 0·55 | 0·61 | 0·65 | | | | |
| 16 | 0·98 | 0·50 | 0 56 | 0·60 | 1·72 | 2·10 | | |
| 18 | 0·91 | 0·50 | 0·48 | 0·50 | 1·45 | 1·80 | 3·69 | 1·60 |
| 20 | 0·79 | 0·40 | 0·43 | 0·45 | 1·19 | 1·45 | 3·42 | 1·45 |
| 23 | 0·73 | 0·40 | 0·36 | 0·40 | 0·89 | 1·10 | 2·25 | 0·95 |
| 26 | 0·69 | 0·35 | 0·34 | 0·35 | 0·75 | 0·90 | 1·54 | 0 65 |
| 30 | 0·62 | 0·35 | 0·29 | 0·30 | 0·57 | 0·70 | 1·28 | 0·55 |
| 33 | | | | | | | 0·93 | 0·40 |
| 35 | | | 0·25 | 0·25 | 0·43 | 0·50 | 0·66 | 0·30 |
| 40 | | | 0·23 | 0·25 | 0·33 | 0·40 | 0·49 | 0·20 |
| 43 | | | | | | | 0·42 | 0·20 |

In fig. 7 are shown curves of $\log_{10} n'$ against the time $t$ for the explosions at initial pressures of 0·4, 0·2, 0·15 and 0·05 atmosphere. The calculated points appear to conform very well to the linear relationship which has been assumed although in all cases there is some divergence at the later periods. This is probably due to two factors, namely, the rising pressure and temperature resulting from adiabatic compression as the volume of inflamed gas increases and also the slowing down of the reaction as the O atom concentration approaches the equilibrium value, or the pseudo-equilibrium value if the presence of excited molecules of $CO_2$ disturbs the normal equilibrium. In addition it must be noted that at the later periods, the difference between the plain and quartz-coated wire temperatures becomes quite small and any errors of measurement will have a correspondingly larger effect.

The values of $g$ at each of the different pressures, as derived from the gradient of the $\log_{10} n'-t$ curves, are given in Table III. It will be seen from this Table that the flame gas temperatures are not very different at the various pressures and also that the values of $g$ are of much the same value at each pressure. This is somewhat strange for it would appear to indicate that the decay of atomic oxygen was due to a first order reaction. Now if reaction (3), namely, $O+CO+M \rightarrow CO_2+M$ was solely responsible for the disappearance of the O atoms the reaction rate would be

Fig. 7.

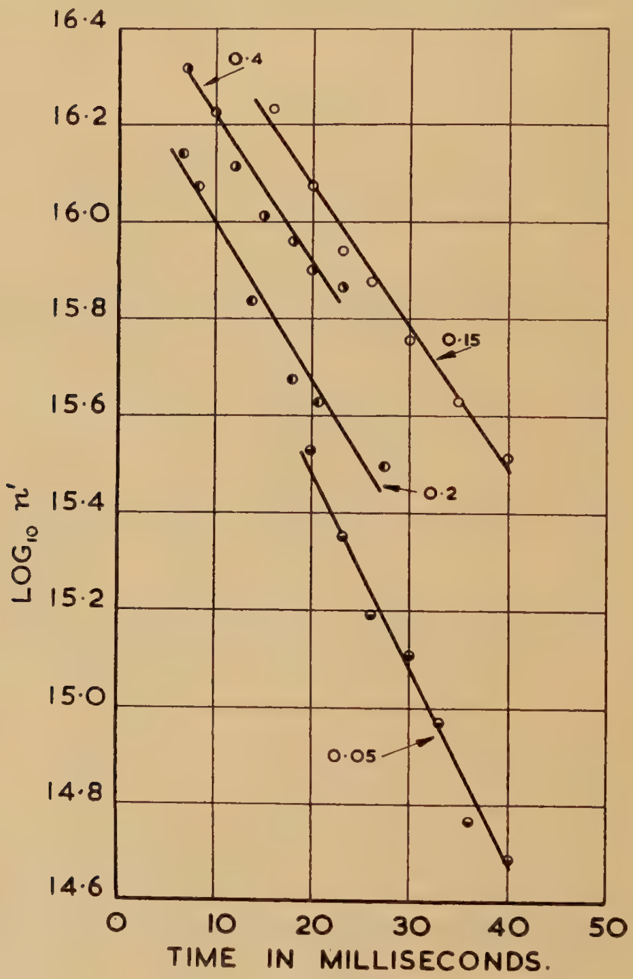

$$\frac{d[O]}{dt} = -k[O][CO][M],$$

where $k$ is the velocity constant for the forward reaction, or

$$g=-k[\mathrm{CO}][\mathrm{M}].$$

Hence $g$ should be proportional to the square of the pressure at any one temperature. The temperature variations shown in Table III. are by no means sufficient to account for the fact that $g$ appears to be independent of pressure. It must be concluded that the reactions occurring in the gas phase are not, in the overall process, due solely to a third order reaction. They must in fact be of such a character as to give the appearance of a much lower order reaction. So little appears to be known of the kinetics of the explosive reaction of CO and $O_2$ that a possible reaction scheme cannot readily be predicted to harmonize with these observations and we prefer, at this stage, to leave the question open.

Attention has previously been directed to the fact that the flame gas temperature derived from the quartz-coated wire temperatures are considerably less than the ideal values. David and co-workers (1944) have also observed this defect of temperature (in their experiments radiation loss corrections were not applied and they assumed that the quartz-coated wire temperatures gave reasonably accurate estimates of flame gas temperature) and they ascribed it to abnormal electronic excitation of a proportion of the $CO_2$ molecules, these being assumed to possess excess intra-molecular energy which they called " latent energy ". There does in fact seem to be little doubt that excited $CO_2$ molecules, possibly in a metastable electronic state, are present in the flame gases resulting from explosions of $CO–O_2$ mixtures. The only doubt is whether they are present in sufficient concentration to account for the whole of the latent energy, a doubt which Egerton and Ubbelohde (1934) have previously expressed.

TABLE III.

| Initial pressure atmospheres | Mean gas gas °C. | $g$ sec$^{-1}$ |
|---|---|---|
| 0·4 | 1280 | 69 |
| 0·2 | 1320 | 74 |
| 0·15 | 1080 | 67 |
| 0·05 | 1320 | 95 |

The atomic oxygen which, from the present work, appears to remain in the flame gases will naturally account for a certain proportion of the total missing energy. A single example will suffice to show that this is only a minor effect. With the explosion at 0·4 atmosphere initial pressure, in which the flame gas temperature is highest and the total missing energy least for the explosions here considered, the atomic oxygen accounts for some 9·5 per cent of the heat of combustion of the mixture at its highest recorded concentration at a time of 0·007 second after the temperature rise commences and this leaves an unaccounted energy of 20 per cent. After the atomic oxygen has well nigh disappeared, at a time of 0·04 second, the unaccounted-energy is still some 20·5 per cent of the heat of combustion of the mixture. The small increase may be, and probably is, due to the radiation loss from the flame gases during the time interval of 0·033 second. Radiation, however, is unlikely to explain the whole discrepancy and the conclusion would seem to support David's views that the energy is held in the flame gases in " latent " form.

Gaydon (1942) has given an alternative explanation of the latent energy in terms of vibrationally excited molecules. According to Gaydon, the presence of water-vapour—and presumably hydrogen—in the CO flame gases should have a marked effect in reducing the magnitude of the vibrational excitation energy. From the present work, however, the explosions of mixtures containing hydrogen show a large amount of missing energy after the elapse of an appreciable time. This appears to discount the views of Gaydon as giving a complete explanation of the phenomenon of latent energy. It seems to us most probable that the true explanation is to be found in a combination of factors such as radiation, electronic excitation, vibrational excitation and the presence of atomic oxygen and like active species. At this stage the relative importance of the first three of these factors cannot be assessed but the final factor does not appear, from the experiments which have been described, to have large influence.

## REFERENCES.

CARSLAW and JAEGER, 1947, *Conduction of Heat in Solids* (Oxford : University Press).

CHAPMAN and COWLING, 1939, *The Mathematical Theory of Non-Uniform Gases* (Cambridge).

DAVID, *et al.*, 1944, *Proc. Inst. Mech. Eng.*, **151,** 236.

EGERTON and UBBELOHDE, 1934, *Nature*, **134,** 848.

GAYDON, 1942, *Spectroscopy and Combustion Theory* (Chapman and Hall).

GAYDON, 1946, *Trans. Faraday Soc.*, **42,** 292.

HINSHELWOOD, 1940, *The Kinetics of Chemical Change* (Oxford : Clarendon Press).

JOST and MÜFFLING, 1938, *Z. Physik. Chem.*, Sec A, **181,** 208.

KONDRATIEVA and KONDRATIEV, 1946, *Acta Physicochim, U.R.S.S.*, **21,** 1.

KONDRATJEW, 1937, *Acta Physicochim., U.R.S.S.*, **6,** 748.

LAIDLER, 1949, *J. Chem. Phys.*, **17,** 221.

LANGMUIR, 1921, *Trans. Faraday Soc.*, **17,** 621.

LEAH, SMEETON, A., 1943, *Phil Mag.*, **34,** 795 ; 1947, *Ibid*,. **37,** 657.

LEAH, SMEETON, A., ROUNTHWAITE, C., and BRADLEY, D., 1950, *Phil. Mag.*, **41,** 468.

LEWIS and VON ELBE, 1934, *J. Chem. Phys.*, **2,** 537 ; 1938, *Combustion Flames and Explosions of Gases* (Cambridge).

RICE, 1940, *Electronic Structure and Chemical Binding* (McGraw-Hill).

SEMENOV, 1935, *Chemical Kinetics and Chain Reactions* (Oxford : University Press).

SMITH, W. V., 1943, *J. Chem. Phys.*, **11,** 110.

TANFORD, 1947, *J. Chem. Phys.*, **5,** 433.

TAYLOR and LAVIN, 1930, *J.A.C.S.*, **52,** 1910.

# XLIII. *The Cut-Off in the Energy Spectrum of Primary Cosmic Radiation.*

By P. J. D. Gething,
Department of Mathematics, Imperial College of Science, London *.

[Received January 30, 1950.]

## Summary.

Janossy's explanation of the cut-off in the observed cosmic ray energy spectrum, viz., that it is due to the action of the Sun's magnetic field, was originally based on Hale's estimate for the dipole moment of the Sun. A recent investigation by Thiessen, however, has led to a much smaller estimate. It appears that, if Janossy's calculations were corrected to allow for this new estimate, the calculated level of the cut-off would be greatly reduced, and consequently there should be a corresponding increase in the total intensity of incoming radiation observable at high magnetic latitudes. The possibility of an alternative explanation of the cut-off is considered, with particular reference to the theories of Milne and Fermi.

1. The energy spectrum of arriving primary cosmic radiation (assumed throughout this paper to consist entirely of protons) is approximately given by :

$$n(\mathrm{E})\,d\mathrm{E}=\mathrm{const}\,.\,d\mathrm{E}/\mathrm{E}^{\gamma}, \quad \ldots \ldots \ldots \quad (1)$$

for E greater than $2\times10^{9}$ eV. In this formula $n(\mathrm{E})\,d\mathrm{E}$ is the number of particles with energies in the range E to $\mathrm{E}+d\mathrm{E}$. The exponent $\gamma$ is estimated to be about 2·8. The fact that no radiation is reaching us of energy less than $2\times10^{9}$ eV., at least down to $3\times10^{7}$ eV., has been established experimentally by observations near the North Geomagnetic Pole (Carmichael and Dymond 1939).

The most generally accepted explanation of this cut-off has been the suggestion due to Janossy (1937), that particles arriving from outside the solar system are deflected by a permanent dipole magnetic field due to the Sun. Particles with momenta less than a certain critical value $\mathrm{P}_1$ would then be unable to cross the Earth's orbit, whereas those with momenta between $\mathrm{P}_1$ and a second critical value $\mathrm{P}_2$ would only be able to arrive at the Earth from certain directions. Particles with momenta greater than $\mathrm{P}_2$, however, could arrive from any direction.

---

* Communicated by E. A. Milne.

The general theory is complicated, but in the equatorial plane of the Sun's dipole field, which is assumed for simplicity to coincide with the plane of the Earth's orbit, the above critical momenta are:

$$P_1=(3-2\sqrt{2})eM/d^2, \qquad (2)$$

$$P_2=eM/d^2, \qquad (3)$$

where $e$ is the charge on the proton, M is the Sun's magnetic moment and $d$ is the distance of the Earth from the Sun.

The cut-off directly observed refers to the momentum spectrum, and occurs at $2\times10^9$ eV./$c$. Taking this value for $P_1$, it follows from (2) that the corresponding magnetic moment of the Sun should be $M=10^{34}$ e.m.u., implying a field intensity on the Sun's surface of about 50 gauss at the poles.

2. When Janossy originally made the above calculations this result appeared to be in good agreement with more direct measurements of the solar field, particularly the observations of Hale (1913). Recently, however, Thiessen (1949) has re-investigated the Sun's field and claims that at the poles it amounts only to about 1·5 gauss, with a probable error of 0·5 gauss.

On Janossy's theory, therefore, the field required to account for the observations of Carmichael and Dymond would be from 30 to 40 times greater than the field observed by Thiessen. The only way of reconciling both sets of observations with Janossy's theory is to suppose that in the last decade or so the Sun's field has decreased about thirty-fold. Such a change, of course, would also affect the total intensity of radiation observed on the Earth. This may be roughly estimated as follows. Let us assume that the cut-off in the momentum spectrum has in fact changed from $2\times10^9$ eV./$c$. to $5\times10^7$ eV./$c$. and that the energy spectrum (1), with $\gamma=2{\cdot}8$, may be extrapolated to cover the corresponding energy range. Owing to the action of the Earth's magnetic field, particles with momenta less than $2\times10^9$ eV./$c$. cannot reach low magnetic latitudes, so that there would be no effective change up to the old "threshold latitude" at about 55° N. (geomag.). Beyond this point, instead of remaining constant, the intensity would continue to increase up to a new threshold latitude which would appear to be at about 70° N. (geomag.). From here to the magnetic pole the intensity would remain constant, but at a level some 15 or 20 times higher than the previous value.

3. If these approximate calculations are correct, it seems unlikely that the effect of a change in the Sun's magnetic field of the order of magnitude implied by the results of Hale and Thiessen respectively could have escaped detection. However, the following sources of possible inaccuracy in the calculations should be noted :—

(i) Observations by Pomerantz and Vallarta (1949) suggest the possibility that the extrapolation below $2\times10^9$ eV. of the energy spectrum law (1), with $\gamma$ unaltered, may not be justified. If, however, y were reduced, the threshold latitude would still change as predicted above, although the change in total intensity might be very much less marked.

(ii) Rosseland (1936) has criticized the common procedure of treating the Sun's field as that of a dipole. Theory suggests that this hypothesis may lead to serious errors in some applications. The dipole field, however, is probably a good enough approximation to deal with the theory of the orbits of the cosmic ray particles, even if it is not a justifiable approximation near the surface of the Sun.

(iii) Formulæ (2) and (3) apply only in the equatorial plane. Moreover, we have considered only possible changes in the value of $P_1$, without reference to $P_2$. Detailed investigation of the cosmic ray orbits depends on numerical integration, but it is unlikely that the conclusions reached above would be drastically modified if more exact calculations were made.

(iv) Formulæ (2) and (3) depend on the assumption that the moment M does not vary with time. Elementary calculations show immediately that the deflection suffered by a particle due to the Sun's field in all but the last few days of its journey towards the Earth is completely negligible. Consider, for example, the field in the equatorial plane at a distance of $3 \times 10^{15}$ cm. (*i. e.* about 200 astronomical units) from the Sun. If M were $10^{34}$ e.m.u., the intensity would be $3{\cdot}7 \times 10^{-13}$ gauss. Now a proton of energy $2 \times 10^{9}$ eV. moving in a uniform field of this strength would describe a circle of radius $2{\cdot}4 \times 10^{19}$ cm., or about 26 light-years. Since the field of the Sun is not uniform, but falls off as $r^{-3}$, and since the nearest stars (which may be magnetically active) are only a few light-years from the Sun, it is apparent that the deflection caused by the Sun beyond $3 \times 10^{15}$ cm. may certainly be ignored. More detailed investigation would probably show that this limit could be reduced. A particle whose speed is very close to that of light takes about 28 hours to travel $3 \times 10^{15}$ cm. in a straight line. Even allowing for the curvature of the orbits, no modification will be needed to the theory of these orbits unless the Sun's field is rapidly fluctuating, with significant variations in a matter of a few days.

4. Since Janossy's theory seems to present some difficulty if Thiessen's observations are correct, it is interesting to enquire whether any other explanation of the cut-off can be found. The only alternative possibilities which seem to have been considered so far are the following :

(i) Hamilton, Heitler and Peng (1943) suggested that primary radiation is, in fact, reaching the Earth below the cut-off value and is escaping detection. Janossy (1947) has criticized this idea, but his reasoning is difficult to follow. The only requirements of their theory is that particles with energies below the critical value should undergo one atomic collision process in the atmosphere, in which the energy is converted to some form in which it cannot be detected by the coincidence counters and ionization chambers; while above the critical value the collision process is presumably different, and the incoming energy is converted to a detectable form.

(ii) Using Milne's theory (1935) that cosmic radiation is primarily due to world-gravitation, George (1948) has obtained a theoretical energy spectrum of about the right form, *i. e.*

$$n(\mathrm{E})\,d\mathrm{E}=\mathrm{const}\,.\,(1-m_0^2c^4/\mathrm{E}^2)\,d\mathrm{E}/\mathrm{E}^3. \qquad . \quad . \quad . \quad . \quad (4)$$

This curve rises rapidly from $n(\mathrm{E})=0$, when $\mathrm{E}=m_0c^2$, (*i. e.* for particles of zero momentum) to a maximum at $\mathrm{E}=(\sqrt{5/3})m_0c^2$, which for protons corresponds to $\mathrm{E}=1{\cdot}2\times10^9$ eV. After this point the curve falls approximately as const./$\mathrm{E}^3$. It therefore includes something closely analogous to a cut-off at its low energy end. Furthermore, it seems that there may also be a true cut-off at some point in the spectrum according to this theory. In Milne's model of the Universe, a particle may be ejected from a fundamental particle or nucleus (these nuclei are identified with the extra-galactic nebulæ) by some subsidiary mechanism, and then accelerated by the combined gravitational field of all the nuclei to a speed arbitrarily close to that of light in a finite time. If inter-galactic space is as transparent as Hubble (1942) claims, then on Milne's theory it would appear that most of the cosmic ray particles which reach us have their origin in other galaxies. Since the nearest extra-galactic system, namely the Large Magellanic Cloud, is about 86,000 light-years away, the vast majority of the cosmic ray particles arriving at the Earth would have been travelling for at least 100,000 years. If there is in fact a minimum distance that the particles must have travelled, the theory that they are accelerated by a gravitational mechanism would appear to imply a corresponding minimum energy which they must have acquired by the time they reach the Earth.

(iii) Fermi's theory (1949), that the cosmic ray particles acquire their high energies from collisions with the magnetic fields associated with drifting interstellar clouds, has recently attracted considerable attention. He points out that if a proton is to be accelerated by this mechanism, its initial energy must be at least $2\times10^8$ eV., otherwise the energy losses due to ionization will exceed the energy gains. Since the rate of gain of energy will be irregular, it may be that this figure must be multiplied by a factor of 5 or 10 to give the particle any reasonable chance of undergoing a net acceleration. If this is the case, then some other mechanism must be found to bring the particles up to such a high "injection energy," but Fermi's calculations on ionization losses may be capable of application to other theories of origin.

## CONCLUSION.

5. Recent observations by Thiessen on the Sun's magnetic field suggest that Janossy's explanation of the cut-off in the energy spectrum of incoming cosmic radiation should be re-examined and compared with

possible alternative theories. Future observations of the Sun's field, in conjunction with observations on the cosmic ray intensity and threshold latitude, should provide a crucial test of Janossy's theory.

I should like to thank Dr. G. J. Whitrow for helpful discussions on this subject.

*Note added in proof.*—Dolbear and Elliot have recently reported (1950, *Nature*, **165**, 353) measurements made at high altitudes of the variations in cosmic ray intensity throughout the solar day. They find that the amplitude of the variations is considerably smaller than the value predicted on the basis of Janossy's theory. This provides further evidence against the acceptance of his theory, which is independent of Thiessen's observations considered above.

## REFERENCES.

CARMICHAEL and DYMOND, 1939, *Proc. Roy. Soc. A*, **171**, 321.
FERMI, 1949, *Phys. Rev.*, **75**, 1169.
GEORGE, 1948, *Phil. Mag.*, **39**, 240.
HALE, 1913, *Astrophys. J.*, **38**, 27.
HAMILTON, HEITLER and PENG, 1943, *Phys. Rev.*, **64**, 78.
HUBBLE, 1942, *American Scientist*, **30**, 101.
JANOSSY, 1937, *Zeit. f. Physik*, **104**, 430.
JANOSSY, 1947, *Commun. Dublin Inst. for Adv. Studies*, Series A, No. 4, 16.
MILNE, 1935, *Relativity, Gravitation and World Structure, O.U.P.*, Chapter XII.
POMERANTZ and VALLARTA, 1949, *Phys. Rev.*, **76**, 1889.
ROSSELAND, 1936, *Theoretical Astrophysics, O.U.P.*, 219.
THIESSEN 1949, *Observatory*, **69**, 228.

# XLIV. CORRESPONDENCE

## *On the Binary and Ternary Photofission of Thorium-232.*

By E. W. Titterton and T. A. Brinkley.

[Received February 21, 1950.]

A recent experiment by Titterton and Goward (1949) has shown that uranium undergoes photofission into three charged fragments. It is therefore of interest to determine whether a similar process occurs in the photofission of thorium which, after uranium is the naturally occurring element most easily fissionable with $\gamma$-rays.

It was expected, from the work of Westöo (1948) that difficulty would be experienced in loading plates with thorium-232 atoms, since his experiments had shown these to be adsorbed at the surface of the emulsion. Preliminary experiments made with $100\mu$ Ilford $D_1$ emulsions employing a variety of presoaking times and concentrations of $Th(NO_3)_4$ $4H_2O$ in water confirmed Westöo's result that the take-up of thorium-232 ions from the solution is slow compared with that for thorium X and thorium B.

However, preswelling of the emulsion layer by a long soaking in water followed by immersion in thorium nitrate solutions of much higher concentration than that used by Westöo, resulted in improvements in penetration of the $^{232}$Th ions. If the concentration is increased too far the sensitivity and mechanical properties of the emulsion are impaired, and it is necessary to make a compromise on this account.

In the experiments to be described, the plates were presoaked in water for 20 minutes at 18° C., were loaded by immersion at the same temperature in a solution of 10 grms. of $Th(NO_3)_4 4H_2O$ in 100 ml. of water for 20 minutes, immersed for two minutes in absolute alcohol and dried in a warm air stream. Under these conditions the sensitivity of the emulsion was unimpaired, and the $^{232}$Th $\alpha$-particles (range $16\mu$) were observed throughout the emulsion layer, although they were not distributed uniformly in depth.

Plates loaded by this method were irradiated with a continuous spectrum of $\gamma$-rays of maximum energy 24 MeV. from the A.E.R.E. Synchrotron. Three irradiations, of 100, 150 and 180 R, were made and the resulting plates showed a fission density of $2{\cdot}5 \times 10^4$ per c.c. at the 150 R level, which, though small, was satisfactory for a preliminary investigation. Comparison of the exposed plates with identically treated, but unirradiated, control plates indicated some fading of tracks in the irradiated plates, especially deep in the emulsion. In an examination involving 2500 binary photofissions five cases of ternary fission involving the emission of a long range light fragment, probably an $\alpha$-particle, have been observed. These events are listed in Table I. and a photomicrograph of one is given in fig. 1. In addition, there are seven cases where a third, short range, particle (which does not appear to be a recoil atom) occurs in the centre $5\mu$ of the fission track. These events may be similar to those found in the slow neutron fission of $^{235}$U where short range fragments of mass $12\pm1$ have been reported (Dewan and Allen 1949).

TABLE I.

| N | $f_1(\mu)$ | $f_2(\mu)$ | $F(\mu)$ | $R_\alpha(\mu)$ | $E_\alpha$(MeV.) | $\phi(^\circ)$ |
|---|---|---|---|---|---|---|
| 1 | 15·1 | 10·2 | 25·3 | 160 | 18·0 | 93 |
| 2 | 14·7 | 10·3 | 25·0 | 133 | 16·3 | 77 |
| 3 | 11·6 | 11·6 | 23·2 | 83 | 12·6 | 71 |
| 4 | 12·9 | 11·0 | 23·9 | 91 | 13·1 | 71 |
| 5 | 13·1 | 12·4 | 25·5 | 68 | 11·2 | 82 |

N=number of event.
$f_1$=range of longer fission fragment.
$f_2$=range of shorter fission fragment.
$F=f_1+f_2$.
$R_\alpha$=range of $\alpha$-particle.
$E_\alpha$=energy of $\alpha$-particle.
$\phi$=angle of emission of $\alpha$-particle relative to long fission fragment.

Fig. 1.

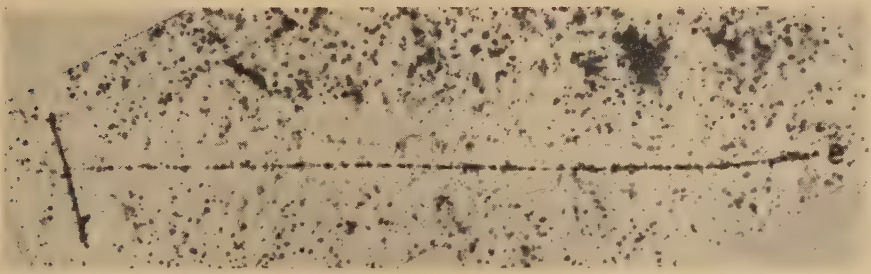

Photomicrograph of Event No. 2. Observer Miss P. A. Port. The two heavy fission fragments and the light, long range particle are wholly contained in the emulsion.

The possibility that the fissions observed are fast-neutron induced has been considered, but the fast neutron flux at the plates has been shown by experiment to be at least 25 times too small to account for the fission rate. Moreover, according to Tsien and Faraggi (1947) thorium-232 does not undergo tripartition with fast neutrons. Because of the long half-life of $^{232}$Th, compared with that of its daughter products, the concentration of $^{232}$Th atoms in the emulsion is far greater than that of any other member of the family. It is therefore reasonable to attribute the observed binary and ternary fission events to the action of $\gamma$-rays on $^{232}$Th nuclei.

A number-range curve, fig. 2 (*a*), was determined for the photofission tracks and is compared with a similar curve, fig. 2 (*b*), for tracks formed by the slow neutron fission of $^{235}$U in a $D_1$ emulsion under conditions of similar emulsion sensitivity. It appears that the energy release in the photofission of $^{232}$Th is smaller than that in the slow neutron fission of $^{235}$U. If it is assumed that the mass spectrum of the fission fragments in the two cases is similar, then from the velocity-range curves for the $^{235}$U fission fragments given by Bohr (1941) it can be shown that, to a first approximation, the ratio of the kinetic energy released in the two cases is equal to the ratio of the squares of the corresponding ranges. Taking $24{\cdot}5\mu$ and $27{\cdot}0\mu$ as the mean ranges

Fig. 2.

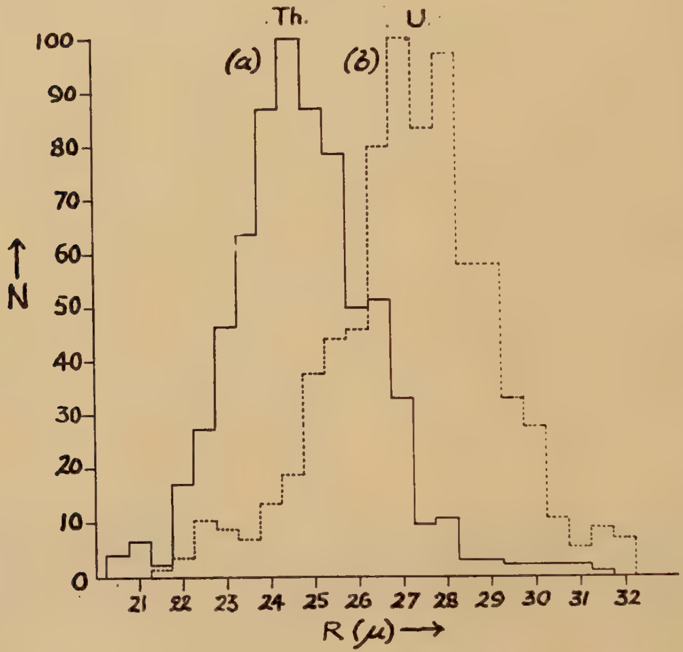

Number-Range curves for binary fission tracks in $D_1$ emulsions :
(*a*) Photofission of Thorium,
(*b*) Slow-neutron fission of $^{235}$U.

$$\frac{\text{Kinetic energy released in } ^{232}\text{Th photofission}}{\text{Kinetic energy released in } ^{235}\text{U slow neutron fission}} = \left(\frac{24{\cdot}5}{27{\cdot}0}\right)^2 = 0{\cdot}82$$

The measured value of the K.E. release in the slow neutron fission of $^{235}$U is given by Brunton and Hanna (1949) as 151·5 MeV. and from this we derive 124±10 MeV. as the mean kinetic energy released in the photofission of $^{232}$Th.

We wish to thank Mr. L. R. H. Metcalfe for help in setting up the experiment and for operating the synchrotron for these exposures.

Atomic Energy Research Establishment,
Harwell, Berks.
16th February, 1950.

E. W. Titterton.
T. A. Brinkley.

### References.

Bohr, 1941, *Phys. Rev.*, **59,** 270.
Brunton and Hanna, 1949, *Phys. Rev.*, **75,** 990.
Dewan and Allen, 1949, *Phys. Rev.*, **76,** 181.
Titterton and Goward, 1949, *Phys. Rev.*, **76,** 142.
Tsien and Faraggi, 1947, *Compte-Rendus*, **225,** 294–6.
Westöo, 1948, *Ark. Mat. As. O. Fys.*, **34 B,** No. 22, 1–8.

---

## *A Temporary Increase in the Neutron Component of Cosmic Rays.*

By N. Adams,
The Physical Laboratories, The University, Manchester.

[Received March 10, 1950.]

A recent report (Forbush, Stinchcomb and Schein 1950), has drawn attention to an abnormality in the cosmic ray intensity on November 19, 1949.

Increases of 43 per cent were found in the ionizing cosmic rays measured at sea level in geomagnetic latitudes 50° and 80°, and an increase of 180 per cent in the rays measured at Climax, Colorado, at an altitude of 11,000 feet. No increase was found at 11,000 feet on the equator. These increases were associated with a radio fade out at 10.33 G.M.T. At about the same time large increases were found in the cosmic ray intensities recorded by two independent systems in these laboratories.

One of these which records ionizing cosmic ray consists of three-fold Geiger–Muller counter telescopes pointing north and south at an angle of 45° to the horizontal (Elliot and Dolbear 1950). This recorded an increase in intensity reaching a maximum of about 12 per cent above normal between 11.00 and 12.00 hrs. Its counting rate had reverted to within 1 per cent of the normal by 14.00 hrs. The other is a neutron intensity recorder and the accompanying figure shows its response for the period 19th–20th November, 1949.

The neutron detector consists of boron–trifluoride filled proportional counters embedded in a " Pile " built of high purity graphite. Its detection efficiency is appreciable for incident neutrons of energies between thermal and perhaps 10 MeV., being greatest for energies 3 to 5 MeV.

The ordinates of the figure represent the observed average counting rate during successive hourly intervals. No hourly readings are available for the period between 13.25 and 16.27 hrs. when the equipment was being tested. However, counting rates taken for periods of a few minutes each and therefore of rather low precision, were obtained during this period at about 15.00 and 16.00 hrs. and are plotted in the figure with appropriate standard deviations as A and B respectively.

The barometric pressure for the period shown in the figure had extreme variations of ±0·1″ Hg about its mean value. Such variations would produce changes of about ∓2·5 per cent in the counting rate of the recorder in normal conditions.

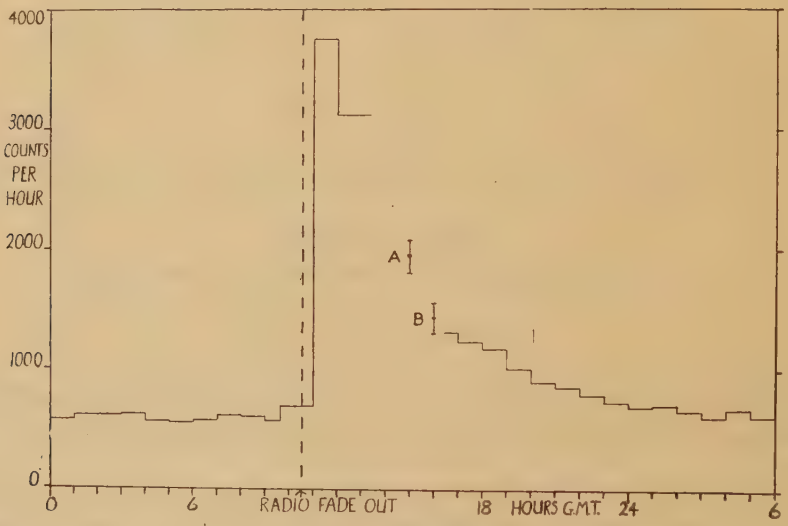

From the moderate increase of counting rate (15 per cent) observed during the period preceding 11.00 hrs. and the enormous increase (550 per cent) in the period 11.00–12.00 hrs. (both compared with the counting rate earlier that morning) is seems reasonable to suppose that the onset of the disturbance occurred only a few minutes before 11.00 hrs.

After reaching a maximum value for the period between 11.00 and 12.00 hrs. the counting rate, so far as readings are available, decreased continually with time and was still significantly above normal in the first hours of November 20th. Thereafter the hourly counting rates showed their usual statistical fluctuation.

Except for the occasion described here no variation of counting rate of root mean square amplitude (averaged over periods of several weeks) greater than 0·3 per cent of the total rate has been found save for the effect of barometic pressure.

The author is indebted to D.W.N. Dolbear and H. Elliot for permission to publish the observations on the ionizing cosmic rays, described here, which have been made by them.

### REFERENCES

FORBUSH, S. E., STINCHCOMB, T. B., and SCHEIN, M., 1950, *Bull. Amer. Phys. Soc.*, **25**, 15.

ELLIOT, H., and DOLBEAR, D. W. N., 1950, *Proc. Phys. Soc.* A, **63**, 137.

---

## *A Temporary Increase in the Neutron Component of Cosmic Rays.*

By N. ADAMS and H. J. J. BRADDICK,
The University, Manchester.

[Received March 8, 1950.]

THE outstanding feature of the result reported above is the very large increase, at sea level, of neutron intensity as compared with ionizing cosmic radiation. This cannot be explained by a uniform increase in all types and energies of incoming cosmic rays.

Although fast neutrons from the sun could reach the earth with only a moderate loss due to decay, the increase cannot be due to the appearance of neutrons at the top of the atmosphere, for the increased rate persists after sunset. The rate was about $2\frac{1}{2}$ times normal at Manchester sunset and was significantly above normal when the nearest point of the atmosphere directly irradiated by the sun, was hundreds of miles away.

The effect must therefore be ascribed to charged particles, and this conclusion is confirmed by the fact that no increase (in ionizing radiation) was observed on the geomagnetic equator. The particles concerned must have momenta between ca. $2\cdot10^9$ eV./*c*., the threshold value at Manchester and ca. $10\cdot19^9$ eV./*c*., the corresponding equatorial value. Particles at the lower end of this range would have rather low efficiencies as meson producers, and any mesons they produced would be completely stopped in the atmosphere, for the minimum ionization loss is ca. $2\cdot10^9$ eV. for a particle which traverses the atmosphere and there are no fluctuations in favour of individual particles. The absorption of neutrons in the atmosphere is of a different type—it takes place in a rather small number of nuclear encounters and is therefore exponential with depth. The altitude and barometric coefficients indicate that neutrons produced near the top of the atmosphere give rise to between 1/300 and 1/1000 of their number at sea level. For comparison, the mixed ionizing radiation at its maximum is about 50 times the corresponding sea level value. An increase in charged cosmic particles which favoured a comparatively narrow band above $3\cdot10^9$ eV. would therefore give rise to a large increase in sea level neutrons combined with a relatively small increase in sea level ionizing radiation.

# XLV. *Notices of New Books and Periodicals received.*

*A General Kinetic Theory of Liquids.* By M. BORN and H. S. GREEN. (Cambridge University Press). Price 10*s*. 6*d*.

IN view of the concise and allusive style imposed on modern publications in the scientific journals, a book consisting only of a collection of papers with a brief appendix has necessary defects as an introduction to the subject of which it treats. The reviewer must then attempt to exhibit its relation to other work in the field, and to criticize its content in more detail than is usually required.

It has been usual to discuss the liquid state of matter in terms of models constructed in analogy with those found fruitful in the solid or gaseous states ; and a good account of the equilibrium properties of normal liquids can be given by such models with reasonably few empirical parameters. This, however, can be done by any model which does not contradict the law of corresponding states, and it has proved much less easy to find any consistent picture of transport processes or to introduce quantum-mechanical effects.

A more fundamental approach is through the use of multiple distribution functions

$$f_h\,(x_1, \dots x_h\,;\ \dot{x}_1, \dots \dot{x}_h\,;\ t),$$

where $f_h$ is the probability density at time $t$ for finding different molecules at $x_1, x_2, \dots x_h$ with velocities $\dot{x}_1, \dots \dot{x}_h$ respectively. The book under consideration contains the contribution of Born and Green to this aspect of the theory, with its generalization in quantum mechanics. In the first paper, the classical distribution functions are introduced and continuity equations established. The introduction of a potential function establishes recurrence relations among the $f_h$.

For the case of thermodynamic equilibrium, these multiple distribution functions were introduced by Onsager (1933) and subsequently used by Kirkwood (1935, 1942). In this case the form of $f_N$, where N is the total number of molecules in the system, is known to be exp $[(F-H)/kT]$, where F is the free energy and H the Hamiltonian of the system. Provided the velocities only appear in the kinetic energy, it is possible to integrate over all values of all the velocities, obtaining multiple densities $n_h$. The $h$-molecule density, $n_h$, is proportional to

$$\exp\,[-(\text{potential of average force on } h \text{ molecules}/kT)],$$

where the average is taken over the canonical assembly. Kirkwood (1935) has suggested that if the potential energy is a sum of two-body terms, then in considering groups of more than two molecules we may assume that the average forces between pairs of molecules can be simply superposed. This leads in particular to an expression for $n_3$ in terms of $n_2$, which Born and Green assume valid in non-equilibrium states also and use to obtain an integral equation for the $n_2$.

The Kirkwood assumption is vital in the development of the theory. Born and Green give a rather misleading reference in the appendix to a result of Sabry quoted by Rodriguez (1949). The assumption is shown to be true for a solid in which the atomic equilibrium positions are on a perfect lattice and interactions are harmonic. It is obviously also true for a perfect gas, but an approximation valid in two extreme cases where the motion can be resolved in terms of normal coordinates simply related to the atomic coordinates is not necessarily so in less simple conditions.

In the second paper, Green insists on the kinetic character of the theory and its independence of statistical mechanics, so finds it necessary to use some form of the H-theorem. This meets the usual difficulty that the H-function, reasonably defined, is strictly constant in the motion of an unperturbed conservative dynamical system, no matter how improbable the initial state, so it is necessary to introduce thermal perturbation. This is represented by a simplified interaction with another similar system, which is no improvement on the use of the Gibbs assembly. A formal derivation of the equation of state from the integral equation for the $n_2$ follows.

For a corrected and more complete treatment of the equation of state the appendix refers to the paper of Rodriguez, which gives two computed isothermals for argon. These show a flattening at high pressures, which may represent the start of the liquid-solid transition region, and a cusp at the foot of the section which represents metastable states of the liquid under tension. This should be the point at which no activation energy is necessary to initiate a bubble: however, its significance depends on the credit one gives to the "unstable" section of the curve. Born and Green refer to forthcoming work of McLellan which should elucidate how far these results depend on the particular mathematical approximations employed.

The third paper in the book deals with transport processes. Born and Green relate the viscosity and thermal conductivity to the distorted distribution functions in the liquid in non-equilibrium conditions. The calculation of these distorted distributions is treated formally here by expansion in terms of the gradients of the intensive thermodynamic variable. Yang (1949 a, b) has discussed self and mutual diffusion in liquids, but none of this work has yet been reduced to numerical calculation.

In the non-equilibrium case, the physical significance of the distribution functions is not altogether clear. Onsager (1931) and Kirkwood (1946) have represented a system out of equilibrium by an assembly with given initial values, *e. g.* of the statistical space moments of intensive properties, or of the coordinates and momenta of specified molecules. This has led Kirkwood to a treatment of transport processes in which time-smoothed distribution functions of $f_h$ obey an extended Langevin equation with friction constants calculable from molecular properties. Kirkwood, Buff and M. S. Green (1949) have obtained a reasonable numerical estimate of the shear viscosity of liquid argon by this approach. The relation between this approach and that of Born and Green is not quite obvious.

The second half of the book, also containing three papers, concerns the quantum mechanics of liquids. The physical system is described by v. Neumann's statistical operator, which is represented by the density matrix in the coordinate representation. Density matrices for smaller numbers of particles are formed from that for the whole system, as in the classical case.

In the first of these papers it is shown that from the equations of motion of the density matrices may be deduced equations formally identical with those of classical hydrodynamics. However, the trace of the stress tensor appearing in those equations is not proportional to the thermodynamic pressure derived from the free energy. This remarkable result has been challenged by de Boer (1949 a) and its basis further elucidated in a reply by Green (1949). It arises from the finite value of the trace of a set of commutators which appear in the expression for the thermodynamic but not the kinetic pressure. Similarly, the kinetic temperature appearing in the equation for heat conduction differs from the thermodynamic temperature.

The second paper contains a clear and instructive account of the relation between the statistical operator and thermal quantities. In the last paper, Green shows that quantum effects permit the rapid reversible interconversion of mechanical and thermal energy, and applies this to a qualitative explanation of anomalous transport phenomena in liquid helium II. In view of the observed difference in behaviour of $He_3$ and $He_4$ at low temperatures, it is unfortunate that the development contains no explicit reference to the statistics obeyed by the atoms of the liquid. It seems possible that since rotational states of low energy correspond to quasi-rigid rotations of comparatively large groups of atoms, the symmetry conditions modify the high-order density matrices corresponding to such groups (*cf.* Teller and Wheeler (1938)).

This book contains a valuable contribution to the kinetic theory of liquids. The reader who wishes to obtain a balanced view of the subject would do well to study it in conjunction with the published work of Kirkwood and the review article on dense gases by de Boer (1949 b). G. WYLLIE.

### REFERENCES.

DE BOER, J., 1949 a, *Physica,* **15,** 843.
DE BOER, J., 1949 b, *Rep. Prog. Phys.,* **12,** 305.
GREEN, H. S., 1949, *Physica,* **15,** 882.
KIRKWOOD, J. C., 1935, *J. Chem. Phys.,* **3,** 300.
KIRKWOOD, J. C. and BOGGS, E. M., 1942, *J. Chem. Phys.,* **10,** 394.
KIRKWOOD, J. C., 1946, *J. Chem. Phys.,* **14,** 180.
KIRKWOOD, J. C., BUFF, H. and GREEN, M. S., 1949, *J. Chem. Phys.,* **17,** 338.
ONSAGER, L., 1931, *Phys. Rev.,* **38,** 405.
ONSAGER, L., 1933, *Chem. Rev.,* **13,** 73.
RODRIGUEZ, A. E., 1949, *Proc. Roy. Soc.* A, **196,** 73.
TELLER, E. and WHEELER, J. A., 1938, *Phys. Rev.,* **53,** 778.
YANG, L. M., 1949 a, *Proc. Roy. Soc.* A, **198,** 94.
YANG, L. M., 1949 b, *Proc. Roy. Soc.* A, **198,** 471.

*The Mathematical Theory of Communication.* By CLAUDE E. SHANNON and WARREN WEAVER. (Urbana, 1949: University of Illinois Press.) [Pp. 117.] Price $2.50.

THE greater part of this volume is substantially a reprint of a paper on this subject by a well-known member of the Bell Telephone Laboratories, published in the Bell System Technical Journal in July and October, 1948. Only a condensed form of the remainder written by the second author has previously appeared; but portions of it might well be read first by those seeking a general view of the subject before embarking on a mathematical treatment.

*The Atmospheres of the Earth and Planets,* edited by GERARD P. KUIPER. (Published by University of Chicago Press, for whom Cambridge University Press act as agents.) [Pp. 366.] 17 plates. Price 60*s.* net.

THIS is the Report of a Symposium held at Chicago in September, 1947. Of the seventeen separate contributions, ten are concerned with various aspects of the atmosphere of the earth, and it mainly falls on Dunham and Kuiper to re-dress the balance with accounts of those of the planets. Nevertheless the intention, to present a comparative study of atmospheres, is genuinely realized, and results in a volume containing much factual material, especially on atmospheric spectroscopy and optics. F. C. F.

---

[*The Editors do not hold themselves responsible for the views expressed by their correspondents.*]